Superconducting weak links

K. K. Likharev

Department of Physics, Moscow State University, Moscow 117234, USSR

This review covers experimental results and theoretical ideas on the properties of superconducting weak links, i.e., weak electrical contacts between superconducting electrodes which exhibit direct (non-tunnel-type) conductivity. When the dimensions of such weak links are sufficiently small, the Josephson effect is observed in them, in other words, a single-valued and 2π -periodic relationship exists between the supercurrent I_S and the phase difference σ of the electrodes. With increasing dimensions, this relationship has a tendency to deviate gradually from the Josephson behavior. This deviation varies, depending on whether the weak link material is a superconductor or a normal metal. The various known types of weak links are described, and special mention is made of those weak links which are most suitable for physical investigations and have various practical applications. The data on the nonstationary (ac) processes in weak links, when the phase difference varies with time, are analyzed. In conclusion the existing concepts about the processes in weak links are briefly summarized and the most urgent outstanding problems are outlined.

CONTENTS

I. INTRODUCTION

In the modern superconductivity literature, the term "weak link" means the conducting junction between bulk superconducting specimens ("electrodes"), the critical current through which is much less than that in the electrodes. The term "weak link" is specifically used to distinguish weakly linked superconducting structures, i.e., those with direct (non-tunnel-type) conductivity, from the well known tunnel junctions.[1]

A. Reasons for interest in weak links

In recent years, weak links have been attracting increasing attention (about one hundred publications per year) largely for the following reasons. It was found, firstly, that the Josephson effect—one of the most interesting macroscopic quantum phenomena—is clearly exhibited in weak links of sufficiently small dimensions, i.e., when the spacing between the superconducting electrodes and the weak link cross section is small. Moreover, it is small-size weak links, i.e., Josephson junctions with non-tunnel-type conductivity, that have the most suitable parameters for the various applications of the Josephson effect,[2] their main advantage over tunnel junctions being low capacitance.

Secondly, in longer weak links (at a larger electrode spacing) the weak link inevitably becomes either a "usual" superconductor if its material exhibits superconductivity at a given temperature, or a "usual" normal conductor if the material is normal[3] at a given temperature. Therefore, a study of weak links makes it possible to examine the way in which the Josephson effect turns into ordinary superconductivity, and thereby gives a deeper insight into the nature of macroscopic quantum effects in superconductors.

A third circumstance is also important. To date, linear (both stationary and nonstationary) electrodynamic processes, as well as nonlinear stationary processes in superconductors, are well understood, at least in principle. Nonetheless, in the field of nonlinear nonstationary phenomena studies have only just begun. Although several fundamental theories have been suggested for these processes, many experimental phenomena are still far from being clear. Weak links are appealing in the study of these phenomena since simple geometry may be realized in them, which enables one to analyze theoretical problems of reduced space dimensionality under relatively simple boundary conditions.

B. Objective and structure of the review

The main objective of our review is to briefly outline the present status of investigations into the physical processes in superconducting weak links. On account of the specific features of the problem, attention has been centered on the relationship between the properties of weak links and their geometrical dimensions. Although the review is confined almost exclusively to physical problems, the reader will undoubtedly find that the author, like others working in this field, continually has in view the utilization of weak links for applications of the Josephson effect.

The main emphasis in the review is on the general physical picture of phenomena rather than on a mere enumeration of experiments or subtle details of various theories. Details regarding the technology of fabrication of various weak links have been omitted, but references to original works are given in the appropriate places.

[1] The processes taking place in superconducting tunnel junctions, including the Josephson effect, are described in monographs by Kulik and Yanson (1970) and Solymar (1972), and in several reviews, for example, by Josephson (1964; 1965), Clarke (1970), and Waldram (1976).

[2] These applications are discussed in the recent reviews by Gubankov and Likharev (1976) and Nad' (1975)—microwave receivers; Giffard *et al.* (1976), Clarke (1977), and Simmonds (1977)—SQUID magnetometers; Anacker (1969), Keyes (1969; 1975), and Zappe (1977)—computer elements. The theory of processes in circuits and systems with Josephson junctions is described by Likharev and Ulrich (1978).

[3] In the theory of superconductivity any material lacking superconducting properties is called "normal."

Some readers may feel that the review is more theoretical than experimental. But the author would like to assert that only relatively simple mathematical tools have been employed throughout. A knowledge thereof is essential for any experimentalist working in such a field as weak superconductivity, where a large number of new unexpected phenomena have been and probably will be discovered and where really good rather than "satisfactory" agreement between theory and experiment is the rule. The review presupposes, on the part of the reader, a knowledge of the basic principles of superconductivity, as laid down, say, in the monograph by De Gennes (1966), or in the excellent textbook by Tinkham (1975).

The review proper begins with Sec. II, which outlines the main types of junctions where the Josephson effect is observed—tunnel junctions and weak links. The specific properties of tunnel junctions are reviewed, and their advantages and disadvantages from the viewpoint of applications. Then a qualitative analysis is made of how the various types of weak links differ from tunnel junctions and from one another.

Section III is devoted to the most explored class of processes in superconducting weak links—stationary (dc) effects in which a constant current I, less than the critical current I_C, flows through the junction. Under these conditions, there is no voltage across the junction, nor does any normal current flow through it. Even within the framework of these processes, it is possible to follow the transition from the Josephson effect to ordinary superconductivity as the length of the weak link increases. For this purpose, a simple model of weak links, the "One-Dimensional Structure with Electrodes in Equilibrium" (ODSEE) model, is introduced and widely used in further discussion.

In Sec. IV we consider in more detail the specific features of various real types of weak links paying particular attention to the extent to which weak links correspond to the ODSEE model. The applications of weak links in various devices based on the Josephson effect are briefly touched upon here. This analysis shows that essentially the same types of weak links are best suited both for physical investigations and for applications.

The next sections (Sec. V and VI) are devoted to the less widely studied nonstationary (ac) processes. Section V is concerned with situations that are the simplest from an experimental standpoint, where a constant current greater than the critical one flows through the weak link. Section VI deals with some effects which are more complicated for experimental investigation but oftentimes more useful for understanding the physical nature of the processes.

All the foregoing pertains to weak links interconnecting two electrodes. In recent years, weakly linked systems consisting of several electrodes have been investigated intensively. Examples of such systems are a single weak link that simultaneously connects more than two electrodes, or a system of several weak links connected in series or in parallel or in any other complex manner. Radically new phenomena are likely to occur in such weak link systems. These are analyzed in Sec. VII, which also deals with distributed ("wide") Josephson junctions, junctions which may be regarded as a parallel connection of a large number of lumped weak links; the importance of these weak link systems for practical applications is discussed at the end of the section.

In conclusion, Sec. VIII outlines the present status of our knowledge of superconducting weak links and suggests the most urgent problems for further investigation.

II. JOSEPHSON EFFECT AND WEAK LINKS

A. Josephson effect

1. General description

The Josephson effect is one of the macroscopic quantum phenomena of superconductivity. In it the current through a weak contact between two relatively bulky superconducting electrodes may contain a component I_S (supercurrent), which is dependent not on the voltage V across the electrodes but on the phase difference

$$\varphi = \chi_2 - \chi_1 , \tag{1}$$

where χ_1 and χ_2 are the phases of the order parameter, Δ, in the electrodes

$$\Delta_{1,2} = |\Delta_{1,2}| \exp(i\chi_{1,2}) . \tag{2}$$

In the simplest ("classical") case, the relationship $I_S(\varphi)$ is sinusoidal

$$I_S = I_C \sin\varphi , \tag{3}$$

where I_C is called the supercurrent amplitude or the critical current.

The phase φ is related to the voltage across the electrodes V by the following expression

$$\frac{d\varphi}{dt} = \frac{2e}{\hbar} V . \tag{4}$$

There is a significant difference between Eqs. (3) and (4) which qualitatively describe the Josephson effect. Equation (3) is an approximate one, and various kinds of deviations of supercurrent from this dependence may be observed in a superconducting weak link of any type. Moreover, the constant I_C involved in Eq. (3) is essentially dependent on the geometry and material of the weak link, the electrode material, temperature, and other factors.

In contrast, Eq. (4) is derived solely from the main principles of quantum mechanics and contains only fundamental constants. That this relation holds to a high degree of accuracy has been experimentally demonstrated (see, for instance, Clarke, 1968; Dan Bracken and Hamilton, 1972; Macfarlane, 1973). This does not mean, certainly, that Eq. (4) is universally applicable. If V is defined as an electrochemical potential difference measured by an ordinary voltmeter, then certain corrections, say, due to rotation of the superconductors (Zimmerman and Mercereau, 1965) have to be introduced into Eq. (4). Besides, Eq. (4) is violated when the equilibrium stationary state of the electrodes is disturbed by the flow of a normal current component; this flow may occur in the neighborhood of a normal specimen (Reiger *et al.*, 1971) or due to heat flow (Ginzburg, 1944; Zavaritskii, 1974; Aronov and Gal'perin, 1974. See also Aronov and Spivak, 1975; Volkov and Zaitzev,

1976; Zaitzev, 1976). We shall disregard these effects and assume Eq. (4) to be exact, which is the case in most experiments on weak links. Thus our task is reduced to establishing a relationship between the current flowing through the weak link and the function $\varphi(t)$.

2. dc and ac effects

All the electrodynamic phenomena taking place at the Josephson contacts are generally divided into stationary (dc) and nonstationary (ac) effects, depending on whether the variables, including the phase difference φ, change with time or not.

If the phase φ remains constant (dc effects), as directly follows from Eq. (4), the voltage across the junction is zero. At the same time, a nonzero supercurrent (3) can flow through the junction. In the dc case, this current must be constant in time and less than the critical current

$$V=0,\ \varphi(t)=\text{const},\ I=I_S(\varphi),\ |I|\leq I_C. \tag{5}$$

Among the nonstationary (ac) effects occurring when the phase changes with time, the most important are Josephson oscillations which inevitably take place if the voltage V at the contact has a dc component $\bar{V}$. As follows from Eq. (4), in this case the phase φ contains a component that increases linearly with time at a rate

$$\omega_V=\overline{\frac{d\varphi}{dt}}=\frac{2e}{\hbar}\bar{V},\ f_V=\frac{\omega_V}{2\pi}=\frac{2e}{h}\bar{V}. \tag{6}$$

The supercurrent, therefore, oscillates in time at a frequency ω_V directly proportional to $\bar{V}$. The proportionality factor ($f_V/\bar{V}\approx 500\text{MHz}/\mu V$) is rather high; consequently, Josephson junctions are highly sensitive to the electromagnetic field.

In ac processes, not only the supercurrent I_S, but other current components can flow through the Josephson junction. Moreover, the supercurrent may depend not only on the instantaneous value of the phase difference, but also on the preceding variations of φ. Therefore the ac effects are always far more complicated than the dc effects. Thus we shall begin our discussion with the dc case.

3. Tunnel junctions and weak links

In the history of prediction and discovery, as well as at the initial stages (from 1962 to 1967 or so) of Josephson effect research, a prominent role was played by tunnel junctions in which two superconducting electrodes are separated by a thin insulating layer [Fig. 1(a)]. Finite conductivity is exhibited in such structures only due to tunneling of electrons through the potential barrier created by an insulator. A finite supercurrent may flow in them owing to the correlated tunneling of the electrons forming a pair. These are the tunnel junctions for which the Josephson effect was theoretically predicted (Josephson, 1962) and its main consequences were observed experimentally: the flow of supercurrent without any voltage drop (Anderson and Rowell, 1963) and the specific magnetic field dependence of the supercurrent (Rowell, 1963). Josephson oscillations were detected both indirectly (Shapiro, 1963; Giaever, 1965) and directly (Yanson *et al.*, 1965) with the help of the same

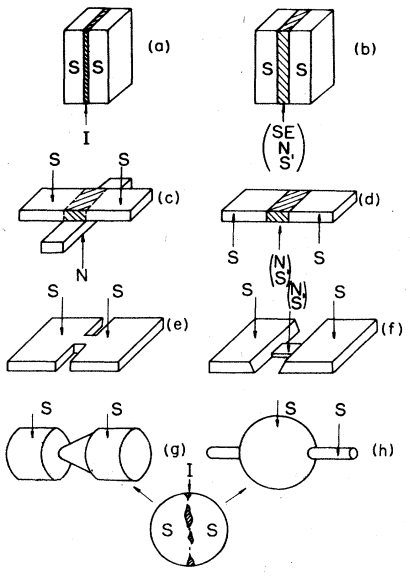

FIG. 1. Different types of structures where the Josephson effect can take place. (a) tunnel junction, i.e., S-I-S sandwich. All others are different weak links, i.e., structures with direct (non-tunnel-type) conductivity; (b)-sandwich; (c)-proximity effect bridge; (d)-ion-implanted bridge; (e)-Dayem bridge; (f)-variable-thickness bridge; (g)-point contact; (h)-blob-type junction. The conducting regions of the two last types of weak links are shown schematically in the circle on the bottom. S stands for superconductor, S' for the superconductor with reduced critical parameters, N for normal metal or alloy, SE for semiconductor (usually highly doped), I stands for insulator. Thin-film structures are shown without the substrate.

structures.

The outstanding role of tunnel junctions has greatly affected further research in the field. Some workers were led to believe that this effect could take place only in tunnel junctions, although the Josephson effect was observed in structures with non-tunnel conductivity as early as 1964 (Anderson and Dayem, 1964; Lambe *et al.*, 1964), and by 1966 all the main processes associated with this effect had already been detected in these structures (weak links) (Zimmerman and Silver, 1964; 1966a, b; Grimes *et al.*, 1966; Dayem and Grimes, 1966). Overestimation of the significance of tunnel junctions has led to deplorable consequences. Firstly, considerable attention has been given to complex and specific processes in tunnel structures which are of minor theoretical and practical importance. Secondly, after the main effects had been experimentally observed and a fairly satisfactory theory of the Josephson effect had been developed (Werthamer, 1966; Larkin and Ovchinnikov, 1966), some investigators got the wrong impression that "everything is quite clear concerning the Josephson effect," and some prominent workers were thus unfortunately misled to abandon further research in the field.[4]

[4]This is reflected in the literature too. Let alone the early surveys, in the existing monographs (Kulik and Yanson, 1970; Solymar, 1972) and even in some recent reviews on the Josephson effect, attention is focused on tunnel junctions.

Therefore, although the use of weak links for practical purposes was begun in 1966–67, the physics of weak links has only become a subject of intensive study since 1974. So far these investigations have produced more questions than answers, and the most significant progress achieved to date is, probably, the recognition of the fact that the Josephson effect is up to now far from being a clearly understood phenomenon, and that tunnel junctions are merely a particular case of Josephson junctions.

This review is devoted to weak links with non-tunnel conductivity; and yet we shall begin with a brief survey of the well known properties of tunnel junctions. This is done, first, for the sake of comparison and, second, because there are cases where the properties of weak links are similar to those of tunnel junctions.

B. Tunnel junctions

1. Basic equations

In most cases the properties of tunnel junctions are adequately described by the existing theory,[5] which is based on two facts:

(i) The thickness of the energy barrier (insulating layer) is of the order of 10^{-7} cm, and is negligibly small compared to all other characteristic lengths in the superconductor, in particular, the mean free path of electrons ℓ. This means that the barrier may be and is described integrally, without introducing the coordinate dependences of any superconductivity parameters (e.g., Δ) inside the barrier.

(ii) The barrier transparency factor T is in most cases so small that the critical current through the junction (usually of order $1-10^2 A/\mathrm{cm}^2$) is far less than the critical current of the electrodes ($10^5-10^7 A/\mathrm{cm}^2$). This makes it possible to calculate the characteristics of the junctions using perturbation theory with respect to the small parameter $T \ll 1$, i.e., to disregard disturbances in the electrodes' state caused by tunnel current.

These facts greatly simplify theoretical analysis; as a result of which as far back as 1963 a complete theory was formulated for the dc case ($V=0$) (Ambegaokar and Baratoff, 1963), and in 1966 a theory for arbitrary $V(t)$ was completed (Werthamer, 1966; Larkin and Ovchinnikov, 1966). A discussion of the theory can be found in the monograph by Kulik and Yanson (1970) or in the report by Poulsen (1973); here we shall quote the main results only.

Consider a junction of such small area that the phase difference and the voltage across the junction are independent of the coordinates in the plane of the barrier, and are interrelated by Eq. (4). Let the voltage contain components at a frequency ω and its harmonics, and possibly a frequency of the Josephson oscillations ω_V [Eq. (6)]. In this case $\exp(i\varphi/2)$ can be expressed in the form of a Fourier series

$$\exp(i\varphi/2)=\sum_n A_n \exp[i(\omega_V/2+n\omega)t]. \tag{7}$$

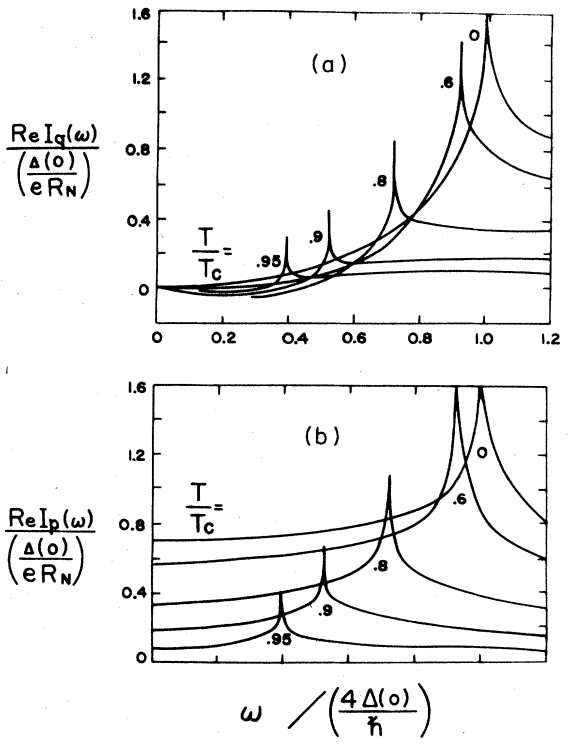

FIG. 2. The amplitudes of supercurrent (I_p) and normal electron (quasiparticle) current (I_q), which are used in tunnel theory [Eq. (8)], for different temperatures T. T_C is the critical temperature of the electrodes, which are taken to be identical. $\Delta(T)$ is the order parameter modulus in the electrodes. R_N is the normal junction resistance. Real parts of amplitudes are even, and imaginary parts are odd functions of the argument.

In this case the current through the junction is of the form (Poulsen, 1973):

$$I(t)=\mathrm{Im}\Big\{\exp(i\varphi/2)\sum_n A_n^* \exp[-i(\omega_V/2+n\omega)t]\, I_q(\omega_V+2n\omega) + A_n \exp[i(\omega_V/2+n\omega)t]\, I_p(\omega_V+2n\omega)\Big\}, \tag{8}$$

where I_p and I_q are complex functions which describe the currents of Cooper pairs and unpaired electrons, respectively.[6] These functions are shown in Fig. 2 for the case where the electrodes are made of the same material. Some curves for electrodes with different critical temperatures T_C are plotted in the paper of Harris (1974).

[5] An exception is the problem of the sign of the "interference" and the "fourth" components of the current (see Sec. V).

[6] As the properties of the unpaired electrons in a superconductor differ slightly from their properties in normal metals, they are generally referred to as "electron-like quasiparticles," "electron-like excitations," and others. For the sake of simplicity, however, we shall use the term "electrons" everywhere, bearing in mind the distinction mentioned above.

2. Basic properties of tunnel junctions

For the dc (zero-voltage) case, we have to change $\omega_V t \to \varphi$ in Eqs. (7) and (8); thus we get

$$I = I_C \sin\varphi\,,\quad I_C = \mathrm{Re}\,I_p(0)\,, \tag{9}$$

which shows that the $I_S(\varphi)$ relationship is always sinusoidal for tunnel junctions. The critical current is given by $\mathrm{Re}\,I_p(0)$ which, for identical electrodes, is

$$I_C = V_C/R_N\,,\quad V_C = \frac{\pi}{2}\,\frac{\Delta(T)}{e}\tanh\frac{\Delta(T)}{2k_BT}\,, \tag{10}$$

where $\Delta(T)$ is the equilibrium value of the energy gap, i.e., the modulus of Δ in electrodes, and R_N is the resistance of the junction in a normal state. An important result is that the product I_CR_N, which is called the characteristic voltage of the junction V_C, does not depend on any parameters of the barrier, and is determined solely by the operating (T) and critical (T_C) temperatures through the well known function $\Delta(T) = k_BT_Cf(T/T_C)$. We recall here that in the microscopic theory (Bardeen *et al.*, 1957) the quantity $\Delta(T)$ is almost constant at low temperatures

$$\Delta(T) \approx \Delta(0)\left\{1 - \left(\frac{2\pi k_BT}{\Delta(0)}\right)\exp\left[-\frac{\Delta(0)}{k_BT}\right]\right\},\ \text{at } T \lesssim 0.6T_C\,, \tag{11}$$

$$\Delta(0) = (\pi/\gamma)k_BT_C\,,\ \gamma \approx 1.78\,,$$

and falls off rapidly as $T \to T_C$

$$\Delta^2(T) \approx \frac{8\pi^2}{7\zeta(3)}k_B^2T_C(T_C - T)\,,\ \text{at } T_C - T \lesssim 0.1T_C\,, \tag{12}$$

$$\zeta(3) \approx 1.202\,.$$

Therefore the critical temperature determines the maximum possible value for the junction voltage ($T \to 0$)

$$\max_T(eV_C) = \frac{\pi}{2}\Delta(0) = \frac{\pi^2}{2\gamma}k_BT_C\,,\quad \max_T(V_C)[\mu V] \approx 240T_C[K]\,. \tag{13}$$

Near T_C, the characteristic voltage is a linear function of temperature with a universal slope

$$V_C = \frac{\pi}{4}\,\frac{\Delta^2}{ek_BT} = \alpha(T_C - T)\,,\quad \alpha = \frac{2\pi^3k_B}{7\zeta(3)e} \approx 635\,\frac{\mu V}{K}\,. \tag{14}$$

If the junction voltage is nonzero, then other components also contribute to the current. For example, for constant $V = \bar{V}$, Eq. (8) directly yields

$$I = \mathrm{Re}\,I_p(\omega_V)\sin\omega_V t + \mathrm{Im}\,I_p(\omega_V)\cos\omega_V t + \mathrm{Im}\,I_q(\omega_V)\,, \tag{15}$$

which shows that the current through the junction is the sum of the oscillating Josephson supercurrent with an amplitude $I_p(\omega_V)$ and a constant normal current $\mathrm{Im}\,I_q(\omega_V)$.

It is obvious from Fig. 2 that at low voltages [$e\bar{V} \lesssim 2\Delta(T)$] the amplitude of the current oscillations is practically constant and equal to the critical current. At a frequency $\omega_V = 4\Delta/\hbar$, i.e., at a voltage

$$\bar{V} = 2\Delta(T)/e\,, \tag{16}$$

the amplitude has a weak (logarithmic) singularity (Riedel, 1964), and the electron current has a step of finite height. This behavior results from the following process: an electron pair from one electrode breaks and one of the electrons passes to another electrode, absorbing an electrostatic energy eV. Equation (16) follows precisely from the condition that this energy should be equal to the pair binding energy 2Δ.

At higher voltages, the electron current $\mathrm{Im}\,I_q$ tends to assume its value in a normal junction, while the amplitude of the supercurrent oscillations falls off approximately as ω_V^{-1}. If the contact junction voltage changes with time, a fourth component $\mathrm{Re}\,I_q$ also contributes to the current.

A large number of phenomena occurring at tunnel junctions may be described by Eqs. (7) and (8) if the real geometry of the junction, its capacitance, possible phase variations in its plane, and several other factors are taken into account. These effects do not fall within the scope of our review since most of them do not take place in weak links.

3. Capacitance and current density

As regards the use of tunnel junctions as Josephson elements in various applications, an analysis of the dynamics of devices based on such elements shows the following. Almost all tunnel junctions prepared by existing techniques have parameters which are quite suitable for practical applications with the important exception of the large intrinsic capacitance of the junction C, a parasitic factor for almost all applications (see, for example, the analysis of Likharev and Ulrich, 1978).

As follows from circuit analysis, the criterion for the negligibly small influence of the capacitance on junction processes is the smallness (compared with unity) of the following dimensionless parameter[7]

$$\beta = \omega_CR_NC = (2e/\hbar)I_CR_N^2C\,, \tag{17}$$

where ω_C is the characteristic frequency of the junction, which is related to its characteristic voltage V_C by the Josephson relation (4)

$$\omega_C = \frac{2e}{\hbar}V_C = \frac{2e}{\hbar}I_CR_N\,. \tag{18}$$

It is clear from Eq. (17) that β is independent of the junction area S, and that β shows whether or not the capacitance shunts the conductance at frequencies $\sim\omega_C$.

In a typical Josephson junction the density of the critical current is $\sim 10^2 A/cm^2$, and the critical temperature of the electrodes is about 10 K, while the electrical thickness of the insulating layer t/ϵ is ~1Å. Hence the following estimates of the parameters

$$C/S = \epsilon/4\pi t \approx 10^{-5}F/cm^2\,,\ V_C \approx 2\times10^{-3}V\,,\ \omega_C \approx 6\times10^{12}s^{-1}\,,$$
$$R_NS = V_C/j_C \approx 2\times10^{-5}\Omega\times cm^2\,,\ \beta \approx 10^3 \gg 1. \tag{19}$$

Thus, in a typical tunnel junction, the capacitance effectively shunts the tunnel conductance. This situation has an adverse effect not only on microwave devices based on the Josephson effect, but also on such applications as magnetometry or computer devices, because the $I-V$ curve, under the effect of capacitance (see, for

[7] For applications at very high frequencies ($\omega \gg \omega_C$) β should be small as compared to $\omega_C/\omega \ll 1$.

example, Likharev and Ulrich, 1978), becomes hysteretic.

From Eq. (17) it is clear that β can be reduced in two different ways: either by increasing the current density j_C (decreasing R_N) or by increasing the electrical thickness of the barrier t/ϵ, the current density being kept the same. Each of these ways gives rise to its own difficulties in the technology of fabrication of tunnel junctions.

Since the publication of Giaver's classic papers (1960), tunnel junctions are usually prepared between two thin superconducting films as follows: first the lower film is evaporated, then it is oxidized to form an insulating layer, and finally the upper superconducting layer is deposited. Even relatively small current densities ($\sim 10^2 A/cm^2$) are attained with an oxide layer as thin as 10°–20 Å at which, it is, indeed, a problem to provide layer uniformity and stability with respect to diffusion. In recent years considerable progress has been made in the technology of fabrication of stable oxide layers, using glow discharge oxidation and suitable electrode materials (Schroen, 1968; Greiner, 1971, 1974; Lahiri, 1976). However, only in a few cases has a current density of $\sim 10^4 A/cm^2$ been obtained (see, for instance, Broom *et al.*, 1975), β being still as large as several tens.[8]

Another method is to increase the thickness of the potential barrier, keeping the current density at the same level (or even increasing it) by using a semiconductor interlayer which provides a lower energy barrier height (see the review by Cardinne *et al.*, 1974, and the papers by Barone *et al.*, 1974; Barone and Russo, 1974; Simmonds, 1974). Recently, junctions having a current density $\sim 10^4 A/cm^2$ and $\beta \sim 1$ have been successfully prepared, using silicon single-crystal membranes ~1000 Å thick as an interlayer (Huang and Van Duzer, 1974, 1975; Schyfter *et al.*, 1977). It should, however, be noted that this rather impressive result was obtained with the help of a semiconductor highly doped with boron to a concentration of $\sim 10^{20}$ cm^{-3}, and hence practically degenerate. The conductivity of such material is of metallic type even at helium temperature. Thus these junctions, which will be discussed in detail below, are one of the types of weak links, namely, S–N–S sandwiches.

As a result of the above-mentioned difficulties in manufacturing tunnel junctions with low capacitance, Josephson weak links, i.e., structures with direct (non-tunnel-type) conductivity, are now used for most applications. The most important exception is in digital device applications (see Footnote 2 for references) where some important development programs are based on the use of tunnel junctions. However, large junction capacitances create some hard problems here as well. The personal point of view of the author is that the real advantage of tunnel junctions in this field is the somewhat more advanced technology of their fabrication, and that the situation can change with time.

[8]Recently a report has been published (Niemeyer and Kose, 1976) on the successful production of junctions with $j_C \approx 2 \times 10^5 A/cm^2$ and $\beta \sim 1$. Nonetheless, so far it is not quite clear whether those junctions possess tunnel-type conductivity.

C. Weak links

1. Main types of weak links

The current in weak links, unlike that in tunnel junctions, flows along a conducting, either normal or superconducting, material. The relative weakness of the link, in other words, the low value of its critical current, is attained differently in different structures whose main types are shown in Fig. 1(b)–(h).

If a layer of normal metal, usually 0.1 to 10 μm thick, is interposed between two superconductors, we obtain an "S-N-S sandwich" junction [Fig. 1(b)]. A finite supercurrent can flow through such a junction due to the well known proximity effect (see, for example, De Gennes, 1966). The effect lies in the fact that if a normal metal and a superconducting metal are brought into proper electric contact, some Cooper pairs will penetrate into the normal metal from the superconductor. Thus in the normal metal there arises a nonzero order parameter Δ, which exponentially decreases within the metal over a distance of the order of "normal coherence length" or "decay length" ξ_N. On the other hand, the values of Δ in the superconductor over distances of the order of coherence length ξ from the boundary will become less than the equilibrium value. Hence, if the thickness of the normal interlayer is not very large, the order parameter will be different from zero throughout the normal metal, and a finite supercurrent may flow through the interlayer.

As a normal interlayer we may use either a "true normal" metal which does not suffer superconducting transition at any temperature (hereafter denoted N), or a superconductor having a critical temperature $0 < T_C < T$ (denoted by N'). Moreover, a sandwich material may also be superconducting ($T_C > T$), in which case the weakness of the link is to be provided by keeping its critical current small compared to that of the electrode material S. In this case the junction is called the S-S'-S sandwich.

A situation closely resembling the sandwich phenomenon can be created in proximity effect bridges[9] [Fig. 1(c)] or in ion-implanted bridges [Fig. 1(d)]. In both cases a section of low critical current, usually of about a few microns long, is made in a narrow strip of superconducting film (about 10^3 Å thick). In the first case this section is formed by the proximity effect with a normal metal underlayer, and in the second case by the implantation of ions into this region (or, in some rare cases, into the main bulk of the film, i.e., into the electrodes). In practice, the only distinction between these structures and sandwiches is that their cross section can be made much smaller because one of the dimensions is formed by thin-film evaporation.

An entirely different method of forming weak links is realized in a constant-thickness bridge[10] [Fig. 1(e)] or in a variable-thickness bridge [Fig. 1(f)]. Low critical current results here from the fact that the width (in the first case) or the width and the thickness (in the second case) of the "span" are far less than those of the electrodes ("banks"). The typical thickness of the bank film

[9]These are sometimes termed "Notarys–Mercereau bridges".

[10]These are generally known as "Dayem bridges."

is again 10^3 Å, while the thickness of the span may be several hundred angstroms. The span length is kept as low as possible, say, a few tenths of a micron.

Of course, both of these methods of producing weak links may be used in combination. For instance, in the bridges with current concentration [Fig. 1(e), (f)], the span and the electrodes may be made of different materials (N, N', or S'). From a practical viewpoint this is more natural in the more sophisticated variable-thickness bridges, because incorporation of a second material would greatly complicate fabrication of Dayem bridges.

The geometry of weak links is more complicated in the two other types of Josephson junctions, i.e., in point contacts [Fig. 1(g)] and in blob-type junctions[11] [Fig. 1(h)]. In the first case the electrical contact is created by weak touching of the two superconducting electrodes, and in the second case by forming a pellet of solder (superconducting at low temperatures) over a length of a superconducting wire.

When the pressure between the electrodes in a point contact increases or when the metal in a blob-type junction solidifies, the oxide layer, which inevitably coats the electrodes, is usually interrupted at many places, thereby forming several metallic shorts between electrodes (Fig. 1, sketch in circle). The typical cross-section area (10^{-13} to 10^{-10} cm^{-2}) of such shorts is generally of the order of the square of the thickness of the oxide layer ($\sim 10^{-6}$ cm), and is much less than the area of mechanical contact between the electrodes. Thus the link weakness in this case is also attained due to the strong current concentration.[12]

Such weak links, especially point contacts, have found wide application due to the simplicity of their fabrication. A significant disadvantage of these structures as subjects for physical research is their poorly defined geometry. Their demerit in practical applications is their irreproducibility.

2. Length and effective length

Any weak link, in fact, is a partition between two superconducting electrodes. It is natural, therefore, that its basic geometrical dimension is its length L. By length we mean the electrode spacing, in other words, the dimension of the weak link in the direction of current flow. In sandwiches, for instance, this length [Fig. 1(a), (b)] is merely the thickness of an interlayer, while in ion-implanted bridges (Fig. 1d) this is the length of a section with changed properties.

However, it is an effective length $L_{\text{eff}} \geq L$ rather than the geometric length that plays a significant role in the processes under discussion. By effective length is meant that length within which the nonlinear effects in a weak link are localized. The point is that nonlinear electrodynamic processes almost inevitably extend somehow or other into the adjacent sections of the electrodes, if only because of the proximity effect: variations in the order parameter in weak links caused by the nonlinear effects lead to changes in $|\Delta|$ in the banks. Of course, the degree of involvement of the electrodes in these nonlinear processes depends strongly on the type of weak link. The lower the conductivity of the material and the greater the current concentration in a weak link, the lesser is the degree of involvement (and consequently, the closer the L_{eff} is to L) (for details, see Sec. IV).

Lack of distinct localization of the nonlinear effects in some structures is a serious drawback from the viewpoint of both physical research and practical applications. From the first standpoint, these effects introduce a noticeable amount of indeterminacy into the geometry of weak links, i.e., they complicate theoretical analysis and interpretation of experimental results. From the second standpoint, extension of the nonlinear effects to the banks prevents realization of weak links whose effective length is less than the coherence length, and, as we shall demonstrate below, the Josephson effect is observed precisely in structures with $L_{\text{eff}} \lesssim \xi$. For this reason, in studying the relationship between the properties of weak links and their length, we shall focus our attention mainly on those weak links for which $L \approx L_{\text{eff}}$ and only in Sec. IV shall we briefly discuss the consequences of the absence of distinct localization of nonlinear effects.

3. Classification of weak links

A reasonable classification of weak links is based on a comparison of the effective length L_{eff} with the characteristic lengths of the material forming the weak link, the coherence length ξ and the mean free path ℓ being most important among them.[13]

Junctions with $L_{\text{eff}} \ll \xi$ will be called "*short*" to distinguish them from "*long*" weak links for which $L_{\text{eff}} \gtrsim \xi$. We shall demonstrate that it is in short weak links where the "ideal" Josephson effect (see Sec. III for definition of the term) is observed, and an increase in this effective length causes considerable deviation from the ideality. For this reason we shall center our attention on the case $L_{\text{eff}} \ll \xi$.

Even in short weak links, however, the processes may differ depending on the mean free path ℓ. From experimental and practical viewpoints, the bridge-type weak links [Fig. 1 (c)–(f)] with exactly known geometry, sufficient normal resistance (say, $R_N \gtrsim 0.1\Omega$), and the possibility of reproducible fabrication are of particular importance. As a rule, the mean free path ℓ in bridges is limited by diffuse scattering on the film surface to a length on the order of a few hundred angstroms, which is far less than L_{eff} (from one tenth of a micron to a few microns). We shall mainly consider such "*dirty*" structures for which

$$\ell \ll L_{\text{eff}}, \tag{20}$$

[11] Sometimes they are referred to as Clarke blobs.

[12] When the resistance of point contact is fairly high ($R_N \gtrsim 10^2\Omega$) the tunnel current through the oxide layer may be quite significant.

[13] A third important length for superconductors, the magnetic field penetration depth λ, which determines the force of current self-limitation (Meissner effect), is not so significant for weak links, and is, generally, compared only with the width of the structure W, i.e., with the characteristic size of the cross section.

although at the end of Sec. III we shall briefly touch upon "*clean*" structures with a large mean free path $\ell \gtrsim L_{\rm eff}$.

The terms "dirty" and "clean" for weak links are not to be confused with the well known dirty and clean limits in the general theory of superconductivity, where they are used to denote the relation between values of ℓ and the BCS coherence length ξ_0.

III. STATIONARY (DC) EFFECTS

First we shall examine stationary phenomena in weak links where the phase difference φ of the order parameter in the electrodes is constant in time. In this case a constant supercurrent I_S less than I_C flows through the weak link, and there is no electric field or normal electron current, these electrons being in equilibrium. The stationary theory of superconductivity may be applied, and a relationship between the supercurrent I_S and the phase difference φ has been found for many important cases.

A. Aslamazov-Larkin theory

The basic principles of how the Josephson effect takes place in weak links with strong current concentration have been explained by Aslamazov and Larkin (1969), referred to below as AL. We shall, therefore, examine their theory in greater detail, although it is directly applicable only under rather stringent assumptions with regard to the geometry and the material of weak links.

1. Ginsburg-Landau equations

Let the temperature T be sufficiently close to the electrode critical temperature T_C. Then the modulus of the order parameter at every point in the structure is relatively small ($|\Delta| \ll k_B T_C$), so that the simple and convenient Ginsburg–Landau (GL) equations (1950) may be applied (see also De Gennes, 1966; Tinkham, 1975). These equations may be expressed as

$$\xi^2(\nabla - i\frac{2e}{\hbar c}\mathbf{A})^2\Delta + [\pm 1 - \frac{|\Delta|^2}{\Delta_0^2}]\Delta = 0, \tag{21a}$$

$$\mathbf{j}_s = C_j \mathrm{Im}[\Delta^*(\nabla - i\frac{2e}{\hbar c}\mathbf{A})\Delta], \tag{21b}$$

where $\mathbf{A}$ is the vector potential, and the coherence length is given by the following expression in the dirty limit ($\ell \ll \xi_0$):

$$\xi^2(T) = \frac{\pi\hbar D}{8k_B(T_C - T)}, \quad \xi(T) \approx 0.852(\xi_0 \ell)^{1/2}\left(\frac{|T_C - T|}{T}\right)^{-1/2}, \tag{22}$$

where $D = v_F\ell/3$ is the diffusion coefficient, and ξ_0 is the size of the Cooper pair

$$\xi_0 = \frac{\hbar v_F}{\pi\Delta(0)} \approx 0.180\frac{\hbar v_F}{k_B T_C}. \tag{23}$$

Δ_0 stands for some characteristic value of $|\Delta|$, which for $T < T_C$ is equal to the equilibrium value (12). For $T > T_C$ (GL equations hold true for this case as well) we may again use Eq. (12) for Δ_0, taking the modulus of $(T_C - T)$; here also we take the minus sign before unity in Eq. (21a). The coefficient C_j in the dirty limit is proportional to normal conductivity σ_N

$$C_j = \frac{c^2\hbar}{8\pi e\lambda^2\Delta_0^2} = \frac{\pi}{4}\frac{\sigma_N}{ek_BT}, \quad \sigma_N = 2e^2N(0)D, \tag{24}$$

where $N(0)$ is the density of states on the Fermi surface.

Equation (21) follows from the microscopic theory of superconductivity under the following restrictions in addition to the requirement that $|\Delta|$ be small (Gor'kov, 1959; see also, De Gennes, 1966).

(i) The order parameter varies slowly over the range of the self-consistency radius, equal approximately to $(\xi_0\ell)^{1/2}$ in the dirty limit.

(ii) The current density varies slowly over the range of the radius of integral coupling between the field and the current; it is of the order of ℓ in the dirty limit.

We shall use GL equations to describe a weak link of characteristic size $L_{\rm eff}$ inside which both Δ and j_S undergo significant changes in the general case, and therefore, the condition of the dirty weak link.

$$\ell \ll L_{\rm eff} \tag{25}$$

should necessarily be satisfied.

2. Linearization of the equation for Δ

Aslamazov and Larkin considered a case in which, although condition (25) holds, nevertheless the length of the weak link is sufficiently small both compared with ξ

$$L_{\rm eff} \ll \xi(T), \tag{26}$$

and compared with magnetic field penetration depth

$$L_{\rm eff} \ll \lambda(T). \tag{27}$$

By virtue of Eq. (26), we can discard all terms except the first ("gradient") term in Eq. (21a). Indeed, the sum of all the discarded terms is not greater than Δ, while the gradient term is of the order of $\Delta(\xi/L)^2$. Inequality (27) shows that the influence of self-shielding, which is responsible for the nonuniform distribution of current over the cross section, is insignificant in the weak link. Formally, this inequality makes it possible to neglect the contribution made by the weak link current to the vector potential A which in principle has to be determined from the Maxwell equation. The remaining part ($\mathbf{A}_0$) is associated with the remote field sources ($r \gg L_{\rm eff}$), and it can be represented in the form of a gradient of some scalar function.[14] Since A is always chosen up to the gradient of an arbitrary function, we may take the gauge to be

$$\mathbf{A} = \mathbf{A}_0 = 0. \tag{28}$$

This means that the magnetic field influence is accounted for by the order parameter phase, which is in this case gauge invariant, i.e., a uniquely defined quantity. It is precisely under this gauge that we examined the Josephson effect in Sec. II.

[14] The only exception is the case where the external magnetic fields are strong: $B \sim \phi_0/L_{\rm eff}^2$, where $\phi_0 = ch/2e$ is the magnetic flux quantum. But, by virtue of Eq. (26), these fields are far stronger than the field $H_{C2} = \phi_0/2\pi\xi^2$ which suppresses the superconductivity in the electrodes.

Hence, under the constraints (26) and (27), Eq. (21a) is reduced to a simple linear Laplace equation

$$\nabla^2\Delta = 0, \tag{29}$$

which makes it possible to solve the problem for an arbitrary weak link geometry. It has to be solved under the following boundary conditions. The order parameter inside the electrodes should tend to the following values

$$\Delta = \begin{cases} \Delta_1 \exp(i\chi_1) & \text{for electrode 1,} \\ \Delta_2 \exp(i\chi_2) & \text{for electrode 2.} \end{cases} \tag{30}$$

The current through the surface σ with the outer space (vacuum or an insulator) should be zero. Hence, by virtue of (21b), we obtain the condition

$$\partial\Delta/\partial n|_\sigma = 0, \tag{31}$$

where $\mathbf{n}$ is normal to the surface.

3. Josephson effect as the interference of wave functions

Aslamazov and Larkin pointed out that the (unique) solution of the problem may be expressed as

$$\Delta = \Delta_1 \exp(i\chi_1) f + \Delta_2 \exp(i\chi_2)(1-f), \tag{32}$$

where $f(\mathbf{r})$ is a real function of the coordinates satisfying the following boundary-value problem

$$\nabla^2 f = 0, \quad \partial f/\partial n|_\sigma = 0,$$

$$f = \begin{cases} 1 & \text{for electrode 1,} \\ 0 & \text{for electrode 2.} \end{cases} \tag{33}$$

Indeed, by substituting Eq. (32) into Eqs. (29)–(31), we find that this solution satisfies both the equation and the boundary conditions. For the time being, supposing that the function f is known, and after substituting Eq. (32) into Eq. (21b), since $\mathbf{A} = 0$, we obtain

$$\mathbf{j}_S(r) = C_j \nabla f(r) \Delta_1 \Delta_2 \sin\varphi. \tag{34}$$

According to (33), the function f does not depend on φ; the current at each point of the weak link is, therefore, proportional to $\sin\varphi$. Consequently the total current is also proportional to $\sin\varphi$. Thus we have already arrived at an important result: if the conditions of the AL theory are satisfied, then the Josephson effect occurs in weak links, i.e., the supercurrent and the phase are governed by Eq. (3).

Now we return to Eq. (32), which gives the distribution of the order parameter in the bulk of the weak link. It shows that inside the weak link ($f \neq 0, 1$) the order parameter is a linear superposition of two terms, each of which is proportional to Δ at one of the electrodes and to the coordinate factor. The latter gradually diminishes as we recede from the electrode into the depths of the weak link. Thus inside the weak link there occurs simple interference of two wave functions whose sources are the condensates of Cooper pairs in the superconducting electrodes. Such interference gives rise to current [Eq. (34)] sinusoidally dependent on the phase difference of the sources; consequently, it is the direct cause of the Josephson effect. So, the AL theory not only demonstrates the existence of the Josephson effect in weak links, but also gives one a clear picture of its physical origin.

4. Magnitude of the critical current

It is impossible to find an analytical expression for the function f for an arbitrarily shaped weak link. To find the critical current I_C (and the characteristic voltage V_C), however, there is no need to determine f. To demonstrate this statement, we shall find the current flowing through the same contact in a normal state (for example, at $T > T_C$). From the obvious relationships $\mathbf{j}_N = \sigma_N \mathbf{E}$ and $\operatorname{div} j_N = 0$, and the definition of the scalar potential ($\mathbf{E} = -\nabla\mu$), again we arrive at the Laplace equation.

$$\nabla^2\mu = 0 \tag{35}$$

with the boundary conditions

$$\mu = \begin{cases} \mu_1 & \text{for electrode 1,} \\ \mu_2 & \text{for electrode 2,} \end{cases} \tag{36}$$

$$\partial\mu/\partial n|_\sigma = 0, \quad \mu_1 - \mu_2 = V.$$

For this problem we can easily express the unique solution as follows

$$\mu = \mu_1 f + \mu_2(1-f), \tag{37}$$

where the function $f(\mathbf{r})$ is the same as in the case of Eq. (32). On calculating the current, we find that

$$\mathbf{j}_N = \sigma_N \mathbf{E} = -\sigma_N \nabla\mu = \sigma_N V \nabla f(\mathbf{r}). \tag{38}$$

By comparing Eqs. (34) and (38) we find that both in the normal and in the superconducting states the current is distributed identically over the bulk of the structure ($\mathbf{j} \propto \nabla f$). The total currents I_S and I_N, therefore, are in the same relation as their densities

$$\frac{I_S}{I_N} = \frac{j_S}{j_N} = \frac{C_j \Delta_1 \Delta_2 \sin\varphi}{\sigma_N V}. \tag{39}$$

But the total current in the normal state is evidently equal to V/R_N, and thus from Eq. (39) we have

$$I_S = I_C \sin\varphi, \quad I_C = \frac{C_j \Delta_1 \Delta_2}{\sigma_N R_N}. \tag{40}$$

For the real case of the dirty limit ($\ell \ll \xi_0$) with the help of Eq. (24) we obtain an especially simple expression[15]

$$V_C = I_C R_N = (\pi/4)\Delta_1\Delta_2/ek_BT. \tag{41}$$

For electrodes made of identical material ($\Delta_1 = \Delta_2 = \Delta$), on comparing Eqs. (41) and (14) we find that as $T \to T_C$, the characteristic voltages V_C for small-size weak links and tunnel junctions are identical, hence the derivative $\alpha = |dV_C/dT|$ is again equal to 635 $\mu V/K$

[15] The factor of 4 in the denominator was missing in the original AL paper.

[Eq. (14)].

In deriving Eq. (41) it should be noted that nowhere were the weak link and the electrodes assumed to be of the same material. Hence the characteristic voltage V_C at the "ideal" Josephson effect is not dependent on the material of the weak link. The material only affects the normal resistance R_N of the contact and consequently the critical current, which is inversely proportional to the resistance.

B. Arbitrary temperatures

The fact that the expressions for $I_S(\varphi)$ and V_C in small-size weak links are the same as the corresponding expressions for tunnel junctions when $T \to T_C$ suggests that the dc Josephson effect may also take place in an identical manner at arbitrary temperatures in these two types of structures. Kulik and Omelyanchuk (1975) in an article hereafter referred to as K0-1, have, however, demonstrated the contrary.

1. General properties of the current-phase relationship

Here we may mention that the phase dependence of the supercurrent has certain general properties which do not depend on the geometry of weak links or the equations that describe them.

Firstly, a change of 2π in the phase χ of the order parameter in any of the electrodes does not change the physical state of the system, since

$$\Delta(\mathbf{r}, t) = |\Delta| e^{i\chi} = |\Delta| e^{i(\chi + 2\pi)} . \tag{42}$$

Therefore the function $I_S(\varphi)$ is always 2π periodic

$$I_S(\varphi + 2\pi) = I_S(\varphi) . \tag{43}$$

Secondly, supercurrent may flow only when there is a gradient of the order parameter phase. Therefore there are no currents across the weak links in the two situations depicted in Fig. 3 (b) and (c). In the first case, the phase shift is zero, while in the second case it is π. As a result, the curve $I_S(\varphi)$ intersects the horizontal axis at $\varphi = \pi n$:

$$I_S(\pi n) = 0 . \tag{44}$$

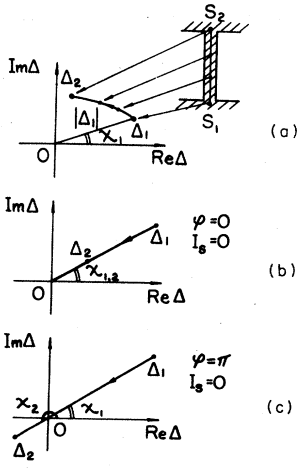

FIG. 3. The representation of process in a weak link on the phase plane of the order parameter Δ (a). Each point on the plane shows a value of Δ in the definite point of the weak link, and finite points of trajectory correspond to the states of the electrodes. Two possible types of phase trajectories corresponding to absence of supercurrent through weak link are shown below: (b) $\varphi = 0 + 2\pi n$; (c) $\varphi = \pi + 2\pi n$.

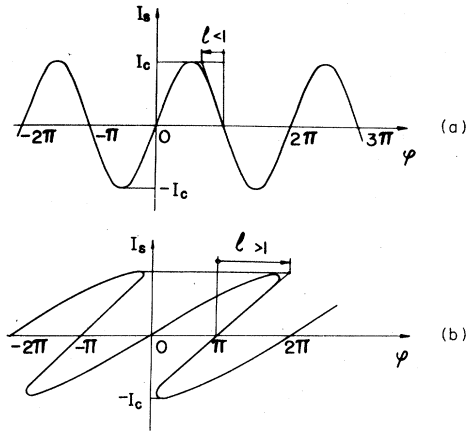

FIG. 4. Possible $I_S(\varphi)$ relationships in weak links (schematically). Function $I_S(\varphi)$ is always odd, and its plot passes through the points $[I_S = 0,\ \varphi = \pi n]$. This function can be either single-valued (a), or multivalued (b). In the first case the parameter $l = I_C (dI_S/d\varphi)^{-1}_{\varphi=\pi}$ of the kinetic inductance is less than unity, and in the second case l is greater than unity.

Moreover, in the superconductor the opposite currents are equivalent;[16] therefore, the function $I_S(\varphi)$ is symmetrical with respect to the origin

$$I_S(-\varphi) = -I_S(\varphi) . \tag{45}$$

Typical examples of $I_S(\varphi)$ functions are schematically shown in Fig. 4. In order to plot the whole curve it suffices to determine only one of its segments, say, the segment joining the points $\varphi = 0$ and $\varphi = \pi$, $I_S = 0$.

It is convenient to characterize the relationship $I_S(\varphi)$ in terms of two constants, namely, the critical current

$$I_C = \max[I_S(\varphi)] , \tag{46}$$

and a dimensionless parameter

$$l = I_C \left(\frac{dI_S}{d\varphi}\right)^{-1}_{\varphi=\pi} + 1 , \tag{47}$$

whose geometrical meaning is evident from Fig. 4. For a sinusoidal $I_S(\varphi)$, $l = 0$; in the case where the curve is inclined towards the right, l increases and becomes more than unity if the function $I_S(\varphi)$ becomes multivalued [Fig. 4(b)].

The quantity l has a simple physical meaning. A function $I_S(\varphi)$ of the type shown in Fig. 4(b) may roughly be described by the expressions

$$\varphi = \varphi_1 + \frac{2e}{\hbar c^2} I_S \mathcal{L}(I_S) , \quad I_S \approx I_C \sin\varphi_1 . \tag{48}$$

By virtue of the Josephson relation (4), Eq. (48) shows that a weak link may be represented in the form of series connection of a "classical" Josephson junction (i.e., junction with $I_S \propto \sin\varphi$) and a nonlinear inductance $\mathcal{L}(I_S)$. Inductance $\mathcal{L}$ is due not to the magnetic field of the current I_S (which is eliminated as we have taken $A = 0$), but to the kinetic energy of the superconducting condensate.

[16] Strictly speaking, only in the absence of a strong (see footnote 14) magnetic field produced by the current.

It is quite evident that this "kinetic" inductance (Sass and Stewart, 1968; Meservey and Tedrow, 1969; Likharev, 1971a) should be particularly great in a very long weak link ($\mathcal{L} \propto L$). Substituting Eq. (48) into Eq. (47), we get

$$\ell = \frac{2e}{\hbar c^2} I_C \mathcal{L}(0) . \tag{49}$$

Therefore ℓ has the meaning of kinetic inductance for a small current, normalized in the manner usual for Josephson junctions (see, for example, Likharev and Ulrich, 1978).

2. Usadel equations

Calculations of the stationary properties of weak links at arbitrary temperatures have become possible primarily because of some previous success in the general theory of superconductivity. Eilenberger (1968) has shown that the highly complicated general equations of stationary superconductivity (Gor'kov, 1958, 1959; see also Abricosov *et al.*, 1962) may be expressed in a fairly simple form. Usadel (1970) reduced the Eilenberger equations for the dirty limit ($\ell \ll \xi_0$) to even simpler equations for the complex functions F which only depend on the point (**r**) and the "Matsubara frequency"

$$\hbar\omega = \pi k_B T(2n+1) . \tag{50}$$

The Usadel equations for F may be expressed in a very simple form if another variable $G = (1 - FF^*)^{1/2}$ is used

$$2\omega F - D(\nabla - i\frac{2e}{\hbar c}\mathbf{A})\left[G\left(\nabla - i\frac{2e}{\hbar c}\mathbf{A}\right)F - F\nabla G\right] = 2\hbar^{-1}\Delta G . \tag{51}$$

All the measurable quantities are derived from the functions F by summing up with respect to ω, i.e., with respect to the integer n (Eq. 50). In particular, the expressions for the order parameter $\Delta(\mathbf{r})$ and the density $j_S(\mathbf{r})$ of the supercurrent are of the form

$$\ln(T_C/T) = \Delta\ln(T_C/T) = 2\pi k_B T \sum_{\omega>0}[(\Delta/\hbar\omega) - F], \tag{52}$$

$$\mathbf{j}_S = \sigma_N(2\pi k_B T/e)\sum_{\omega>0}\mathrm{Im}\left[F^*\left(\nabla - i\frac{2e}{\hbar c}\mathbf{A}\right)F\right] . \tag{53}$$

From these expressions it is clear that the use of the Usadel equations is only slightly more complicated (involves one more additional summation) than the use of GL equations (21). Thus, for example, for a uniform specimen with no current ($\nabla = \mathbf{A} = 0$), from (51) we get

$$\Delta = |\Delta|, \; F = \Delta/[(\hbar\omega)^2 + \Delta^2]^{1/2}, \tag{54}$$

and the self-consistency equation for Δ(52) takes the form:

$$2\pi k_B T \sum_{\omega>0}\left[\frac{1}{\hbar\omega} - \frac{1}{[(\hbar\omega)^2 + \Delta^2]^{1/2}}\right] = \ln\frac{T_C}{T} . \tag{55}$$

Its solution gives the well known function $\Delta(T)$ and the asymptotes (11) and (12), in particular.

For $T \approx T_C$, Eqs. (50) and (53) may be transformed into GL equations (21). In so doing, we must recall that $|F| \to 0$, $|\Delta| \to 0$, and $G \approx 1 - FF^*/2$ as $T \to T_C$. The space scale of Δ variations has become relatively large: $\nabla \sim \xi^{-1}(T) \ll (\hbar D/\omega)^{-1/2}$, and therefore the gradient term in (51) is small. Hence from Eq. (51) we get

$$\frac{\Delta}{\hbar\omega} - F \approx -\frac{\hbar D}{2(\hbar\omega)^2}\left(\nabla - i\frac{2e}{\hbar c}\mathbf{A}\right)^2\Delta + \frac{\Delta|\Delta|^2}{2(\hbar\omega)^3} . \tag{56}$$

After substituting this expression into Eqs. (52) and (53) and summing up with respect to ω:

$$\sum_{\omega>0}(\hbar\omega)^{-2} = \frac{\pi^2}{2(2\pi k_B T)^2}, \; \sum_{\omega>0}(\hbar\omega)^{-3} = \frac{7\zeta(3)}{(2\pi k_B T)^3}, \tag{57}$$

we obtain GL equations (21) with parameters $\xi(T)$ and C_j corresponding to the dirty limit.

3. Kulik-Omelyanchuk (KO-1) theory

If a weak link is sufficiently small, the gradient term alone can be retained in Eq. (51), as was assumed in the AL theory with GL equations. Kulik and Omelyanchuk (1975) have thus simplified it for the case of one-dimensional geometry [$F = F(x)$], but we shall find the solution for the arbitrary shape of a weak link. Let us introduce (following M. Yu. Kupriyanov) the function $\phi(r, \omega)$ in such a way that

$$F = \phi[(\hbar\omega)^2 + \phi\phi^*]^{-1/2}, \; G = \hbar\omega[(\hbar\omega)^2 + \phi\phi^*]^{-1/2} . \tag{58}$$

Equating the gradient term in (51) to zero means in terms of ϕ

$$\nabla(G^2\nabla\phi) = 0 . \tag{59}$$

According to Eqs. (54) and (58), the value of ϕ in the electrodes is equal to Δ. Therefore the boundary conditions for ϕ are the same as for Δ in the AL theory [Eqs. (30) and (31)].

Now we find by direct substitution that for $\Delta_1 = \Delta_2 = \Delta$ the solution of our problem is

$$\phi = \exp[(\chi_1 + \chi_2)/2]\left\{\Delta\cos\frac{\varphi}{2} + i\delta\tan\left[(1-2f)\arctan\frac{\Delta\sin(\varphi/2)}{\delta}\right]\right\}, \tag{60}$$

$$\delta^2 = \Delta^2\cos^2(\varphi/2) + (\hbar\omega)^2 ,$$

where f is the same as in the AL theory [Eq. (33)]. After calculating the current density $\mathbf{j}_S$ by Eq. (53), and then comparing it with the current density in the normal state (38), we obtain the expression for the current

$$I_S(\varphi)R_N = \frac{2\pi k_B T}{e}\sum_{\omega>0}\frac{2\Delta\cos(\varphi/2)}{\delta}\arctan\frac{\Delta\sin(\varphi/2)}{\delta} . \tag{61}$$

For $T \to T_C$, this function is reduced to Eq. (40) of the AL theory, i.e., $I_S(\varphi)$ is a sinusoidal function, while V_C depends linearly on $(T_C - T)$ (14). But at lower temperatures the function is somewhat distorted (Fig. 5). In particular, the derivative $(dI_S/d\varphi)_\pi$ tends logarithmically to infinity as $T \to 0$. The characteristic voltage in the KO – 1 theory depends on temperature as shown in Fig. 6, and attains its maximum as $T \to 0$

$$\max_T[eV_C] \approx 2.07\Delta(0), \; \max_T V_C[\mu V] \approx 316 T_C[K], \tag{62}$$

which is 32% greater than the maximum value of V_C for

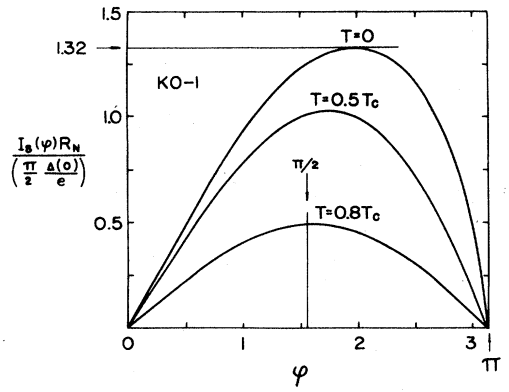

FIG. 5. $I_S(\varphi)$ relationship for a short dirty weak link ($l \ll L \ll (l\,\xi_0)^{1/2}$) according to the KO-1 theory at various temperatures. Because of the 2π-periodicity of the $I_S(\varphi)$ function it is shown only on the $[0, \pi]$ segment. Temperature dependence of critical current is shown in Fig. 6, and $l(T)$ is shown in Fig. 9(b) by the line labeled $L/\xi_N = 0$.

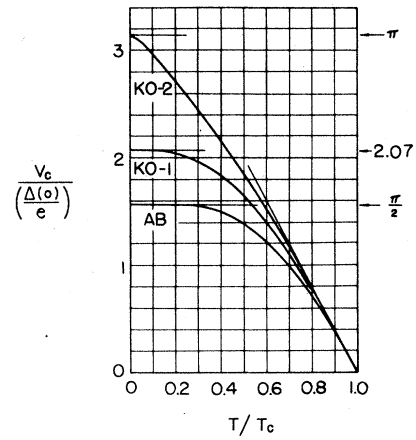

FIG. 6. Temperature dependences of critical current for different small weak links. (AB) tunnel theory (Ambegaokar and Baratoff, 1963); (KO-1) dirty case ($l \ll L \ll \xi$) (Kulik and Omelyanchuk, 1975); (KO-2) clean case ($L \ll l, \xi$) (Kulik and Omelyanchuk, 1977).

tunnel junctions [Eq. (13)].

The fact that even the simplest dc properties of small-size weak links differ from those of tunnel junctions clearly shows the significant distinction between these two structures. If the mean free path of electrons l is much shorter than the effective weak link length L_{eff}, as is assumed in the KO – 1 theory, then electrons are strongly scattered inside a weak link and are sensitive to the "field" (Δ) distribution inside the weak link. As a result, a self-consistent distribution of the order parameter[17] Δ is established inside the link. In the case of tunnel structures, however, scattering of the electrons inside the insulating layer is small, and it is impossible to introduce local values of the order parameter inside the layer. This is the difference in the conductivity mechanism that is responsible for the specific behavior of supercurrent at lower temperatures.

C. Effect of finite length

Now we shall examine the effects of increased length of the weak link, assuming that its cross section as before is negligibly small. For such an analysis we have to use a particular weak link model.

1. One-dimensional structure with electrodes in equilibrium (ODSEE) model

The simplest and the most natural model for the weak link is the "One-Dimensional Structure with Electrodes in Equilibrium" (ODSEE) model in which the following two conditions are assumed to be valid:

(i) The cross section S of a weak link is small ($\ll \lambda^2$) and constant in the direction of current flow throughout the length L of the structure. As a result, all the variables may be taken to be constants along the cross section, i.e., they are functions of the coordinate x in the current direction alone

$$f = f(x), \text{ at } 0 < x < L. \tag{63}$$

(ii) Nonlinear processes are localized over the length L, i.e., the modulus of the order parameter at the boundary of the weak link is equal to its equilibrium value in the electrodes ("banks")

$$|\Delta(0)| = \Delta_1, \ |\Delta(L)| = \Delta_2. \tag{64}$$

In other words, the effective link length L_{eff} is equal to its geometrical length L.

The first of these conditions, as can be seen from Fig. 1, is satisfied in all weak links except for Dayem bridges [Fig. 1(e)] and for structures with random geometry, say, point contacts and blob-type junctions.

As regards the second condition, we may note that it is a rather more stringent one. It is easier to satisfy this condition in structures with strong current concentration, say, in variable-thickness bridges [Fig. 1(f)]. In Sec. VI we shall show that for any material of the bridge and banks (electrodes) this condition holds true if the span film thickness is sufficiently small. In contrast, for the second condition to hold true in structures without current concentration [Fig. 1(b)–(d)], certain significant conditions must be satisfied with regard to the link and electrode materials. Roughly speaking, it is necessary that the normal conductivity σ_N of the link material be small compared to the normal conductivity of the electrodes (see Sec. VI. A). Therefore results derived within the framework of the ODSEE model have limited application for structures without strong current concentration.

The ODSEE model has, in fact, been applied in many theoretical works without specifically mentioning the conditions under which the model holds valid. This has led to a number of errors in the interpretation of experi-

[17] In the KO-1 theory the order parameter is equal to

$$\Delta(r) = \Delta \exp[i(\chi_1 + \chi_2)/2]\left\{\cos\frac{\varphi}{2} + i[1 - 2f(\mathbf{r})]\sin\frac{\varphi}{2}\right\},$$

only if the critical temperature T_C' of the weak link material is not very close to zero: $T_C'/T_C \gtrsim \xi_0 l/L^2$.

mental data, although the quantitative results obtained with the help of this model are valid, of course, for any weak link if $L_{\rm eff}$ is substituted for L.

2. Temperatures close to the critical temperature

We shall begin with a case for which the GL equations (21) are applicable (Likharev and Yakobson, 1975a). This naturally restricts us to a region in which the critical temperatures of both the weak link material (T_C') and the electrode material (T_C) are close to the physical temperature and, consequently, to each other

$$(T_C - T),\ |T_C' - T| \ll T. \tag{65}$$

The sign of $(T_C' - T)$ indicates whether the bridge material is superconducting (S', $T_C' > T$), or normal (N', $T_C' < T$). GL equations are applicable in both cases, and for the ODSEE model they can be simplified as follows

$$\psi'' + \psi(\pm 1 - |\psi|^2) = 0, \tag{66a}$$

$$J = \mathrm{Im}(\psi^* \psi'), \tag{66b}$$

where ψ is the order parameter normalized with respect to its characteristic value Δ_0 in the weak link, x is normalized to $\xi(T)$ (22), and the current is normalized to $I_0 A^{-2}$. Here I_0 is just the critical current which the weak link would have had at $L = \xi$ if the "classical" Josephson effect had taken place at this length (i.e., if the AL theory were valid)

$$I_0 = \frac{\pi}{4}\frac{\Delta^2}{k_B T e R_N}\frac{L}{\xi} = \frac{c\phi_0 S}{8\pi^2\lambda^2\xi}A^2, \quad R_N = \frac{L}{\sigma_N S}. \tag{67}$$

In $I_0 A^{-2}$ units the depairing current (Ginzburg, 1958; see also De Gennes, 1966) is equal to $2/3\sqrt{3} \approx 0.385$.

The parameter A is defined by the expression

$$A^2 = (T_C - T)/|T_C' - T| \tag{68}$$

and, according to Eq. (12), it represents the ratio of the equilibrium value of $|\Delta|$ at the electrodes to its characteristic value (Δ_0) in weak link material. If the materials are the same, then $A = 1$. Using this notation, the boundary conditions [Eq. (64)] can be written as follows (for $\Delta_1 = \Delta_2 = \Delta$)

$$\psi(0) = A\exp(i\chi_1), \quad \psi(L/\xi) = A\exp(i\chi_2). \tag{69}$$

The solution of Eq. (66) may be expressed in terms of special functions (Mamaladze and Cheishvili, 1966; Baratoff *et al.*, 1970; Christiansen *et al.*, 1971), but only by recourse to numerical methods may we determine the constants contained in these functions. It is therefore more convenient (especially for $T_C > T$) to solve these equations numerically, using the analytical expression available for the first integral. We shall cite the main results obtained from the work of Likharev and Yakobson (1975a).

If the weak link length L is sufficiently small

$$L \ll \xi,\ \xi/A, \tag{70}$$

the solution of Eq. (66) is close to solution (32) derived in the AL model. Since the function $f(\mathbf{r})$ for this geometry is $(1 - x/L)$, the AL solution takes the form

$$\psi_{\rm AL} = A[(1 - x/L)\exp(i\chi_1) + (x/L)\exp(i\chi_2)]. \tag{71}$$

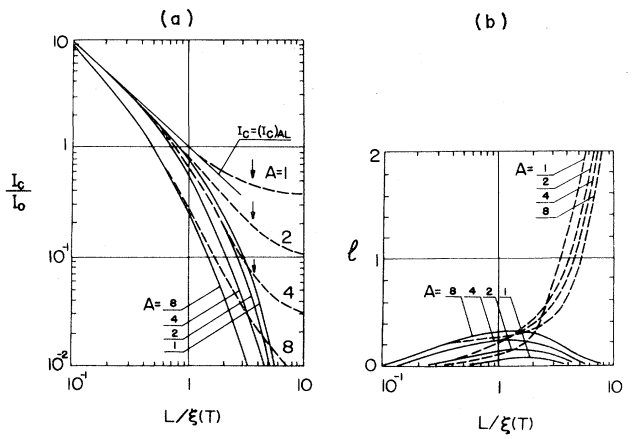

FIG. 7. Critical current (a) and parameter l (b) as a function of weak link length in the framework of the ODSEE model, as obtained from GL equations (Likharev and Yakobson, 1975a). Solid lines correspond to S-N'-S structures ($T > T_C'$), and dashed lines to S-S'-S structures ($T < T_C'$). Parameter A is determined by Eq. (68) and is equal to unity if the materials of the electrodes and weak link are the same. Thin line shows I_C, following from the AL theory.

Assuming Eq. (70), it is easy to find the first approximations in L for ψ and then for the current [signs are to be taken according to Eq. (21a)]

$$I_S = I_0\frac{\xi}{L}\left\{\left[1 \pm \frac{1}{6}\left(\frac{L}{\xi}\right)^2 - \frac{1}{10}\left(\frac{\mathrm{AL}}{\xi}\right)^2\right]\sin\varphi - \frac{1}{30}\left(\frac{L}{\xi}\right)^2\sin 2\varphi\right\}. \tag{72}$$

This equation clearly shows that the corrections for Eq. (40), which describes the "classical" Josephson effect, are small even when L is of the order of ξ or ξ/A. Since the normal resistance of a weak link R_N is proportional to its length L, the characteristic voltage V_C in the region defined by Eq. (70) is approximately constant and is equal to Eq. (14). A further increase in the link length will give rise to effects radically different in S-N'-S and S-S'-S structures. The variations in the critical current I_C and in the factor ℓ with changing length are shown in Fig. 7 by solid lines ($T > T_C'$) and dashed lines ($T < T_C'$), respectively.

For $T > T_C'$ (S-N'-S structure) an increase in L above a few ξ entails a drop in the critical current, the function $I_S(\varphi)$ remaining almost sinusoidal ($\ell \approx 0$). For $L \gg \xi$ from Eq. (66) we readily obtain the following analytical expression

$$I_S = I_0 8[1 + (1 + A^2/2)^{1/2}]^{-2}\exp(-L/\xi)\sin\varphi. \tag{73}$$

This drop results from the fact that in the proximity effect the order parameter in a normal substance decreases exponentially with the distance from its interface with the superconductor. Exponential decrease in the critical current as $L/\xi \to \infty$ is typical of S-N-S structures (see De Gennes, 1966; Aslamazov *et al.*, 1968; Clarke, 1969), but the exact value of the factor before the exponent depends significantly on the boundary conditions.

If $T < T_C'$, we are dealing with a weak link of the

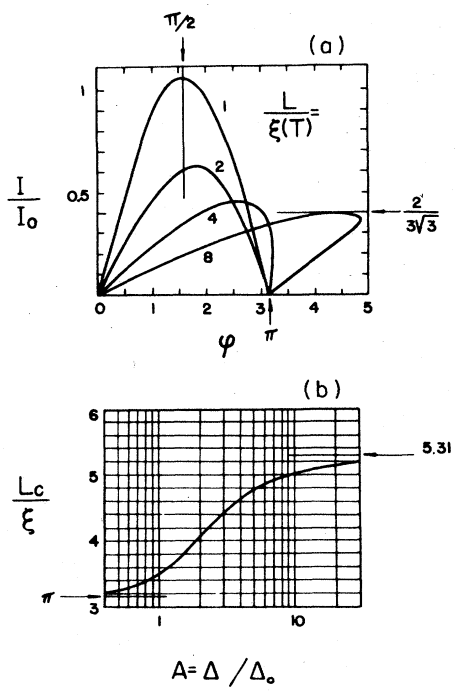

FIG. 8. The deformation of the $I_S(\varphi)$ relationship as the S-S'-S weak link length increases. This deformation shows the transition from the "ideal" Josephson effect to the depairing effect (a). It happens at the length $L = L_C$, when the $I_S(\varphi)$ relationship becomes multivalent. L_C is of the order of the coherence length of weak link material $\xi(T)$ for any A; $L \approx 3.49\,\xi(T)$ at $A = 1$. After Likharev *et al.*, 1974; Likharev and Yakobson, 1975a.

S-S'-S type. For this structure, with increasing weak link length the critical current at first diminishes, then when $L \gtrsim 10\xi$ it tends to a constant value. Here radical changes take place in the shape of the $I_S(\varphi)$ function, as shown in Fig. 8. The parameter of kinetic inductance ℓ grows with increasing length L, and for a critical length L_C it becomes greater than unity, i.e., the function $I_S(\varphi)$ becomes multivalued [see Fig. 4(b)].

For long lengths ($L \ll \xi$), the shape of this function is similar to that of a cubic parabola

$$I_S = \frac{I_0}{A^2}\left\{\frac{\varphi}{(L/\xi)} - \left[\frac{\varphi}{(L/\xi)}\right]^3\right\}, \tag{74}$$

and the critical current is almost constant

$$I_C = \frac{2}{3\sqrt{3}} I_0 A^{-2}. \tag{75}$$

This means that here we are dealing with the well known depairing effect due to diminution in the equilibrium number of Cooper pairs (i.e., $|\Delta|^2$), with the current growth taking place uniformly throughout the entire length of the weak link.[18] The unstable reverse branch of the $I_S(\varphi)$ function joining the point $I_S = I_C$ to the point $I_S = 0$, $\varphi = \pi$ corresponds to the sharp drop of $|\Delta|$ in the middle of the weak link, i.e., to the nucleation of the "phase-slip center" of a length $\sim\xi(T)$. In long weak links with small cross-section inhomogeneities the location of this center will be determined primarily by the narrowest part of the structure.

In this way, with an increase in the length of a superconducting weak link (superconducting "filament" or "channel"), the Josephson effect becomes the depairing effect. It is the length $L = L_C$, where $I_S(\varphi)$ becomes multivalued, that may be assumed as the cutoff point of the transformation. In the succeeding pages we shall show that this critical length is, indeed, highly significant for the processes taking place in the weak link. Its dependence on the parameter A is shown in Fig. 8(b), from which it is clear that L_C is always of the order of several coherence lengths of the weak link material.

Before we proceed further, we shall make one important remark. If the temperature tends to the critical temperature of the weak link, then, according to Eq. (22), $\xi \to \infty$ for any length $L/\xi \to 0$, and as may be imagined from Fig. 7(a), the "classical" Josephson effect should be observed. However, when $T \approx T_C'$, A tends to infinity as $(T_C' - T)^{-1/2}$ [Eq. (68)], and it can easily be verified that the critical current does not exhibit any singularity. This corresponds to the fact that, for $T \approx T_C'$, it is the condition $L \lesssim \xi/A$ that limits the validity of the AL theory. From Eqs. (22) and (68), it is obvious that ξ/A is the coherence length of the weak link material formally taken at a temperature equal to $T - (T_C - T_C')$.

3. *S-N-S* structure at arbitrary temperatures

Likharev (1976) has evaluated the effect of the length on the function $I_S(\varphi)$ at arbitrary temperatures for a particularly important case where the weak link is made of "ideal" normal material, having a critical temperature $T_C' = 0$ (S-N-S structure). According to Eq. (50) here $|\Delta| = 0$ for $0 < x < L$, so we are dealing with gapless superconductivity (De Gennes, 1966). The right-hand side of the Usadel equation (51) vanishes, making it possible to find analytically the first integral of this equation, and to solve the problem numerically within the framework of the ODSEE model in a relatively simple manner.

Figure 9 shows the results of such a calculation. The link length has been normalized with respect to the coherence length of the weak link material that naturally follows from Eq. (51)

$$\xi_N(T) = \left(\frac{\hbar D}{2\pi k_B T}\right)^{1/2} \approx 0.58\left(\frac{\hbar v_F}{2\pi k_B T}\,\ell\right)^{1/2}, \tag{76}$$

taken again at a temperature equal to the critical temperature of the banks.

The plots for $L/\xi_N = 0$ show the results of the KO – 1 theory. From Fig. 9(a), it is evident that this theory is satisfactory for lengths[19] $L \lesssim \xi_N(T_C)$. When the bridge length is increased, the critical current decreases—exponentially at $T \approx T_C$

[18] Note that the Josephson supercurrent in weak links may be much greater than the depairing current (Fig. 7).

[19] But not for $L_{\text{eff}} < \xi_N(T)$, as was stated in the original KO-1 paper.

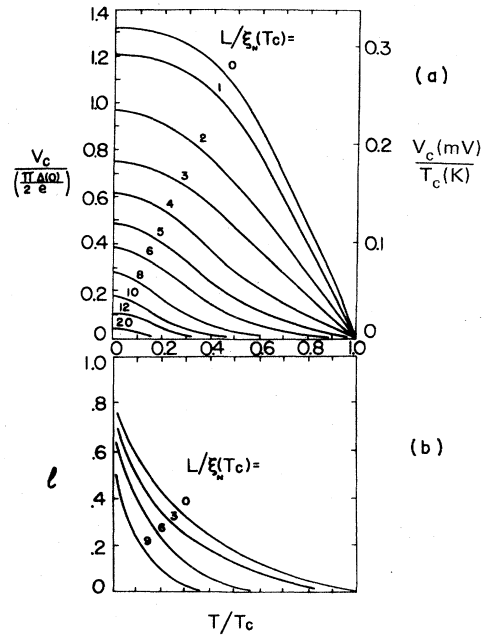

FIG. 9. Temperature dependences of critical current (a) and kinetic inductance parameter l (b) for an S-N-S structure, with zero critical temperature for the weak link material ($T_C'=0$). Plots are calculated from Usadel equations [(51) and (53)] within the framework of the ODSEE model. $\xi_N(T_C)$ is the decay length of weak link material, if taken at the critical temperature of the electrodes. After Likharev, 1976.

$$I_S R_N = \frac{\pi\Delta^2}{4ek_BT}\sum_{n\geq 0}\frac{8}{\pi^2(2n+1)^2}\frac{\ell_n}{\sinh\ell_n}\sin\varphi\,,$$

$$\ell_n=(2n+1)^{1/2}\frac{L}{\xi_N(T)}\,,$$

$$I_S R_N \to \frac{4}{\pi}\frac{\Delta^2}{ek_BT}(L/\xi_N)\exp(-L/\xi_N)\sin\varphi,\ \text{at } L/\xi_N\to\infty\,,$$

and more slowly at $T\to 0$

$$I_C R_N \propto L^{-2},\ \text{at } \xi_N(T_C)\ll L\ll\xi_N(T)\,. \tag{78}$$

As is obvious from Fig. 9(b), the function $I_S(\varphi)$ is always single-valued ($\ell<1$) and is significantly nonsinusoidal only at very low temperatures.

4. Dependence of $I_S(\varphi)$ on length-discussion

Let us use the term *"ideal Josephson effect"* for the case where the $I_S(\varphi)$ relationship is single-valued and V_C is comparable with its value in the tunnel junction (10). As we could see, in "dirty" weak links the "ideal" Josephson effect is conserved up to a certain characteristic length of the weak link. With the help of the calculations carried out for $T_C'\approx T$ and $T_C'=0$, the condition for such an "ideal" effect may be formulated generally as follows

$$L\lesssim(2-4)\min[\xi(T),\xi(T_C)]\,, \tag{79}$$

where ξ is the coherence length of the weak link material. This relationship shows that this material merely fulfills certain "transport" functions, thereby aiding the transfer of the wave functions of the superconducting condensate of the electrodes deep inside the weak link where their interference—Josephson effect—occurs. The parameter ξ characterizing these transport properties is affected by velocity on the Fermi surface v_F of the material alone, under a fixed ℓ. v_F is almost the same for the majority of the known conducting metals, both superconductors and normal materials.

Therefore, for the Josephson effect to be observed in a certain weak link, the link material need not necessarily possess any special "superconducting" properties in the sense of having a finite critical temperature T_C'. Superconducting properties should be exhibited only by the electrode material, because $|\Delta|$ at the boundaries of the weak link is proportional to T_C, and an increase in this parameter entails an increase in V_C.

D. Clean structures

Now we shall briefly examine the properties of "clean" weak links in which the mean free path of electrons ℓ is greater than or comparable with the length L of the weak link. Such a relationship is more often encountered in microshorts of point contacts than in bridge-type structures, i.e., in those cases where the exact shape of the weak link is unknown. We shall, therefore, start our discussion with the most important case of a sufficiently small weak link ($L_{\text{eff}}\ll\ell,\xi_0$) of arbitrary shape. Recently Kulik and Omelyanchuk (1977) advanced a theory, referred to as KO-2, to describe the Josephson effect in such structures.

1. Eilenberger equations

The GL equations or the Usadel equations can no longer be used here, and thus we need to employ more general Eilenberger equations (1968). These equations have been derived for complex functions f and g, each of which depends not only on the point ($\mathbf{r}$) and the Matsubara frequency ω, but also on the spatial direction which is formally represented by a vector $\mathbf{v}_F$. These functions are interrelated by the equality

$$f^\dagger f+g^2=1\,, \tag{80}$$

where, for the sake of convenience, a new function $f^\dagger$ is introduced, defined by the following expression

$$f^\dagger(\mathbf{r},\mathbf{v}_F,\omega)=f^*(\mathbf{r},-\mathbf{v}_F,\omega)\,. \tag{81}$$

The Eilenberger equation for f looks quite simple

$$\left[2\omega+\mathbf{v}_F\left(\nabla-i\frac{2e}{\hbar c}\right)\mathbf{A}\right]f=2\hbar^{-1}\Delta g+\tau^{-1}(g\langle f\rangle-f\langle g\rangle)\,, \tag{82}$$

where the order parameter Δ depends only on $\mathbf{r}$, the angular brackets stand for averaging over all the directions of the vector $\mathbf{v}_F$, and $\tau=\ell/v_F$ is the time of the electron mean free path. For the system of equations to be closed, Eqs. (80)–(82) have to be supplemented with a self-consistency equation for $\Delta(\mathbf{r})$

$$\Delta\ln\frac{T_C}{T}=2\pi k_BT\sum_{\omega>0}\left(\frac{\Delta}{\hbar\omega}-\langle f\rangle\right) \tag{83}$$

and an equation for the supercurrent (in principle, joint-

ly with the Maxwell equations)

$$\mathbf{j}_S = -i2eN(0)2\pi k_B T \sum_{\omega>0} \langle \mathbf{v}_F g \rangle . \tag{84}$$

The system of Eqs. (80)–(84) is valid for any relationship between ξ_0 and ℓ. In the "dirty limit," f, g, and Δ vary only at distances $\sim \xi \approx (\ell\xi_0)^{1/2} \gg \ell$, and in addition are almost isotropic. In this situation the Eilenberger equations are satisfied by a solution of the following type:

$$f(\mathbf{r}, \mathbf{v}_F, \omega) = F(\mathbf{r}, \omega) + \mathbf{v}_F\left(\nabla - i\frac{2e}{\hbar c}\mathbf{A}\right)F_1(\mathbf{r}, \omega) , \tag{85}$$

in which the second term is small. Direct substitution of Eq. (85) into Eqs. (80)–(84) gives the Usadel equations (51)–(53).

For a uniform superconductor carrying no current ($\nabla = \mathbf{A} = 0$), at any ratio between ℓ and ξ_0, we obtain Eqs. (54) and (55) for F and Δ, respectively, which give the usual results of the BCS theory.

2. Weak links of small dimensions

In this case we may examine two regions separately: parts of the electrodes of size $r \sim \xi_0 \ell$, surrounding the weak link, and a region of size $r \sim L_{\text{eff}}$ around the weak link. As will be shown below, in the electrodes the quantities Δ, $\langle f \rangle$, and $\langle g \rangle$ may be taken to be constant and equal to their equilibrium values

$$\begin{aligned} &\langle f \rangle = \langle f^+ \rangle^* = (\Delta/E)\exp(i\chi_{1,2}), \quad \langle g \rangle = \hbar\omega/E , \\ &\Delta = \Delta_{1,2}\exp(i\chi_{1,2}), \quad E^2 = (\hbar\omega)^2 + \Delta^2 , \end{aligned} \tag{86}$$

as they vary only over distances $\sim L_{\text{eff}}$. So Eq. (82) for f and the equations for f^+ and g derived from Eqs. (80)–(82) form a linear system (just as in Sec. II. A and B, we assume that $L_{\text{eff}} \ll \lambda$ and therefore $\mathbf{A} = 0$)

$$\begin{aligned} &(2\hbar\omega + \hbar\tau^{-1}\langle g \rangle + \hbar v_F \partial/\partial s) f - \tilde{\Delta} g = 0 , \\ &(2\hbar\omega + \hbar\tau^{-1}\langle g \rangle - \hbar v_F \partial/\partial s) f^+ - \tilde{\Delta} g^* = 0 , \\ &\tilde{\Delta}^* f - \tilde{\Delta} f^+ - (\hbar v_F \partial/\partial s) g = 0 , \\ &2\tilde{\Delta} = 2\Delta + \hbar\tau^{-1}\langle f \rangle , \end{aligned} \tag{87}$$

where s is the coordinate along the "trajectory," i.e., a line in the direction of $\mathbf{v}_F$. The solution to this system is easily found

$$f = \sum_\kappa f_\kappa e^{\kappa s} , \quad g = \sum_\kappa g_\kappa e^{\kappa s} , \tag{88}$$

where for κ we have three values:

$$\kappa = \kappa_0, \pm\kappa_1 , \quad \kappa_0 = 0, \kappa_1 = (E + \hbar\tau^{-1}/2)/\hbar v_F . \tag{89}$$

This solution describes the relaxation of f and g towards their equilibrium values [Eq. (86)] at distances $\sim \min(\xi_0, \ell) \gg L_{\text{eff}}$. Along a trajectory, f_κ and g_κ are constants, but these constants vary on different trajectories. For the trajectories which do not pass through the weak link (Fig. 10) we may take f and g to be constants, i.e., only the terms with $\kappa = 0$ are to be included in the sum [Eq. (88)]. Then it follows directly from Eqs. (87) that on these trajectories f and g are equal to their equilibrium values [Eq. (86)].

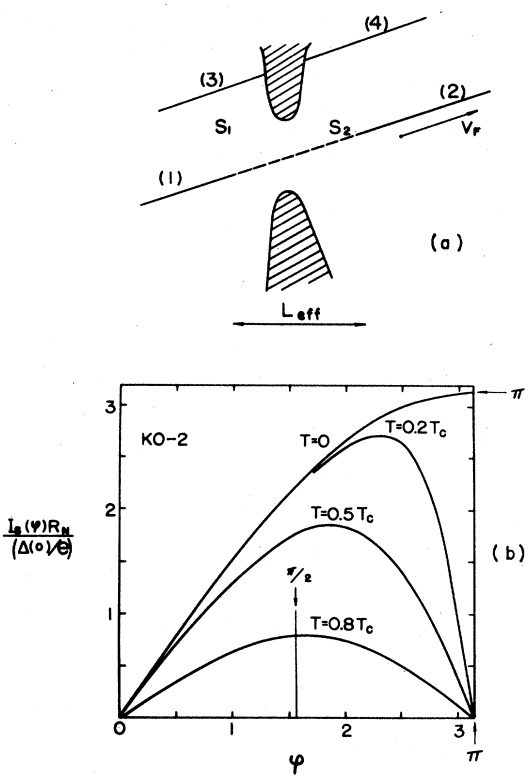

FIG. 10. The KO-2 theory for clean small weak links ($L_{\text{eff}} \ll l, \xi_0$). (a) Two types of electron trajectories in the weak link region: (1) "incoming" part of through trajectory; (2) "outgoing" part of this trajectory; (3) and (4) nonthrough trajectories. (b) Current-phase relationship for different temperatures. Temperature dependence of critical current is shown in Fig. 6.

Along those trajectories passing through the weak link, f and g cannot be constant, since for $\chi_1 \neq \chi_2$ the values of f in the electrodes are different. Since f and g are finite as $s \to \pm\infty$, therefore for the "outgoing" part of a through trajectory we have

$$f_o = \langle f \rangle + \tilde{f}_o \exp(-\kappa_1 s) , \quad g_o = \langle g \rangle + \tilde{g}_o \exp(-\kappa_1 s) , \tag{90}$$

and for the "incoming" part of this trajectory

$$f_i = \langle f \rangle^* + \tilde{f}_i \exp(+\kappa_1 s) , \quad g_i = \langle g \rangle + \tilde{g}_i \exp(+\kappa_1 s) . \tag{91}$$

What remains now is to find $\tilde{f}$ and $\tilde{g}$. For this purpose first we have to substitute Eqs. (90) and (91) into Eqs. (87), and thus derive a relationship between $\tilde{f}$ and $\tilde{g}$:

$$f_o = g_o \frac{2\Delta + \hbar\tau^{-1}\langle f \rangle}{2\hbar\omega - \hbar\tau^{-1}\langle g \rangle - \hbar v_F \kappa_1} ; \tag{92}$$

for f_i and g_i the sign of the term containing κ_1 has to be reversed. Then, we consider a region of size $\sim L_{\text{eff}}$. In this region the main term in Eq. (82) is the gradient one, because it alone is of the order of v_F/L_{eff}, while the remaining terms are $\sim v_F/\xi_0$ or v_F/ℓ ($f, g \sim 1$). Thus we obtain a simple equation:

$$\mathbf{v}_F \nabla f = 0 , \tag{93}$$

which shows that f (and consequently g) remains con-

stant on a trajectory at a distance of the order of $L_{\rm eff}$. Hence in Eqs. (90) and (91) the values of f and g in the weak link region ($s=0$) may be regarded as being the same, both on the incoming and on the outgoing parts of the trajectory. This gives

$$\langle f\rangle+\tilde{f}_o=\langle f\rangle^*+\tilde{f}_i,\ \tilde{g}_o=\tilde{g}_i\,. \tag{94}$$

From Eqs. (92) and (94) we get, taking $\chi_1=-\chi_2=-\varphi/2$

$$\tilde{g}=i\sin\frac{\varphi}{2}\,\frac{\Delta^2}{E\,[E\cos(\varphi/2)+i\hbar\omega\sin(\varphi/2)]}\,. \tag{95}$$

Now substituting this value into Eq. (84), and using the expression for the resistance of a structure in the normal state (Omelyanchuk *et al.*, 1977),

$$R_N^{-1}=e^2v_F N(0)S\,, \tag{96}$$

we finally obtain the result

$$I_SR_N=\frac{\pi\Delta}{e}\sin(\varphi/2)\tanh\frac{\Delta\cos(\varphi/2)}{2k_BT}\,, \tag{97}$$

which does not depend on the ratio between ℓ and ξ_0.

It now only remains for us to verify the validity of our initial assumption that $\langle f\rangle$ and $\langle g\rangle$ are constants in the region $r\gg L_{\rm eff}$. For averaging we have to take for f and g the equilibrium values [Eq. (86)] on nonthrough trajectories, and perturbed values [Eqs. (90) and (91)] on the through trajectories. The number of the latter trajectories in the region under consideration is small, as a weak link is "observed" within the small solid angle $\Omega(r)\ll 4\pi$. The values of $\langle f\rangle$ and $\langle g\rangle$ (and consequently the value of Δ, too) therefore differ from the equilibrium values only by a quantity of the order of $\Omega/4\pi\ll 1$. Thus $\langle f\rangle$, $\langle g\rangle$, and Δ vary greatly only in the immediate neighborhood of a weak link ($r\sim L_{\rm eff}$) where $\Omega\sim 2\pi$.

3. Discussion

Figure 10(b) shows the phase dependence of the supercurrent, defined by Eq. (97), while the KO-2 curve in Fig. 6 shows the dependence $V_C(T)$. The $I_S(\varphi)$ relationship is sinusoidal for $T\approx T_C$ and V_C is again defined by Eq. (14), but at lower temperatures the results are quite different from those predicted by the tunnel theory or the KO-1 theory either. For $T=0$, the current-phase relationship is highly nonsinusoidal, and suffers jumps at $\varphi=\pi+2\pi n$, while V_C is twice the value given by the tunnel theory

$$\max_T[eV_C]=\pi\Delta(0),\ \max_T[V_C]\,[\mu V]\approx 480T_C[K]\,. \tag{98}$$

Such a marked discrepancy shows an essential distinction in the physics of the processes in these three types of Josephson structures. In order to discover the causes of this discrepancy, we shall analyze the structure of the Eilenberger functions f for these three cases. For "clean" weak links, f has just been calculated and is expressed by Eqs. (86) and (90). For "dirty" links the form of $f\approx F$ is given by Eqs. (58) and (60). Therefore it remains to describe the tunnel junction in the same terms.

This is easily done by adding a small perturbation due to tunneling from the other electrode to the equilibrium functions of each electrode [Eq. (86)]

$$f_{1,2}=(\Delta/E)\exp(i\chi_{1,2})+T_p(\Delta\hbar\omega/E^2)\exp(i\chi_{2,1})\,, \tag{99}$$

where the probability T_p of electron tunneling depends on the direction of momentum $\mathbf{p}_F$. Substituting Eq. (99) into the definition of g [Eq. (80)], we obtain

$$g=(\hbar\omega/E)+iT_p(\Delta^2/E^2)\sin\varphi\,, \tag{100}$$

and by virtue of the relationship between T_p and R_N,

$$R_N^{-1}=j_NS/V=(2eN(0)/V)\,|\langle\mathbf{v}_FT_p\,\mathrm{sign}(\mathbf{v}_F)_x\rangle|S\,, \tag{101}$$

we arrive at the result derived by Ambegaokar and Baratoff [Eqs. (9), and (10)]. Equation (99) shows that the results of the tunnel theory are only valid when a clean "mixture" (i.e., interference) of states induced by neighboring electrodes exists at all distances ($\sim\ell,\xi_0$) significant in the superconductivity theory. This will be so, of course, not only for the case of tunnel junctions.

For instance, as demonstrated by Zorin and Likharev (1978a), if two electrodes are separated by a thin opaque barrier with a large number of minute ports ($p_FL_{\rm eff}/\hbar\ll 1$), the wave functions of such a structure *in toto* coincide with the functions of a tunnel junction. For this type of weak link, therefore, all the results predicted in the tunnel theory are applicable (nonetheless, the relative capacitance of these structures may, as in other types of weak links, be much less than that of tunnel junctions: $\beta\lesssim 1$).

For "dirty" weak links the functions f are almost isotropic (Usadel approximation), but they change considerably in space at distances $L_{\rm eff}$ greater than ℓ. This is precisely the cause of the difference in the results obtained within the framework of the KO-1 and tunnel theories. Finally, the functions f for a "clean" weak link change strongly both in the coordinate space (at distances $\sim\ell,\xi_0\gg L_{\rm eff}$) and in the momentum space (a significant difference between transparent and nontransparent trajectories). A still more essential distinction between the results of KO-2 and tunnel theories is associated with this.

Thus there is a noticeable difference in the stationary properties of weak links, even among those which are short compared to $\xi(T)$.

4. Pure one-dimensional structures

Of course, how "clean" weak links behave when their length is increased is a question of considerable interest. So far, this feature has only been studied for one-dimensional $S-N-S$ structures, i.e., in the case where a weak link material has zero critical temperature. Moreover, in these calculations, it was assumed that the condition

$$L\gg\min[\xi_0,(\xi_0\ell)^{1/2}]\,, \tag{102}$$

is satisfied, and was thus possible to disregard the proximity effect throughout a major part of the structure, and to assume that (Kulik, 1969b)

$$\Delta=0,\ 0\leq x\leq L\,. \tag{103}$$

In such a model the $I_S(\varphi)$ relationships for $T=0$ (Ishii, 1970, 1972) and for $T\neq 0$ (Svidzinskii *et al.*, 1971, 1973; Bardeen and Johnson, 1972; see also the introduction to

the paper by Bezuglyi *et al.*, 1975) have been calculated for $\ell = \infty$. The influence of a finite mean free path ($\ell \sim L$) has been treated by Kulik and Mitzai (1975).[20]

Here we shall not examine the results reported in these papers. The reason is that the equations derived by Kulik and Mitzai (1975) cannot be converted at $l \ll \xi_0$, L into the results following from the Usadel equations, [into Eq. (78), in particular], which hold true in this case. The author of this review feels that in the analysis of clean $S-N-S$ structures some error has probably crept into the determination of boundary conditions. Fortunately, there is a method by which we can clarify this situation: that is to make an analysis of such $S-N-S$ structures using the Eilenberger equations, where the boundary conditions are quite clear, rather than the complex formalism of the above papers.

E. $I_S(\varphi)$ relationship and Josephson effect

So far in the preceding pages we have assumed that the cross section of a weak link is so small that the current self-shielding (i.e., actually the Meissner effect) may be disregarded. This condition may be formulated in the form of a constraint on the maximum transverse dimension of the weak link cross section, i.e., the

$$W \ll \lambda_{\text{eff}} , \tag{104}$$

where λ_{eff} denotes some characteristic size of the self-shielding region (magnetic field penetration). As we shall see in Sec. VII, it depends substantially on both the density of the critical current in the weak link, and the geometry of the structure, and is usually much larger than L. But, even for very small widths ($W \sim \xi$), the uniform flow of the condensate, i.e., the uniform distribution of variables over the weak link cross section, may prove to be unstable with respect to the formation of vortex lines carrying one or several magnetic flux quanta (Abricosov, 1957; see also De Gennes, 1966).

1. Abricosov vortices

In a superconducting specimen of sizes far greater than ξ and λ, every Abricosov vortex is an axial symmetric formation. The order parameter is zero on the vortex axis and tends to its equilibrium value at a distance of $\sim\xi$ from the axis, thereby forming a normal "core" of the vortex. A persistent ring supercurrent flows around the core at distances of about λ. The magnetic field of total flux ϕ_0 (or $n\phi_0$) directed along the vortex axis is screened by this current from the remaining portion of the superconductor. The electromagnetic region of the vortex readily suffers deformation, and this is just what happens when the vortices are of high density in a strong magnetic field or when the vortices penetrate to a specimen of small size ($\ll\lambda$).

The vortices may penetrate into a superconducting specimen only from the side of the boundary with vacuum (insulator),[21] under the influence of either an external magnetic field or a current flowing through the specimen itself. These two cases differ essentially in the behavior of the vortices after penetration into the speciman. In both cases a Lorentz force of linear density

$$\mathbf{f} = \frac{\phi_0}{c}[\mathbf{n}\times\mathbf{j}] \tag{105}$$

acts on the core of each vortex, where $\mathbf{n}$ is the direction of the vortex axis. A contribution to the current density $\mathbf{j}$ is made by all the currents on the vortex axis, including the circulating currents of other vortices.

If the vortices are generated under the action of an external magnetic field, the force [Eq. (105)] is directed from all the boundaries towards the center of the specimen, and a steady distribution of the vortices (static mixed state) is established in the specimen. On the other hand, if the vortices are created by the current in the specimen itself, the Lorentz force pushes the vortices in a direction normal to the current, i.e., along the cross section, and tends to establish a continuous flow of additional vortices across the conductor (dynamic mixed state), the dc voltage drop in this case being nonzero.

An analysis of conditions for vortex formation in samples of constant cross section, thin film strips for example (Likharev, 1971a, b), and considerable body of experimental data show that even when $W \ll \lambda_{\text{eff}}$, the critical current I_{C1} for vortex penetration may be small (much lower than the depairing current). Moreover, I_{C1} may essentially depend on small-scale ($\sim\xi$) inhomogeneities at the point where the vortex penetrates into the specimen, a fact which makes I_{C1} almost irreproducible in experiments.

It is, therefore, quite likely that the calculations of critical currents I_C in weak links may prove to be inadequate, because the vortex motion across the weak links can start at much lower currents. Fortunately, this does not occur in the most interesting case of very short weak links: the reason is that *Abricosov vortices simply cannot exist in such structures.*

2. Abricosov vortices in weak links

Following Likharev (1975b), we consider a solitary vortex which has penetrated into a weak link, within the framework of the ODSEE model in which a weak link is regarded as a span between two unperturbed bulk electrodes. Since the energy of a vortex is proportional to its length, its axis is always normal to the maximum size of the cross section, say for example, to the plane of the thin film bridge. In addition, the vortex experiences strong repulstion from the bulk superconducting banks (Likharev, 1971d). Therefore its axis is located in the middle between the electrodes (Fig. 11).

We shall carry out an analysis within the framework of the GL equations (21), and it is now necessary to assume that Δ and $\mathbf{j}_S$ may depend both on x and y (Fig. 11).

[20] The specific influence of an external magnetic field on such structures (at $l = \infty$) has been considered by Antsygina *et al.* (1975). Bezuglyi *et al.* (1975) have examined such structures with low transparency of the S–N boundary.

[21] Another possible process is the formation of a pair of antipolar vortices at the internal points of the specimen under the influence of current. This process is energetically less advantageous.

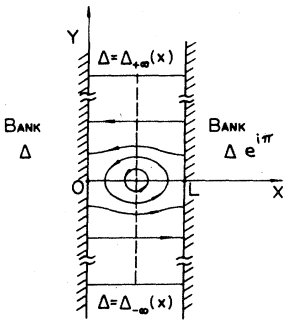

FIG. 11. Abricosov vortex inside a weak link at $L > L_C (l > 1)$. Thin lines show (schematically) the lines of supercurrent which circulate around the vortex axis. Phase difference of the banks is equal to π.

Representing Δ in Cartesian form as

$$\Delta = R(x, y) + I(x, y), \tag{106}$$

from Eq. (21a) we obtain the following equations for real R and I

$$\xi^2 \nabla^2 R + [\pm 1 - (R^2 + I^2)/\Delta_0^2] R = 0, \tag{107a}$$

$$\xi^2 \nabla^2 I + [\pm 1 - (R^2 + I^2)/\Delta_0^2] I = 0. \tag{107b}$$

As a rule, these equations do not easily yield to solution, but the ODSEE model offers a means of making a complete analysis, as the boundary conditions for Δ are very simple [Eq. (64)]. Since the phases in the electrodes can only change at distances $\sim \lambda_{\text{eff}}$ (see Sec. VII), under the condition (104), they are constant for each electrode. Moreover, as χ is always determined up to a constant, take $\chi_1 = 0$; hence on the first bank ($x = 0$) we have

$$R(0, y) = \Delta, \quad I(0, y) = 0. \tag{108}$$

When we pass round the vortex by angle π, the phase of the order parameter likewise should change by π, therefore the phase at the second bank is π, and

$$R(L, y) = -\Delta, \quad I(L, y) = 0. \tag{109}$$

In order to derive the boundary conditions on the lateral sides of the weak link, let us first consider the case where $W \gg L$. Thus, far from the vortex center (which we take as the origin of the transverse coordinate y) Δ should tend to a uniform solution

$$R(x, \pm\infty) = R_{\pm\infty}(x), \tag{110a}$$

$$I(x, \pm\infty) = I_{\pm\infty}(x), \tag{110b}$$

which is just the same as the one we derived earlier (Sec. IV.C). Now we shall analyze the solutions of the problem [Eqs. (107)–(110)].

3. "Explosion" of core

If the function $I_S(\varphi)$ is multivalued ($l > 1$), several (at least, three) values of I_S and consequently the same number of uniform solutions $\Delta(x)$ (Fig. 4) correspond to the value $\varphi = \pi$, which we now require. The current on the two different sides of the vortex flows in opposite directions and therefore the solutions giving different signs to $I_S(\varphi)$ have to be taken as $y \to \pm\infty$. As is clear from Fig. 3, a nonzero value of I corresponds to a nonzero current:

$$I_{+\infty} = -I_{-\infty} \neq 0, \text{ at } l > 1. \tag{111}$$

In this case the solution of the system of equations (107) describes the core of an Abricosov vortex of a shape close to that of an ordinary axial-symmetric vortex, the only difference being that the current distribution around the core is distorted by the banks (Fig. 11). These distortions may be treated as the positive mirror images of the vortex at the banks (Likharev, 1971d). The core suffers slight distortion on decreasing L, becoming somewhat flattened along the x direction as it is stretched out in the y direction.

The situation is radically different when L is less than $L_C (l < 1)$. The one-dimensional problem for this case has only one solution with $\varphi = \pi$, which, according to Fig. 4(c), has $I_S = 0$; consequently $\chi = \text{const}$ and

$$I_{+\infty} = I_{-\infty} = 0, \text{ at } l < 1. \tag{112}$$

Thus the differential equation for I(107b) has zero boundary conditions [Eqs. (108)–(110), (112)] at all boundaries and only a trivial solution in the whole domain

$$I(x, y) = 0, \quad \Delta(x, y) = \Delta_{\pm\infty}(x) = R_{\pm\infty}(x), \tag{113}$$

which gives rise to a zero current density in the whole bulk of the weak link

$$\mathbf{j}_S(x, y) = 0. \tag{114}$$

Thus, when $l < 1$, the vortex core ceases to exist. The numerical solution of the system (107) shows that noticeable deformation of the core (expansion along the y axis) begins only for values of L several percent higher than L_C; consequently, the *vortex core literally suffers an "explosion"* when the link length becomes equal to the critical length.

Where does the vortex disappear to at the time of explosion? To answer this question we have to consider a weak link of sufficient width ($W \gtrsim \lambda_{\text{eff}}$) so that an electromagnetic region of the vortex may be embedded inside the link. If an Abricosov vortex exists in a weak link, the circulating current [say, $(j_S)_x(L/2, y)$] builds up when $0 \lesssim y \lesssim L$, and then gradually decays in the region $L \lesssim y \lesssim \lambda_{\text{eff}}$. After the explosion of the core, the current will grow at distances $0 \lesssim y \lesssim \lambda_{\text{eff}}$, and with a further increase in y will diminish at distances of the same order. This structure is the well known Josephson vortex with only one characteristic dimension $\lambda_{\text{eff}} \gg L$ (see, for example, Kulik and Yanson, 1970). Thus, after core explosion, the vortex remains where it was, but its nature suffers transformation, i.e., an *Abricosov vortex is transformed into a Josephson vortex.*

In the course of penetration and motion of the Josephson vortices, the currents in the weak link vary only at great distances ($\sim \lambda_{\text{eff}}$); hence they do not disrupt the uniformity of current in weak links of small cross section ($W \sim \xi$). Thus all the calculations made previously are applicable to these narrow structures as well.

The fact that there are no solutions of Eq. (107) describing Abricosov vortices is in no way connected with the particular form of these equations. Therefore, even if the equations differ from the GL ones (for example, Usadel equations are valid), the conclusions remain the same: if in a weak link the dependence of the supercurrent density on the phase difference is single-valued, two-dimensional structures of the Abricosov vortex type may not exist in them. For example, in $S-N-S$-type

weak links, as we have already seen, $I_s(\varphi)$ is always a single-valued function, and consequently Abricosov vortices cannot under any circumstance exist in such a weak link for any length of the structure.

4. Critical length versus link width

In the preceding section we analyzed a case where the link width W, i.e., the maximum size of the weak link cross section, is much greater than $L \sim \xi(T)$. It is worthwhile examining the way in which the critical length (below which Abricosov vortices are forbidden) of a weak link changes with decreasing width. Such calculations have been carried out for a rectangular weak link ($0 \leq x \leq L$, $-W/2 \leq y \leq W/2$) by Kupriyanov *et al.* (1975).

In these calculations the last of the boundary conditions (110) has to be replaced by more general ones

$$\frac{\partial R}{\partial y}\left(x, \frac{\pm W}{2}\right) = 0, \quad \frac{\partial I}{\partial y}\left(x; \frac{\pm W}{2}\right) = 0, \tag{115}$$

which follow from the condition of absence of current flow through the lateral edges of the weak link. Here it is impossible to find an analytical expression for the critical length, and Eqs. (107) were solved numerically. The results are shown in Fig. 12 by a solid line for the case where $A = 1$, i.e., the weak link and the electrodes are made of the same material $T_C' = T_C$. However, the vertical asymptote

$$W \to W_C \approx 4.41\xi(T), \text{ as } L/\xi \to \infty, \tag{116}$$

does not depend on T_C'. The effective critical length increases with the decreasing width W, and reaches the asymptote (116), so that Abricosov vortices cannot exist in the center of a strip less than W_C in width at any length.

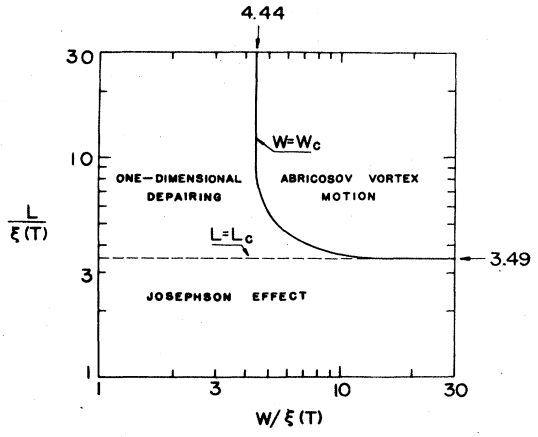

FIG. 12. Variety of possible sizes of dirty weak links (is correct qualitatively at $T \approx T_C = T_C'$). Solid line separates the region of large sizes, where Abricosov vortex appearance is possible, from the region of small lengths and/or small widths, where dc state is destroyed only due to one-dimensional instabilities, with all variables changing only along weak link length (x-axis). Dashed line corresponds to $L = L_C$ and separates the range of small length, where the Josephson effect with single-valued $I_S(\varphi)$ relationship takes place. After Likharev, 1971d; Kupriyanov *et al.*, 1975.

It should be emphasized that the results calculated for finite widths are somewhat uncertain. In the calculations a vortex was assumed to exist in a static position at the center of the weak link. Such a position, however, on account of the attraction toward the lateral edges, is unstable, and a vortex may be sustained in the center only with the help of an external magnetic field applied parallel to the vortex field. If $W \gg L$, the fields necessary for this purpose prove to be rather weak ($\ll H_{C2}$), and there is no need to introduce any corrections into the calculations. For $W \sim L \sim \xi$, the field should be quite strong, so that the asymptote (116) does not define a strict lower limit to W_C for any condition. When $B \approx H_{C2}$, in particular, the lower boundary shifts leftwards to values $\approx 3\xi(T)$.

In contrast, when vortex motion occurs under the action of the current passing through the weak link alone, the boundary may move from the position shown to the right only. In fact, as follows from our previous analysis, if $W < W_C$ the vortex core spreads out along the y axis normal to the current direction, thereby forming a one-dimensional structure $\Delta = \Delta(x)$. When $W \geq W_C$, Abricosov vortices may penetrate only under very large currents which move at high speeds. The finite relaxation time of the order parameters (see Secs. IV and V) likewise enhances the tendency for the vortices to "spread out" in the direction of the flux flow, i.e., along the y axis. Therefore, in the absence of a strong external magnetic field, disruption of the stationary state at $W < W_C$ may be thought of as taking place in a one-dimensional way, and consequently, the theory developed above for $I_S(\varphi)$ under this assumption is valid.

5. Limits of Josephson effect

We now have all the information needed to answer the question, to what length may the Josephson effect be supposed to take place in a superconducting weak link? Conflicting opinions have been expressed regarding this question, partly due to vagueness in defining the Josephson effect.

In particular, the current step pattern on I-V curves of a weak link under microwave irradiation has often been taken as evidence of this effect. These steps appear at voltages $\overline{V} = V_{m,n}$ related to the frequency ω of microwaves by an expression

$$V_{m,n} = \frac{m}{n}\frac{\hbar\omega}{2e} \ (m, n \text{ are integers}), \tag{117}$$

which is a generalization of the Josephson law [Eq. (6)]. These steps are the consequence of the expression for the "classical" Josephson effect (for details, see Sec. VI). However, they may also appear in weak links of very large dimensions ($L, W \gg \xi, \lambda$). Indeed, suppose that a large number of Abricosov vortices move simultaneously in a large structure. In the absence of inhomogeneities, they will tend to form an ordered spatial structure, say, move in m lines with identical frequency in each line. Upon application of an external microwave field, penetration of the vortices into the specimen may be locked in by the nth harmonic of frequency ω. Thus $n\omega/2\pi$ vortices per second will pass along each line. Since the intersection of the specimen

by one flux quantum, according to the induction law, generates a voltage pulse across the electrodes

$$c\int V dt = \phi_0 = \frac{ch}{2e}\,, \tag{118}$$

and the voltage in lines is summable, we find that the mean voltage at a weak link is indeed given by the expression (117):

$$\overline{V} = \sum_m \frac{1}{T}\int V dt = m\times\frac{2\pi}{n\omega}\times\frac{h}{2e} = V_{m,n}\,. \tag{119}$$

Coherent motion of the vortices and current steps at voltages (117) have actually been observed in superconducting films as long as a few millimeters (Fiory, 1971) and in variable-thickness bridges of dimensions much greater than ξ (Gubankov *et al.*, 1973). Moreover, in such large structures it is also possible to record ac voltage at frequencies given by Eq. (117) (Martinoli *et al.*, 1976). These experiments clearly demonstrate that coherence effects in superconductivity are of a common nature.

Nonetheless, it should be stressed that even small inhomogeneities of the sample will lead to the pinning of Abricosov vortices (see, for example, Campbell and Evetts, 1972; Shmidt and Mkrtchyan, 1974) and to differences in the velocities of the vortices in different lines, and hence to the vanishing of coherent effects. In addition, such large structures do not possess the single-valued $I_s(\varphi)$ function generally used in applications of the Josephson effect. An even more significant argument from an experimental viewpoint is that all structures admitting the appearance of small instabilities ($\sim\xi$) are almost irreproducible because unavoidable inhomogeneities determine substantially the formation of these instabilities.

It is therefore reasonable to believe that the "ideal" Josephson effect takes place only when the function $I_s(\varphi)$ is single-valued, and when, consequently, the development of instabilities is impossible. For weak links made of superconducting materials, this condition is satisfied at lengths L less than the critical length L_c found above, i.e., below the dotted line in Fig. 12, which shows the different regions for different behaviors of weak links. In the region characterized by large lengths and short widths the stationary state is disrupted by the depairing effect and by the formation of a "phase slip center" or centers at the weakest point(s) (see, for example, Skocpol *et al.*, 1974b,c). In the region characterized by large lengths and large widths the stationary state is disrupted due to the penetration of Abricosov vortices; their motion has been treated by Likharev (1971d), Schmid and Hauger (1973), Larkin and Ovchinnikov (1973), and Aslamazov and Larkin (1975).

Despite interest in these nonstationary processes, we shall mainly consider the nonstationary processes in relatively short links for which $I_s(\varphi)$ is a single-valued function, i.e., in which almost the "ideal" Josephson effect takes place. Before dwelling on this topic, however, we have to outline the experimental situation in the area of stationary effects. It requires an analysis of various types of weak links and their agreement with the theoretical models used above.

IV. TYPES OF WEAK LINKS

In this section we shall briefly outline the basic types of weak links and evaluate their suitability for pure physical purposes (comparison with theory) and for the main applications of the Josephson effect. Most of the theoretical results for weak links have been derived within the framework of the ODSEE model (see Sec. III.C), in which simple boundary conditions [Eq. (64)] are assumed. In the first instance, we shall, therefore, examine the processes in the electrodes that might lead to deviations from these conditions in real weak links.

A. Nonlinear processes in the electrodes

We shall discuss only the processes which give rise to a deviation of $|\Delta|$ at the weak link–electrode interface from the equilibrium value, i.e., the nonlinear processes. Such linear processes as linear changes of the phase χ in the electrodes under the action of current through a weak link ($\mathbf{j}_s \propto \nabla\chi$) are consistent with the ODSEE model provided the condition (104) is valid, because noticeable changes in χ along the weak link–bank interface may take place only over $\lambda_{\rm eff}$.

1. Proximity effect

Even in the absence of any current through a weak link, the proximity effect is observed at its interface with the electrodes: the values of $|\Delta|$ on either side of the interface tend to each other, i.e., deviate from their equilibrium values. These variations extend into the depths of the weak link and the electrodes to distances of the order of the coherence lengths of these materials. When a supercurrent I_s comparable to I_c flows through a weak link, it changes $|\Delta|$ in the weak link appreciably. Thus, if the proximity effect is significant, then $|\Delta|$ at the interface will suffer significant changes, leading to considerable deviations from the ODSEE model. Consequently, this effect cannot be avoided even if the weak link and the electrodes are made of the same material.

2. Suppression of superconductivity by a current

The critical current of short weak links, in which the Josephson effect takes place, may be rather large. For example, it is obvious from Fig. 7, that with diminishing link length the current can notably exceed the depairing current of the weak link material. This current, on entering the electrodes, can likewise produce the depairing effect accompanied by suppression of the order parameter. Therefore, for the ODSEE model to be valid [condition (64)] it is necessary that the current in the electrodes be, for some reason (say, change of material or cross section), much less than the depairing current.

3. Consequences of nonlinear effects in the banks

If at least one of the aforementioned effects occurs in the banks, then the ODSEE model is no longer applicable, and the situation, in principle, has to be reexamined. It is, however, obvious that if nonlinear effects extend into the electrodes a distance δ, then the weak link will behave qualitatively in the same manner

as in the ODSEE model, but with a different effective length

$$L_{\text{eff}} \approx L + 2\delta . \tag{120}$$

We shall now consider some particular types of weakly linked structures, using the high or low current concentration in the weak link as the criterion in classifying them.

B. Structures without current concentration

The largest deviations from the ODSEE model may be observed in structures with no current concentration, where the electrodes have the same cross section as the weak link [Fig.1(a)-(d)].

1. Specific features of structures without current concentration

Both the above-mentioned nonlinear effects are strongly exhibited in these structures. Consider, for example, the case of a dirty structure ($\ell \ll \xi_0$) of length $\sim\xi'$ (primes show weak link parameters) at a temperature not very close to the critical temperature. As follows from Eq. (53), the density of the depairing current of the electrodes ($F \sim 1, \nabla \sim \xi^{-1}$) is of the order

$$j_{dp} \approx \frac{\sigma_N \Delta}{e\xi} , \tag{121}$$

and the Josephson current of a weak link is of the order ($\nabla \sim L^{-1}$)

$$j_C \approx \frac{\sigma_N' \Delta}{eL} \approx \frac{\sigma_N' \Delta}{e\xi'} . \tag{122}$$

Hence, in order that there may be no depairing effect at the banks, the following condition

$$\frac{\sigma_N'}{\xi'} \ll \frac{\sigma_N}{\xi} \tag{123}$$

should be satisfied. As for the proximity effect, we shall take into account the fact that the functions F and the quantities $\sigma_N \nabla F$ should be continuous on the plane of the boundary of two materials. This guarantees the continuity of the current and is in agreement with the boundary conditions of Zaitsev (1966). The deviation of F in the electrodes from the equilibrium value is of the order of $\xi \nabla F$, and is, therefore, much less than that in the weak link, if

$$\xi' |\nabla F'| \gg \xi |\nabla F| , \tag{124}$$

which again results in the condition (123) for the ratio of the parameters of the materials.

Since

$$\sigma_N/\xi \propto N(0)(v_F \ell)^{1/2} \tag{125}$$

we find that condition (64) of the ODSEE model holds true in "one-dimensional" weak links (with no current concentration) only for the interlayer made either of dirty material (small ℓ) or of low concentration of conduction electrons n [in the free electron (gas) model $N(0)v_F^{1/2} \propto n^{1/2} m_e$].

If, however, σ_N/ξ is of the same order in the electrodes as in the weak link, then the effective length of the weak link (120) is of the order of $(L + 2\xi)$ i.e., it cannot be made less than ξ by diminishing L. From Figs. 7 and 8, it is evident that in such weak links it is impossible to provide the "ideal" Josephson effect with almost sinusoidal $I_S(\varphi)$ relationship and large V_C. This is confirmed by the calculations carried out for the processes taking place in such structures (De Gennes, 1966; Galaiko *et al.*, 1969; Baratoff *et al.*, 1970; Blackburn *et al.*, 1972, 1975; Volkov, 1974).

Here we should mention yet another situation complicating the use of structures without current concentration for comparison with theory. We know that the basic dc characteristics of a weak link are the temperature dependence of the critical current $I_C(T)$ and the phase dependence of the supercurrent $I_S(\varphi)$, the latter carrying more information. One difficulty in the measurement of the $I_S(\varphi)$ relationship in one dimensional structures is that even in the absence of nonlinear effects the phase χ grows linearly into the electrode depth ($j_x = \text{const}$, $\partial\chi/\partial x = \text{const}$). If, in addition, the current is close to the critical depairing current, then a 2π increase in the phase takes place even at small distances $\sim\xi$ ($\sim 10^{-5}$ cm). Therefore the "three-dimensional" electrodes, across which the phase difference $\varphi = \chi_2 - \chi_1$ is measured by one method or another (Fulton and Dynes, 1970; Jackel *et al.*, 1974, 1976a; Waldram and Lumley, 1975; Meservey and Tedrow, 1975; Rifkin and Deaver, 1976), have to be connected to the "one-dimensional" electrodes at a distance of $\sim\xi$, and this does, strictly speaking, have some influence on the processes occurring in a weak link.

We shall now take up some specific one-dimensional structures.

2. Sandwiches

Sandwiches are, as a rule, fabricated by sequential evaporation of the various layers, on a substrate. The interlayer thickness, depending on the materials used, varies from 10^{-5} to 10^{-3} cm. Experiments have been carried out mainly with sandwiches containing a relatively dirty normal metal interlayer (Clarke, 1969, 1971; Bolton and Douglas, 1971; Sheperd, 1972); similar structures were investigated by Bondarenko *et al.* (1970a). The value of σ_N/ξ in these studies was of the same order in a normal metal and in the electrodes, hence the boundary conditions were noticeably different from those of the ODSEE model. In experiments with interlayers much thicker than ξ', it may, however, be possible to measure ξ' and its temperature dependence, as in this case the proportionality between I_C and $\exp(-L/\xi')$ [see Eqs. (73) and (77)] does not depend on the boundary conditions. It would, moreover, be worthwhile to study the function $I_C(T)$ for relatively clean sandwiches ($\ell \sim L, \xi_0$) and to compare them with the theoretical calculations (see Sec. III.D).

From the point of view of device applications it should be noted that sandwiches are rather unsatisfactory, as they have very low V_C ($\sim 10^{-7}$ V or even less) and R_N. For instance, in small-size sandwiches with an area of 10×10 microns and a normal metal interlayer thickness of 0.1 μm, the normal resistance is of the order of $10^{-5}\Omega$ (for $\sigma_N^{-1} \approx 10^{-6}\Omega$ cm). Such values of V_C and R_N

are too low for any application of the Josephson effect (see Likharev and Ulrich, 1978).

Thus sandwiches with an "ordinary" metal interlayer are of rather limited interest. In contrast, the "ideal" Josephson effect can be realized by using a poorly conducting interlayer (low σ_N'/ξ'). This is just the situation that probably takes place in $S-SE-S$ type junctions with a doped silicon interlayer (Huang and Van Duzer, 1974, 1975; Schyfter *et al.*, 1977; Hu *et al.*, 1978). In using semiconductors, the situation does, however, become complicated due to the Schottky barriers appearing at the interlayer-electrode interfaces. Under these conditions the tunneling process at the interface interferes with the direct conductivity inside the semiconductor. An important problem today in weak superconductivity is that of working out further experiments and developing a comprehensive theory, at least, for the dc processes in these structures.

From the practical viewpoint, $S-SE-S$ type sandwiches not only provide a means of raising V_C to the maximum possible values, but also of increasing considerably the normal resistance of structures, while keeping the capacitance negligibly small. Sandwiches with $V_C \geq 1$ mV and R_N of about 0.5 Ω at an area ~50 μm^2 have already been fabricated (Schyfter *et al.*, 1977). Such structures are quite suitable for most of the microwave devices, especially those which use arrays of such junctions (see Sec. VII). Moreover, these sandwiches are quite promising for utilization in Josephson cryotrons.

3. Proximity effect bridges

Proximity effect microbridges do not, in their physical processes, differ from $S-S'-S$ or $S-N'-S$-type sandwiches (depending on the extent to which the critical temperature of the span is suppressed by the proximity effect). Their advantage over sandwiches is their small cross section and, consequently, their relatively high resistance R_N (which may reach 10^{-2} to $10^{-1}\Omega$), which simplify both the measurements and the practical applications of these microbridges. A definite drawback is the need to provide the smallest possible dimension ($L \sim \xi$) not in thickness, but in plane of the structure. However, even when this dimension is relatively large (of the order of one micron), the condition $L \leq \xi'(T)$ can be satisfied in a narrow range near the critical temperature of the link material T_C'.

These structures may have a single-valued $I_S(\varphi)$, but their V_C, as it follows, say, from Fig. 7, is low

$$V_C \sim (V_C)_{\max} \exp[-L/\xi'(T_C)] \ll (V_C)_{\max} . \tag{126}$$

In the early realizations of proximity effect microbridges, where their structures were almost one-dimensional [Fig 1(c)], values of V_C were in the range of a few nanovolts (Notarys and Mercereau, 1971; Kirschman, 1971), i.e., about 10^6 times less than the maximum possible values which are of the order of a few millivolts [Eq. (62)]. Later, these bridges had to be modified: the entire film was placed over a normal metal film, the span superconductivity being weakened by the decreasing thickness, which stimulated the suppression of $|\Delta|$ due to the proximity effect (Mercereau, 1974; Kirschman *et al.*, 1975). Current concentration occurs in such structures, the suppression of $|\Delta|$ at the banks is reduced (see below), and V_C increases. However, due to lack of a very great difference between the thicknesses of the span and the banks, the characteristic values of V_C even in such modified bridges do not exceed tens of microvolts.

The smallness of V_C and R_N restricts the applications of proximity effect microbridges to ac SQUIDs (Kirschman *et al.*, 1975; Falco and Parker, 1975); dc SQUIDs based on these bridges feature rather poor characteristics (Decker and Mercereau, 1973).

4. Ion-implanted microbridges

Recently several papers have been published dealing with a new method of preparation of one-dimensional weak links by implantation of ions into superconducting films. Implantation may be carried out in the span (Arrington and Deaver, 1975; Kirschman *et al.*, 1977; Rachford *et al.*, 1977; Boone *et al.*, 1977) if it diminishes the film critical parameters, or in the banks (E. Harris, 1975; Harris and Laibowitz, 1977) in the opposite case. The physical properties of these microbridges [Fig. 1(d)] are close to the one-dimensional structures already discussed and they can have a rather limited application in physics or engineering.

One work (Harris and Laibowitz, 1977) is worthy of special mention: the banks were subjected to irradiation and thus their critical temperature was increased. As ℓ and $(\xi \sim \xi_0 \ell)^{1/2}$ diminished at banks in this process, the effective length L_{eff} was close to the physical value. Therefore, for moderate current densities, the boundary conditions for Δ were close to those of the ODSEE model, allowing verification of the theory discussed in Sec. III on the effect of length on the critical current of weak links at $T \approx T_C \approx T_C'$.

C. Dayem bridges

The only example of structures with weak current concentration is the constant-thickness bridge [the Dayem bridge, Fig. 1(e)] in which the concentration occurs in only one direction, i.e., along the film width.

1. Specific features of the processes in Dayem bridges

The concentration of current even in one direction improves the correspondence of the weak link to the ODSEE model. However, in Dayem bridges the weak link and the banks are made of the same material ($\sigma_N/\xi = \text{const}$). Hence the banks are easily involved in nonlinear processes. Indeed, current-induced suppression of $|\Delta|$ has the greatest influence in that region where the current density J is comparable with the maximum one ($J_{\max}$). The length of this region, as is evident from Fig. 13

$$L_{\text{eff}} \approx \max(L, W) , \tag{127}$$

is always greater than the bridge geometrical length L.

Moreover, even if L_{eff} is less than ξ, the simple AL and KO-1 theories are not applicable to Dayem bridges because, as can easily be verified, the function f diverges (rather weakly, as $\ln r$) on receding from the bridge into banks. Therefore any theory of the AL type

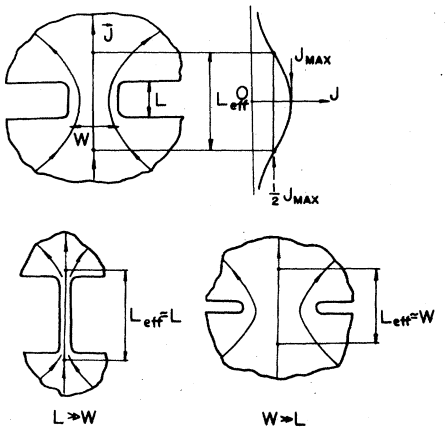

FIG. 13. Current concentration in Dayem bridges at various relationships of their length L and width W. Figure shows that current density falls off at the lengths $L_{\rm eff} \approx \max[L, W]$.

has to be reconstructed to be valid for Dayem bridges. This work has been carried out by Volkov (1973), who assumed the bridge to be bounded within hyperbolas with centers separated by a distance $2a \ll \xi$. The same result has been shown to hold valid for any shape (Likharev and Yakobson, 1975a), if the bridge boundaries at small distances ($r \ll \xi$) tend to lines emerging from one point.

The Volkov theory gives the following expression for the critical current

$$I_C = V_C / R_N(\xi), \tag{128}$$

where V_C, as in the AL theory, is expressed by Eq. (14), but $R_N(\xi)$ is the normal resistance of the bridge part inside a circle of radius ξ

$$R_N(\xi) \approx 2R_\square \ln(\xi / L_{\rm eff}), \quad R_\square = (\sigma_N d)^{-1}, \tag{129}$$

where $R_\square$ is the normal (residual) resistance of the film per square. Even in the vicinity of T_C, the function $I_C(T)$ is evidently different from linear (see also Klapwijk *et al.*, 1977b).

For Dayem bridges the $I_S(\varphi)$ relationship, just as in the case of one-dimensional structures, is somewhat uncertain, as it is not clear between which points the phase difference φ has to be taken. Since even at distances of $r \gg \xi$ inside the banks the current decreases slowly ($j_S \propto r^{-1}$), the phase continues to grow ($\propto \ln r$). Suppose that we are measuring the phase difference between bulk superconducting electrodes connected to the banks at $r \gg \xi$ (in this case they do not affect the processes occurring in the bridge). Then, as follows from Eqs. (21b) and (24), for $d \lesssim 2\lambda, dL_{\rm eff} \lesssim \lambda^2$

$$\varphi_r = I_S \frac{16e\lambda^2}{c^2\hbar d} \ln \frac{r}{L_{\rm eff}} + \text{const}(r). \tag{130}$$

On comparing Eq. (130) with Eq. (48), we see that the electrodes make a contribution l_R to the effective kinetic inductance proportional to $\ln r$. In the dirty limit, using Eq. (24) and Eqs. (128) and (129), we obtain

$$l_R \approx \frac{1}{\pi} \ln(r / L_{\rm eff}) \gg 1 . \tag{131}$$

Even the minimum value of this contribution (when $r \sim \xi$) is of the order of unity.

Thus the dependences $I_S(\varphi_R)$ measured for Dayem bridges should be multivalued even when $L_{\rm eff} \ll \xi$, as was observed in the experiments (Jackel *et al.*, 1975, 1976a).

2. Large and small bridges

The aforementioned results apply, in fact, to small-size bridges. Historically, starting with the pioneering work of Anderson and Dayem (1964),[22] for a few years research was concentrated on bridges of relatively large size[23] ($L, W \approx 1-2$ μm) which, for the material used (Sn, In), satisfied the relation $L_{\rm eff} \lesssim \xi$ only in a narrow temperature range close to T_C. Since this range was of the order of the phase transition width, the superconducting parameters of the film in this range were essentially inhomogeneous, and a comparison with the theory was impossible. At other temperatures, the bridge dimensions were noticeably greater than ξ, and the uniform flow of the condensate was disrupted by penetration of Abricosov vortices (see Sec. III.E, and Fig. 12).

It is doubtful whether such large Dayem bridges could ever prove useful in any physical research or application, maybe with the exception of SQUIDs with relatively low sensitivity (see below). However, it is still more unfortunate that in the last few years considerable effort has been expended in fabricating constant-thickness bridges from such hard superconductors as Nb, Nb_3Sn, NbN, and others (Janoko *et al.*, 1971, 1973, 1975; Laibowitz *et al.*, 1975; Fujita *et al.*, 1975; Holdeman and Peters, 1975, 1976; Golovashkin *et al.*, 1976, 1978; Wu and Falco, 1977; Balla *et al.*, 1977; Rachford *et al.*, 1977). These films have extremely low coherence length (~ a few hundred angstroms or even less), and therefore remain "large" even if the bridge dimensions are as small as 0.1 – 0.2 μm.

The main hurdle in microbridge fabrication in the early seventies was the formation of their sizes, usually by superposition of masks during film evaporation.[24] Therefore, quite a significant advancement at that time was the "double scratch" technique (Gregers-Hansen *et al.*, 1971, 1972) by which microbridges from soft materials (Sn, In, Al) of sizes of about 0.2 to 0.5 μm could be prepared without complex special equipment. Such sizes are quite sufficient for $L_{\rm eff}$ to be less than ξ in a noticeable temperature range close to T_C, and consequently most of the phenomena associated with the Josephson effect can be observed (Gregers-Hansen *et al.*, 1971, 1972a, b; Gregers-Hansen and Levinsen, 1971; Jahn and Kao, 1973; Chiao *et al.*, 1974; Pedersen *et al.*, 1977).

Further progress in microbridge fabrication technology has been made in utilizing such methods as electron

[22] Almost at the same time these bridges began to be studied by other groups (Parks and Mochel, 1964; Lambe *et al.*, 1964).

[23] A review of early work on Dayem bridges may be found in an article by Likharev (1971d).

[24] Only a recent communication (Dmitriev *et al.*, 1976) reports the preparation of submicron-size bridges by this method.

lithography (Laibowitz, 1973; Laibowitz *et al.*, 1974, 1975; Auracher and Van Duzer, 1974; McCarthy and Stanko, 1974; Jillie *et al.*, 1975, 1976, 1977). These methods make possible high reproducibility in fabricating film structures with microbridges of submicron dimension.

3. Application of Dayem bridges

The main shortcoming of Dayem bridges from the application viewpoint is their low resistance R_N which is of the same order as the resistance per square $R_\square$ [Eq. (129)] and does not usually exceed a few tenths of an ohm.[25] It is not possible to increase R_N by decreasing the film thickness d or by raising R with impurities, because ℓ would decrease and the coherence length $\xi \propto \ell^{1/2}$ would become less than $L_{\rm eff}$. Low resistance also causes strong heating effects (see Sec. V) and this further restricts the operating range of Dayem bridges close to T_c.

Moreover, the large value of l deteriorates parameters of the Dayem bridge as elements of those Josephson effect devices where the weak link is connected to the superconducting ring. For such devices, it is generally necessary that their main parameter l_Σ be

$$l_\Sigma = l_R + l\,, \quad l_R = \frac{2e}{\hbar c^2}\,\mathfrak{L}_R I_C\,, \tag{132}$$

where $\mathfrak{L}_R$ is the ring inductance, to be less or slightly more than unity (for references see Footnote 2). A value of $l_\Sigma \gg 1$ leads to a loss of sensitivity proportional to l_Σ in ac SQUIDs, and proportional to l_Σ^{-1} in dc SQUIDs. If $l > 1$, then l_Σ can never be made less than unity for any inductance $\mathfrak{L}_R$. This is why ac SQUIDs (Goodkind and Stolfa, 1970; Murata *et al.*, 1976) and dc SQUIDs (Richter and Albrecht, 1973; Albrecht, 1976; Carelli and Modena, 1976; Kravchenko *et al.*, 1976; Lobanov *et al.*, 1976) utilizing Dayem bridges did not have very high sensitivity and had a narrow operating temperature range.

Likewise, as $l \gg 1$, the Dayem bridges are not suitable for use as quantron-type computer elements (Dynes *et al.*, 1973; Anacker and Zappe, 1973; Likharev, 1974a, 1977a,b; Likharev *et al.*, 1976; Hurrell, 1977). Finally, diffraction-type cryotrons cannot be based on these bridges either (see Sec. VII), as their width cannot be much greater than the effective length [Eq. (127)]. In all probability, Dayem bridges can prove useful only in several microwave devices if their microwave impedance is increased by connecting several bridges in series (see Sec. VI).

D. Structures with strong current concentration

In these structures both the weak link cross-section dimensions are much less than those of the electrodes, and therefore the current concentration now takes place in two dimensions. For example, in variable-thickness bridges [Fig. 1(f)] the current is concentrated along both the thickness and the width of the film. In addition to these bridges, random microshorts in point contacts [Fig. 1(g)], blob-type junctions [Fig. 1(h)], and similar other structures belong to the class of high current concentration structures.

1. Special features of strong current concentration structures

The ODSEE model can easily be realized in these structures (Likharev, 1971d). Indeed, consider the proximity effect near the weak link–bank interface. The volume segment V' of the link contained in a distance $\sim\xi'$ from this interface is considerably less than the corresponding volume segment V of the bank at a distance $\sim\xi$ from the interface. Therefore a deviation in $|\Delta|$ from the equilibrium value at the bank would cause a much greater increase in the free energy $\Delta F \propto V$ than that created by the same deviation of $|\Delta|$ in a weak link: $\Delta F' \propto V'$. Although the order parameter in these structures is suppressed in the banks to depths $\sim\xi$ from the weak link, the amplitude of these changes is negligibly small. Hence the value of $|\Delta|$ at the boundaries remains close to the equilibrium values in the electrodes, and this happens irrespective of the materials of the links and banks.[26]

Similarly, the second possible nonlinear effect also decreases, namely, suppression of $|\Delta|$ in the electrodes due to the current flow through the weak link. For example, in a variable-thickness bridge the current, on entering the banks from the span, rapidly diverges throughout the thickness and width. The current density is, therefore, high (of the same order as the depairing current) only at distances of the order of bridge film thickness d' from the interface, and the bridge effective length $L_{\rm eff}$ is almost the same as its geometrical length L. A detailed analysis (Likharev and Yakobson, 1975c) shows that the main condition [Eq. (64)] of the ODSEE model can be satisfied with any materials by decreasing the weak link cross section.

Structures with a current concentration in two dimensions have one more advantage in that the phase difference at the weak link can easily be measured. In fact, as the current in the banks diverges in two directions, its density decreases as r^{-2} with increasing distance from the weak link, and consequently the phase drop at the banks is finite

$$\varphi_r \propto \int^r j_S\,dr = \text{const}\,(r) + Cr^{-1}\,. \tag{133}$$

Moreover, it is easy to show that with the decreasing weak link cross section this phase drop decreases (for instance, in variable-thickness bridges it is of the order of d'/L) and is usually very small. Therefore the phase difference between two remote points on the electrodes is almost exactly equal to the phase difference φ between the boundaries of the weak link and

[25] The only exception is a work (Froome and Beck, 1976) in which Dayem bridges were reported to have R_N of the order of a few ohms. It is not clear whether the condition $L_{\rm eff} \lesssim \xi$ was satisfied in these experiments.

[26] With the exception, of course, of the unlikely case where the normal conductivity of the bank material is much less than that of the weak link material.

electrodes, which is the subject of calculation in the ODSEE model.

2. Point contacts and similar structures

Point contacts [see the review by Zimmerman (1972), and also paper by Gubankov *et al.* (1972)] are usually fabricated by lightly pressing a sharp needle point (the radius of the tip being no greater than a few tenths of a micron) onto the planar surface of another electrode; they can, however, be formed by several other methods (see, for example, Bondarenko *et al.*, 1970a; Yanson, 1975). Numerous conducting microshorts are, as a rule, developed between electrodes in the oxide layer at the contact surface. The shape and exact dimensions of these shorts do not readily yield to investigation. By studying the magnetic field dependence of the critical current, we can only infer that the cross-section areas of these microshorts are much less than the area of mechanical contact between the electrodes.

Microshorts are responsible for the mechanical instability and total irreproducibility of the point contacts. While the first drawback can, to some extent, be eliminated using special mechanical adjusting systems (see, for example, Contaldo, 1967; Zimmerman *et al.*, 1970; Nad′, 1971; Buhrman *et al.*, 1971; King, 1971; Edrich *et al.*, 1974; Kulikov *et al.*, 1974; Soerensen, 1974; Antyukh and Nad′, 1975; Macfarlane, 1976; Neumaier, 1976; Cross and Blaney, 1977), the second shortcoming is insuperable, hindering both theoretical investigations and practical applications of point contacts.

Therefore, from the viewpoint of physical research, point contacts are only useful in verifying those theories where the geometrical structure of the weak link is unimportant. It would be very worthwhile to verify experimentally the KO-1 and KO-2 theories in particular, and the applicability of the tunnel theory to systems of very small microshorts (see Sec. II.C). So far such investigations have not been carried out, and only some evidence is available that $I_S(\varphi)$ functions can be single valued in point contacts (Jackel *et al.*, 1974, 1976a; Rifkin and Deaver, 1976).

As regards the device applications, we may note that point contacts with the desired electrical characteristics can usually be prepared using repeated formation with mechanical adjusting or weak electrical discharges. The characteristic voltage V_C, in particular, can be made to attain the maximum possible theoretical value (i.e., ~3 mV at $T \sim 10$ K and $T \lesssim T_C/2$), while the normal resistance can be varied from $\sim 10^2$ to $10^{-2}\Omega$, the function $I_S(\varphi)$ being almost sinusoidal. As a result of these convenient properties and ease of fabrication, point contacts find extensive application in all types of Josephson effect devices, with the exception of computers, where reproducibility is essential.

Recent advances in thin-film weak link fabrication technology, however, leave no doubt that point contacts will gradually be superseded in all fields of device applications by reproducible types of weak links. This situation is equally true of similar structures like blob-type junctions (Clarke, 1966; Manikopoulos and Hannam, 1973), microshorts in oxide films (Bondarenko *et al.*, 1970a, 1976; Yanson, 1975; Lum and Van Duzer, 1975), and similar junctions, their only distinction from point contacts being still greater intrinsic capacitance, which complicates their applications.

3. Variable-thickness bridges

These bridges (Likharev, 1971d) are practically the only reproducible structures in which the ODSEE model is valid, i.e., the only means of avoiding nonlinear effects at the banks, for any length of the structure and for any (including identical) materials of weak link and electrodes. Even the first experiments with variable-thickness bridges (Gubankov *et al.*, 1973) confirmed the main conclusion of the theory that nonlinear effects are localized at the span film.[27] The relatively small-size tin bridges prepared in the same group (Gubankov *et al.*, 1975, 1976, 1977) exhibited satisfactory Josephson properties at T close to T_C.

Similar bridges were fabricated almost at the same time by another research group (Klapwijk and Veenstra, 1974; Klapwijk and Mooij, 1975; Klapwijk *et al.*, 1977) with a view to reducing energy dissipation (and, consequently, self-heating) by diminishing the span film thickness d'. Indeed, for fixed $\bar{V}$ and planar sizes, self-heating decreases proportionally to d'. As a result, even at temperatures far from the critical temperature, multivaluedness in the I-V curves can be avoided.

In Sec. III we have already pointed out that normal metals can function as weak links just as well as superconducting metals if they have similar values of v_F. On the other hand, we have a wider choice of normal metals (Au, Ag, Cu, Al, and others) having high values of v_F (~10^8 cm/s) than the choice of such superconductors (Sn, In). For both these classes of metals, ξ at temperatures far from the critical one is ~$0.1 - 0.2$ μm for the real mean free paths ($\ell \sim d' \sim 10^{-5}$ cm), so that bridges with an L measuring a few tenths of a micron exhibit the "ideal" Josephson effect. Besides, the normal metals listed above have sufficiently high melting points so as to safeguard against accidental burnouts. These arguments (Likharev, 1976) stimulated others (Komarovskikh *et al.*, 1975) to fabricate $S-N-S$-type bridges with niobium banks and a gold span. The resistance of such bridges was relatively high (~0.4Ω for a width of ~10 μm) and self-heating was low even at temperatures far below T_C, where V_C was quite high (~400 μV).

Some other groups, as well, have recently reported success in preparing "genuine" variable-thickness bridges. Octavio *et al.* (1977a, b) succeeded in fabricating tin microbridges in which self-heating noticeably suppressed the Josephson effect only at voltages as large as ~3 mV. Boone *et al.* (1977) and Wang *et al.* (1977) have prepared microbridges with a tin and niobium span, while Yeh and Buhrman (1977) used lead. Sandell *et al.* (1977) used electron lithography to make indium variable-thickness bridges.

Some other structures closely resemble variable-

[27] In these experiments the bridges were of large dimensions ($L, W >> \xi$) and their resistive state was associated with Abricosov vortex motion.

thickness bridges in their properties. For instance, the properties of proximity bridges after the above-mentioned modifications (Mercereau, 1974), which somewhat weaken the nonlinear effects at the banks, become more similar to those of the ODSEE model. The $S-N-S$-type structures studied by Romanagan *et al.* (1975) and Gilabert *et al.* (1975) are also similar to variable-thickness bridges. However, owing to their large L, the Josephson effect was observed in them only at temperatures very close to T_C, so that the V_C's of these bridges were rather low.

$S-N-S$-type microbridges with Bi spans are described by Ohta *et al.* (1974). As a result of the low conductivity of bismuth and its moderate ξ, the ODSEE model should be valid for such structures, despite the relatively thick bridge span. Their merit from the point of view of device application is their high resistance R_N.

Furthermore, in bridges prepared by the "double scratch" method (see Sec. IV.C), if the first scratch (on the substrate) is quite shallow, the span thickness too becomes less than the bank thickness. Thus the properties of such bridges are close (though not identical) to those calculated in the ODSEE model. In particular, measurements have shown that for these bridges the $I_S(\varphi)$ relation is quite often single-valued (Jackel *et al.*, 1976a).

Finally, in an effort to reduce the cross section of structures with a semiconductor interlayer, Schyfter *et al.* (1977) and also Kandyba *et al.* (1978) fabricated "coplanar" structures, which are, in reality, $S-N-S$ bridges in which a doped surface layer of the semiconductor substrate serves as the span. These structures have one serious drawback in that one of the planar dimensions (L) has to be kept rather small (~0.1 μm), because the coherence length of the doped semiconductor is several times less than that of normal metals listed above. Their indisputable merit is relatively high normal resistance.

Naturally, variable-thickness bridges and similar structures are quite convenient in physical research into the processes occurring in weak links, especially the little studied nonstationary (ac) processes (see below). Such investigations have already been started; for instance, the basic principles of the theory of dc processes in weak links have been experimentally verified (Gubankov *et al.* 1976), and the first results with regard to ac processes have been published (Gubankov *et al.*, 1977; Octavio *et al.*, 1977b).

As regards applications, it is generally felt that variable-thickness bridges, given a proper choice of materials for the span and the banks, may meet almost all the practical requirements. Therefore, with advances in production technology (variable-thickness bridges are more complicated to produce than any other type of bridges) these weak links could certainly be incorporated into many of the Josephson effect devices. A serious competitor to them is, in all probability, the class of small-area sandwiches with an interlayer made of doped semiconductor or any other normal material of relatively high normal resistance.

E. Controllable weak links

Once fabricated, the weak links considered in the previous pages should last indefinitely. Other types of weak links have been fabricated (or only conceived) which may exist only under continuous external influence.

Volkov (1971) theoretically examined a weak link between two sections of superconducting film separated by a region whose superconductivity is suppressed by incident electromagnetic waves, say, light. It was believed that suppression is effected by the nonzero mean square of the electrodynamic field.

After it was found (Testardi, 1971) that light pulses have a strong effect on superconductivity, it became evident that this effect takes place primarily due to photon breaking of the Cooper pairs, and the consequent establishment of nonequilibrium (higher) concentration of normal electrons and phonons [see reviews by Langenberg (1975) and by Chang and Scalapino (1977)]. Therefore another approach for weak links created by local irradiation of light was proposed (Wong *et al.*, 1976, 1977). The authors believe that these structures are a particular kind of controllable weak link (CLINK) in which $|\Delta|$ is suppressed owing to the increased concentration of quasiparticles: normal electrons and phonons. In the same paper other methods of fabricating CLINKs were examined, in particular, by injection of quasiparticles through an additional tunnel junction. The first experiments (see also Gilabert *et al.*, 1977) have shown that the processes in the system are far more complicated than what follows from an analysis based on simple phenomenological equations for the quasiparticle distribution proposed by Rothwarf and Taylor (1967).

Dolan and Lukens (1977) reported production of weak links by the action of a magnetic field on a short section of thin film strip. Outside parts were shielded from the field action with the help of another superconducting film.

Bevza *et al.* (1976) produced a weak link in a narrow strip, using suppression of $|\Delta|$ by a current flowing in a transversal strip. The whole structure was in the form of a cross. Suppression was probably effected by quasiparticles generated in the "control" strip, which is the first to attain its normal state.

It must be admitted that the structures created by means of external actions can be of use in studying the physics of these actions, say, of excitation and relaxation of the quasiparticles (see Secs. V, VI). Nonetheless, according to our classification, all these structures fall into the class of one-dimensional ones, i.e., do not have any noticeable current concentration at the weak link. Therefore, the banks are extensively involved in nonlinear processes, which gives rise to difficulties in their theoretical description.

V. JOSEPHSON OSCILLATIONS AND I-V CURVE

The ac processes in weak links are not as well understood as the dc processes, mainly due to the lack of appropriate microscopic theories. Thus we are compelled to describe these processes on the basis of equations derived strictly for some particular cases, or on a phenomenological basis. We shall begin our discussion with those processes that take place in the following simple experiment: a weak link is connected in series to a circuit with dc current $I=\bar{I}$.

So long as the current through the weak link is less

than the critical one, it is transported by the superconducting condensate (I_S), the phase φ is constant in time, and the voltage between the electrodes is zero. If the current exceeds the critical one, it cannot be transported by only the condensate; consequently, at least a part should be transported by normal electrons. But this "normal" current gives rise to a nonzero potential difference V with $\overline{V} \neq 0$. Hence the phase difference φ begins to change with the frequency ω_V [Eq. (6)].

In such an ac process, in the majority of weak links, the supercurrent I_S is a periodic function of the phase; thus the supercurrent oscillations occur in the element with this Josephson frequency, and probably with its harmonics, too. The manner in which this process (Josephson oscillations) occurs, and the consequent appearance of the current-voltage curves ($I-V$ curves), depends not only on the physics of conduction through the weak link, but also on the capacitance of the structure.

A. Influence of intrinsic capacitance

1. Impedance relationship

Josephson oscillations in real experiments have extremely high frequencies. Indeed, the typical voltage across a weak link is given by a factor $V_C = I_C R_N$ which, as we have seen in Sec. III, may be of the order of $k_B T/e$. In ordinary cases where T_C is of the order of several kelvin, we have $(V_C)_{\max} \sim 10^{-3}$ V and the frequency ω_C determined from Eq. (6) is about 10^{12} s^{-1}. Of course, $\overline{V}$ and ω_V may be far less; nevertheless, the arguments given below are equally applicable even to $\omega_V \sim 10^8 - 10^9$ s^{-1}.

At such high frequencies, the external electrodynamical system has a very large impedance Z_e as compared to that of the weak link. Indeed, $|Z_e|$ is usually on the order of the wave resistance of free space $4\pi/c \approx 377\Omega$. This is significantly greater than the intrinsic impedance of the weak link $|Z| \lesssim R_N$. Therefore the electric charge carried by the oscillating supercurrent cannot pass through an external circuit, and consequently at each moment the supercurrent should be compensated either by the normal current I_N or by the displacement current $I_D = C\,dV/dt$, where C is the capacitance between the electrodes.

The relation $|Z_e| \gg |Z|$, which holds true for the vast majority of weak links not switched into special low-ohmic electrodynamic structures, precisely explains why an experiment with a constant current rather than constant voltage across the weak link is the simplest. If we attempt to set a constant voltage with the help of a source having low dc internal resistance ($R_e \ll |Z|$), the impedance relationship at the Josephson frequencies will, nevertheless, be the other way round, and it is again the current, but not the voltage, that will be constant in time. The dc resistance R_e only determines the slope of the "load line" $\overline{V} = E - R_e \overline{I}$ in the $[\overline{I}, \overline{V}]$ plane, but not the shape of the $I-V$ curves.

2. Capacitance, Josephson oscillations and *I-V* curve

We now consider the conditions under which not only the current, but also the voltage V across the weak link may be constant in time. The effective impedance of the normal current I_N is on the order of normal resistance R_N, while the impedance due to the displacement current is $(i\omega C)^{-1}$. Therefore, if the condition

$$\omega C R_N \gg 1 \tag{134}$$

is satisfied at the frequency of the ac process, the ac component of the voltage is totally shunted by the capacitance of the structure, hence $V(t) \approx \overline{V}$. In other words, under the condition (134) the oscillating supercurrent is fully compensated by the displacement current. Therefore the normal current I_N and the voltage are constants. Substituting the characteristic frequency of the Josephson oscillations [Eq. (18)] into Eq. (134), we obtain the condition $\beta \gg 1$ [Eq. (17)] (Stewart, 1968; McCumber, 1968). If it is satisfied, then for any voltage across the contacts, the voltage may be regarded constant in time, and phase φ varies according to the simple linear relationship

$$\varphi = \omega_V t + \text{const}, \quad \omega_V = (2e/\hbar)\overline{V}\,. \tag{135}$$

In contrast, if the capacitance of the structure is small ($\beta \ll 1$), then a significant ac voltage at the Josephson oscillation frequency and its harmonics is present across the junction. In this case the displacement current may be neglected in the analysis.

The influence of weak link capacitance on the ac electrodynamics is reflected in the shape of weak link I-V curves. The effect of capacitance is illustrated in the following example. Let the relation $I_S = I_C \sin\varphi$ be true for a transient process. If the capacitance is large, the phase will change by the linear rule (135), and therefore there will be no constant component in the supercurrent

$$\overline{I}_S = I_C\,\overline{\sin}(\omega_V t + \text{const}) = 0\,, \tag{136}$$

i.e., the supercurrent will not contribute to $\overline{I}$ when $\overline{V} \neq 0$. If, however, $\beta \ll 1$, the phase will change at $\overline{I} \gtrsim I_C$ in a sharply nonlinear manner, the greater part of the period being close to $\pi/2 + 2\pi n$. Therefore the contribution of supercurrent in the $I-V$ curve is highly significant

$$\overline{I}_S \approx I_C \sin(\pi/2) = I_C\,. \tag{137}$$

3. Capacitance of weakly linked superconductors

While for the tunnel junctions the capacitance is usually quite high ($\beta \gg 1$), for the majority of weak links it is negligibly small

$$\beta \ll 1\,. \tag{138}$$

The displacement current in metals is comparable with the conduction current only at very high frequencies, namely, of the order of the plasma frequency ω_p or the inverse scattering time v_F/ℓ, both being $\sim 10^{14} - 10^{15}$ s^{-1} (see, for example, Ziman, 1972). Therefore in structures where the entire space between superconducting electrodes is completely filled with metal (say, in $S-N-S$ or $S-S'-S$-type sandwiches), the value of β is $\sim \omega_C/\omega_p \ll 1$.

In strong current concentration structures, R_N is proportional to the area of the weak link alone, while C

is proportional to a much greater area of the electrodes; therefore β becomes somewhat greater. In most cases, however, β remains much less than unity, the exception being the blob-type junctions [Fig. 1(h)] and some specially fabricated point contacts [Fig. 1(g)], for which the ratio of the electrode area to the area of conducting regions is as large as 10^4–10^6.

Thus, for the majority of weak links, the displacement current is negligibly small. This is the reason for the great practical interest in weak links, since capacitance has a parasitic action on the useful characteristics of Josephson junctions. But, on the other hand, this creates some difficulties in studying the processes in weak links, since even in simple experiments the voltage cannot be assumed to be constant in time, and the phase varies according to a more complicated relation than the linear dependence of Eq. (135).

B. General pattern of *I-V* curve

Although some details of the experimentally observed $I-V$ curves are as yet obscure, still their general pattern is more or less clear. We shall illustrate this with special reference to a case in which weak links may be described by tunnel theory [Eqs. (7) and (8)].

1. *I-V* curves in tunnel theory

In order to determine the $I-V$ curve of a structure with negligibly small capacitance within the framework of the tunnel theory, we have to find the frequency ω_V and coefficients A_n for which the current I [Eq. (8)] is constant and equal to a given value. Here in Eqs. (7) and (8) we may take $\omega=\omega_V$ because the voltage and phase oscillate only with the Josephson frequency and its harmonics.

Such a procedure has been carried out by McDonald *et al.* (1976) for the case $T=0$, and by Zorin and Likharev (1977) for an arbitrary temperature. Their calculated results are shown in Fig. 14 by solid lines. For the sake of comparison, the dashed lines in the same figure show the $\mathrm{Im}I_q(2e\overline{V}/\hbar)$ curves, which according to Eq. (15) represent the $I-V$ curve of a tunnel junction with high capacitance. We shall discuss the origin of the $I-V$ curves of weak links ($\beta \ll 1$, solid lines).

In the low-voltage range ($\overline{V} \ll V_C$) the mean current almost equals the critical level, due, as already mentioned, to the specific nature of the phase motion in this region. During the greater part of the Josephson oscillation period, the phase is close to $\pi/2$. Therefore the mean supercurrent is close to I_C(137). Once in each period the phase jumps by 2π, during which a voltage pulse of area ϕ_0/c [Eq. (118)] is generated at the weak link. This quick process, during which the current is transported primarily by normal electrons, lasts for a time of the order of

$$\tau_j=(\omega_C)^{-1}=\hbar/2eV_C\,, \tag{139}$$

and therefore the amplitude of the voltage pulse is

$$V_{\max}\approx\phi_0/c\tau_j=V_C\,. \tag{140}$$

As a consequence of these pulses, the weak link voltage spectrum is quite rich and contains about $V_C/\overline{V}\gg 1$ harmonics of the Josephson frequency.

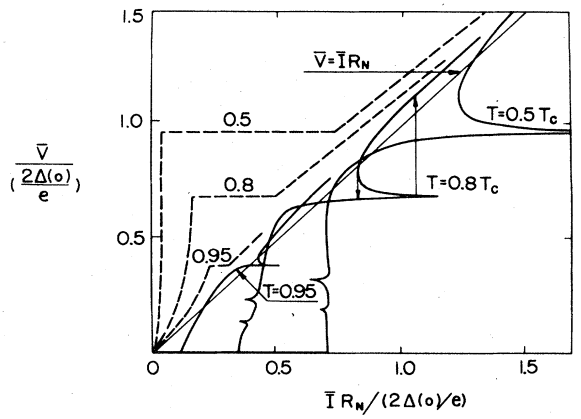

FIG. 14. $I-V$ curves of Josephson junctions within the framework of tunnel theory for negligibly small capacitance ($\beta \ll 1$, solid lines) and large capacitance ($\beta \gg 1$, dashed lines) at various temperatures. $I-V$ curves of weak links ($\beta \ll 1$) show singularities at voltages $\overline{V}=2\Delta/(2n+1)e$. Arrows show the approximate hysteresis occurring at the $I-V$ curve for $T/T_C=0.8$ when Riedel singularity is slightly smoothed.

In the high-voltage range, in contrast, the current is mainly transported by normal electrons, i.e., by the phase-independent component $\mathrm{Im}I_q$. Hence the voltage is almost constant in time

$$\overline{V}\approx\overline{I}R_N\,. \tag{141}$$

The phase changes almost by the linear relationship (135), supercurrent oscillates according to the same rule (15), and therefore its contribution to $\overline{I}$ is small. Thus, as $\overline{I}\to\infty$, the $I-V$ curve tends to the line (141) corresponding to normal resistance. This behavior, common to any type of weak link, may be regarded as "destruction of the superconductivity" only in a very narrow sense of the term. For example, in the tunnel theory, the supercurrent does have quite a finite amplitude despite the fact that $\overline{I}_S=0$, and can have a noticeable influence on other effects, for instance, the emission of microwave radiation at frequency ω_V. Therefore those parts of the $I-V$ curve where $\overline{V}\neq 0$ are preferably called "resistive" rather than "normal."

In the intermediate-voltage range ($\overline{V}\sim V_C$) the current transport mechanism gradually changes from that of a supercurrent to that of a normal current. Figure 14 shows that in the case of the tunnel theory, certain peaks at voltages

$$V_n=2\Delta(T)/(2n+1)e\,, \tag{142}$$

the so-called "odd subharmonics of the gap," are superimposed on this gradual transition. They appear as a result of the fact that for each such voltage, the argument of one of the terms in Eq. (8) is of the value $4\Delta(T)/\hbar$, at which the real parts of this component have a singularity (Fig. 2). Physically, this means that electron tunneling with absorption of the quantum of the nth oscillation harmonic is possible at the voltage of Eq. (142).

2. Current relaxation time

Using the tunnel theory as an illustration, we have demonstrated that the current is periodically redistributed

between the normal and the superfluid components in the process of Josephson oscillations in weak links. In this theory redistribution occurs in a time of the order of τ_j [Eq. (139)], which, according to the expression for V_C [Eqs. (10)–(14)], is $\sim \hbar/\Delta$ when $T \to 0$, and $\sim \hbar k_B T/\Delta^2$ when $T \to T_C$. This is why we may regard the constant $\omega_C = \tau_j^{-1}$ as the characteristic frequency of the Josephson junction.

As follows from the microscopic theory of superconductivity (Mattis and Bardeen, 1958), τ_j is the characteristic time of linear processes in any superconducting specimen. It is reasonable to call τ_j the current relaxation time because it describes the result of the following simple experiment. Suppose that, starting from the moment $t = 0$, a constant current is made to flow in a long ($L \gg \xi$), thin ($S \ll \lambda^2$) superconductor. At the initial moment this current will be transported by normal electrons. Then in a time τ_j the superconducting condensate will be accelerated to an equilibrium velocity at which the whole current will be carried solely by the condensate and, consequently, the electrical field will vanish.

From Eqs. (7) and (8) it follows that τ_j is the only characteristic time in tunnel theory. Hence even in such a nonlinear effect as the Josephson effect, it is possible to have only one relaxation process, namely, relaxation of the current. Therefore, order parameter relaxation times or nonequilibrium excitation relaxation times, which have a significant bearing on the dynamics of other nonstationary effects in superconductors, do not appear in tunnel theory. This is because the electrodes are constantly in a state of equilibrium.

As a result, the Josephson effect in tunnel junctions is at present the only one of the nonlinear effects in superconductors for which a complete microscopic theory of nonstationary processes exists. Unfortunately, this theory is not adequate to describe weak links of finite dimensions ($Lp_F/\hbar \gtrsim 1$).

3. Resistively shunted junction (RSJ) model

When the temperature is close to the critical temperature, the characteristic voltage [Eq. (14)] in the tunnel theory becomes much less than the gap voltage $2\Delta/e$. Thus, in the low-voltage range

$$\overline{V} \lesssim 2\Delta/e\,, \tag{143}$$

the equations of the tunnel theory can be highly simplified. Indeed, as is obvious from Fig. 2, in this range we may take

$$\mathrm{Re}\, I_p \approx I_C,\quad \mathrm{Im}\, I_q \approx V/R_N,\quad |\mathrm{Re}\, I_p|,\ |\mathrm{Im}\, I_p| \ll I_C \tag{144}$$

and, retaining only two main terms in Eq. (8), we get

$$I = I_C \sin\varphi + V/R_N,\quad d\varphi/dt = (2e/\hbar)V\,. \tag{145}$$

This equation is known as the Resistively Shunted Junction (RSJ) model.

In this model the time dependence of the phase satisfies a simple first-order differential equation.

$$\omega_C^{-1}\, d\varphi/dt + \sin\varphi = I(t)/I_C\,. \tag{146}$$

Consequently it is relatively easy to analyze qualitatively many processes in the Josephson junction and in circuits with these junctions. Such an analysis can be found, for example, in the review of Vystavkin *et al.* (1974), and in the monograph of Likharev and Ulrich (1977).

For the simple process of Josephson oscillations ($I = \overline{I}$ = const) we easily obtain the following expressions (Aslamazov et al., 1968; McCumber, 1968; Stewart, 1968; Aslamazov and Larkin, 1969)

$$\overline{V} = V_C[(\overline{I}/I_C)^2 - 1]^{1/2} \geq 0,\ \text{at}\ \overline{I} \geq I_C\,, \tag{147}$$

$$V(t) = V_C\, \frac{(\overline{V}/V_C)^2}{(\overline{I}/I_C) - \cos\omega_V t}\,. \tag{148}$$

Equation (147) shows that the I–V curve in the RSJ model has hyperbolic resistive branches, while Eq. (148) gives a quantitative description of those features of the Josephson oscillations which we discussed qualitatively in the previous pages.

The RSJ model is really significant, in that it gives a correct description of not only a very restricted class of weak links, which obey the tunnel theory, but also of almost any weak link at temperatures close enough to the critical one.

4. RSJ model in weak links

In the same paper in which they advance a theory to explain the dc Josephson effect in small weak links, Aslamazov and Larkin (1969) suggest that the ac processes occurring in weak links might be described by the RSJ model [Eq. (145)]. The logic of their argument runs approximately as follows:

The equation for the order parameter (21a) in a nonstationary case should contain some terms which depend on the time evolution of the order parameter. But if the weak link length tends to zero for a constant speed ($\sim \omega_C$) of Δ change, the magnitude of time-dependent terms should remain the same, while the gradient term grows as L^{-2}. Therefore, when $L \to 0$, the time-dependent terms may be neglected, and thus the Laplace equation (31), which leads to the solution (34), may be used as before.

In the equation for the current (21b), we have to take the normal current $\mathbf{j}_N$ into account when $V \neq 0$. An analysis of the linear nonstationary processes in superconductors (Mattis and Bardeen, 1958) shows that, for moderate frequencies ($\hbar\omega \ll 2\Delta$), we can use the same expression for the supercurrent as in the stationary case, but with the addition of the normal current

$$\mathbf{j}_N(t) = \sum_\omega \sigma(\omega)\mathbf{E}_\omega e^{i\omega t},\quad \text{when}\ \mathbf{E}(t) = \sum_\omega \mathbf{E}_\omega e^{i\omega t}\,. \tag{149}$$

If $T \to T_C$, for all frequencies $\sigma(\omega)$ tends to σ_N, the conductivity of a material in its normal state. Hence we have

$$\mathbf{j}_N = \sigma_N \mathbf{E},\quad \text{when}\ T \to T_C\,. \tag{150}$$

It is therefore natural to assume that for such nonlinear processes as the Josephson effect, we may also use Eq. (150), adding the current $\mathbf{j}_N$ to the supercurrent $\mathbf{j}_S$ [Eq. (21b)]. Thus, after repeating all the calculations of the AL theory, we arrive at Eq. (145), i.e., at the RSJ model. Nonetheless, it may be noted that the exact conditions for the applicability of this model are far from being clear.

5. Main deviations from the RSJ model

Experiments with a variety of weak links of sufficiently small dimensions ($L, W \lesssim \xi$) have shown that near the critical temperature the $I-V$ curves are indeed close to the pattern predicted by the RSJ model, provided account is taken of the influence of intrinsic and external fluctuations which are significant when $T \to T_C$. This influence is large if the critical current of a weak link is less than or comparable to the characteristic amplitudes of external (usually relatively low-frequency) interferences I_{fl} and of the intrinsic thermal noise of the junction I_{fh} (see, for example, Likharev and Ulrich, 1977). I_{fh} depends on temperature only

$$I_{fh} = 2ek_B T/\hbar, \quad I_{fh}[\mu\text{A}] \approx 0.042T[\text{K}], \tag{151}$$

while I_{fl} depends on the experimental setup, and may be as high as 10–30 μA. By appropriate filtering, it can, however, be kept below I_{fh}.

Fluctuations smooth out the $I-V$ curves as shown in Fig. 15. Therefore, as $I_C(T)$ increases, at first an "embryo" with a characteristic size $I_f = \max[I_{fh}, I_{fl}]$ is formed on the $I-V$ straight line of a normal junction, its amplitude increasing as I_C^2. With a further increase in the current ($I_C \gtrsim I_f$), the $I-V$ curve becomes nearly hyperbolic [Eq. (147)], with only the angles of transition from the superconducting region to the resistive branches being smoothed out. In well designed setups, where $I_{fl} \lesssim I_{fh}$, the influence of fluctuations is hardly noticeable

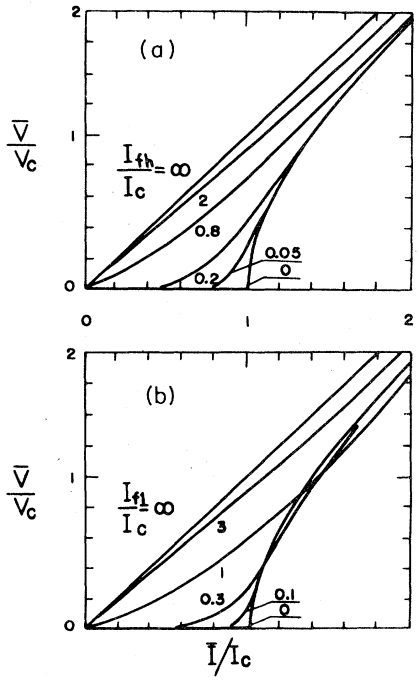

FIG. 15. Smoothing of $I-V$ curve (a) by the intrinsic thermal noise and (b) by low-frequency external interferences. $I-V$ curves are taken according the RSJ model, intrinsic noise is considered as white (δ-correlated), and external fluctuations are expected to have normal (Gauss) distribution (after Stratonovich, 1967; Ambegaokar and Halperin, 1969; Kanter and Vernon, 1970).

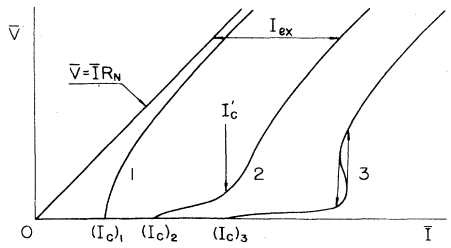

FIG. 16. $I-V$ curve of a short weak link according to the RSJ model (1) and experimental $I-V$ curves showing (2, 3) the excess current effect; (2, 3) "bump" and (3) hysteresis at lower temperatures (3) (schematically).

at critical currents of more than tens of μA.

Nevertheless, the $I-V$ curves of small weak links[28] are more or less close to the hyperbolic form only in a narrow region near T_C (Fig. 16). At lower temperatures, at least three peculiarities not consistent with the RSJ model appear on the $I-V$ curves (see, for example, Clarke and Lindelof, 1976; Gubankov *et al.*, 1977; Klapwijk *et al.*, 1977b):

(i) As the current increases, the voltage tends to a straight line

$$\bar V = R_N(\bar I - I_{ex}) = \bar I R_N - V_{def}, \tag{152}$$

which is shifted up the I axis by an "excess current" I_{ex} relative to the normal $I-V$ curve, or in other words, by an amount V_{def} down the V axis. The excess current is usually of the order of I_C (Pankove, 1966).

(ii) As soon as the current I exceeds I_C, the voltage grows relatively slowly in the first stages with a slope

$$R_d = d\bar V/d\bar I \ll R_N, \tag{153}$$

and thereafter, when the current attains a specific value I_C' the voltage begins to increase rapidly, so that the differential resistance R_d sharply increases and then proceeds almost as in the RSJ model. This behavior is usually referred to as a "bump" on the $I-V$ curve.

(iii) When the temperature falls to a certain value, the differential resistance at points above the bump becomes infinite, and a further reduction in T gives rise to a negative slope region on the $I-V$ curves. If the internal resistance of the current source is high ($R_e \gg R_N$), it results in the hysteresis observed on the $\bar V(\bar I)$ dependence (Fig. 16).

At present, at least one theoretical explanation has been found for each of these phenomena within the framework of the models, which are all generalizations of the RSJ model. Let us start discussion of the models.[29]

---

[28] Here and in the succeeding pages we shall discuss only the best investigated case of dirty weak links ($l \ll L$), of which all the bridges are a particular case. In relatively pure structures, in addition to the peculiarities listed below, some small singularities are observed on $I-V$ curves at voltages $V_n = 2\Delta/ne$; see, for example, Puma and Deaver, 1971; Gregers-Hansen *et al.*, 1973. They were also discussed by Werthamer (1966), and by Hasselberg *et al.* (1974).

[29] The $I-V$ curves of wide weak links ($W \gtrsim \lambda_{eff}$) have peculiarities of their own; see Sec. VII.

C. Description by time-dependent Ginzburg-Landau (TDGL) equations

1. TDGL approximation

The main difficulty in the microscopic theory of nonlinear nonstationary effects in superconductors (Gor'kov and Eliashberg, 1968) lies in the fact that the gap in the electron energy spectrum changes with the variations in $|\Delta|$, together with the position of square-root singularity in the density of the electron states (Bardeen *et al.*, 1957). But in some cases this singularity does not exist, although the order parameter is finite in magnitude. This happens, for instance, in strong magnetic fields or in superconductors with a high concentration of paramagnetic impurities (see, for example, De Gennes, 1966).

Gor'kov and Eliashberg (1968b) have shown that the microscopic theory for this case allows for a simple way of generalizing GL equations [Eqs. (21)] in a nonstationary case.[30] These Time-Dependent Ginzburg-Landau (TDGL) equations differ from the stationary equations (21) in that their right-hand sides contain new terms

$$\tau_\Delta\left(\frac{\partial}{\partial t}+i\frac{2e}{\hbar}\mu\right)\Delta\,, \tag{154a}$$

$$\sigma_N\left(-\nabla\mu-\frac{1}{c}\frac{\partial \mathbf{A}}{\partial t}\right). \tag{154b}$$

Here μ and $\mathbf{A}$ are the scalar and vector potentials of the electromagnetic field; hence Eq. (154b) gives the normal current $\sigma_N\mathbf{E}$.

Let a uniform specimen ($\nabla=0$), free of current ($\mu=\mathbf{A}=0$), exist in a state with $\Delta=0$ at $T<T_C$. From Eq. (21a), after adding (154a), it follows that the initial stage of the Δ variation will be described by the equation

$$\tau_\Delta(\partial\Delta/\partial t)=\Delta\,. \tag{155}$$

Hence it is obvious that the constant τ_Δ has the meaning of a characteristic time of the order parameter modulus relaxation. For the case examined by Gor'kov and Eliashberg (1968b) the time constants τ_Δ and τ_j are related by the equation

$$\tau_\Delta/\tau_j=12\,. \tag{156}$$

However, the TDGL equations have repeatedly been examined for their feasibility for the usual ("gap") superconductors (Maki, 1963; Schmid, 1966; Abrahams and Tsuneto, 1966). In such a phenomenological generalization of GL equations, the ratio between τ_Δ and τ_j remains close to Eq. (156). Indeed, substituting the expression for ξ in the dirty limit into (21a), and rewriting it in the form of a stationary diffusion equation (for the sake of simplicity, we shall take $\mathbf{A}=0$)

$$D\nabla^2\Delta+\frac{8k_B(T_C-T)}{\pi\hbar}\left[\pm 1-\frac{|\Delta|^2}{\Delta_0^2}\right]\Delta=0\,. \tag{157}$$

If we assume that Eq. (157) can be generalized as an ordinary diffusion equation by the mere addition of $\partial\Delta/\partial t$, then we obtain the first TDGL equation with

$$\tau_\Delta=\pi\hbar/8k_B(T_C-T)\,. \tag{158}$$

Now using Eqs. (14) and (18) for $\omega_C=\tau_j^{-1}$ at $T\approx T_C$, we find

$$\tau_\Delta=(\pi^4/14\zeta(3))\tau_j\approx 5.79\,\tau_j\,, \tag{159}$$

which differs from Eq. (156) only by a factor of about 2. Of course, extreme caution should be taken in using this value, as the TDGL generalization is not justified in the case of gap superconductors.[31]

2. Boundary effects and TDGL equations

The TDGL equations not only provide a simple means of describing the relaxation of $|\Delta|$ in time, but also give a simple description of a radically different, but equally fundamental process, that is, of the flow of current normal to the interface between normal and superconducting phases (Reiger et al., 1971; Yu and Mercereau, 1972; Volkov, 1974). Similar effects occur during the motion of Abricosov vortices (Kupriyanov and Likharev, 1972).

We shall rewrite these equations for a one-dimensional geometry $\Delta=\Delta(x)$, again considering the case of small cross sections and low fields, where we may take $\mathbf{A}=0$.

$$\tau_\Delta\left(\frac{\partial\Delta}{\partial t}+i\frac{2e}{\hbar}\mu\right)\Delta=\xi^2\frac{\partial\Delta^2}{\partial x^2}+\Delta\left(\pm 1-\frac{|\Delta|^2}{\Delta_0^2}\right), \tag{160a}$$

$$j=C_j\,\mathrm{Im}\left(\Delta^*\frac{\partial}{\partial x}\Delta\right)-\sigma_N\frac{\partial\mu}{\partial x}. \tag{160b}$$

After expressing Δ in the form $|\Delta|\exp(i\chi)$, and separating the real and imaginary parts in (160a), we find that the latter give only the natural equality $\partial j/\partial x=0$. After differentiating (160b) with respect to x, we obtain a system of equations equivalent to (160)

$$\tau_\Delta\frac{\partial|\Delta|}{\partial t}=\xi^2\frac{\partial^2|\Delta|}{\partial x^2}+\left[\pm 1-\frac{|\Delta|^2}{\Delta_0^2}-\left(\xi\frac{\partial\chi}{\partial x}\right)^2\right]|\Delta|\,, \tag{161a}$$

$$\tau_\Delta\left(\frac{\hbar}{2e}\frac{\partial\chi}{\partial t}+\mu\right)(|\Delta|^2/\Delta_0^2)=\xi^2\tau_j\frac{\partial^2\mu}{\partial x^2}. \tag{161b}$$

The first equation describes relaxation of $|\Delta|$ to the stationary value $|\Delta|(x)$ in time, while the second gives the time and space variations of μ, i.e., of the electrical field.

Let, for instance, the distribution $\Delta(x)$ be established at the interface between a normal and a superconducting phase in the absence of current. The order parameter changes, according to Eq. (161a), at a distance $\sim\xi$ from 0 in the N phase to Δ_0 in the S phase (Fig. 17). Now if a weak current is induced to flow through the S-N interface [see the experiments of Pippard *et al.* (1971), Yu and Mercereau (1972, 1975), Harding *et al.* (1974)], $\xi\partial\chi/\partial x$ in (161a) will be small, the distribution $\Delta(x)$ will not change, and Eq. (161b) will have a solution

$$\partial\chi/\partial t=-(2e/\hbar)\mu_p=\mathrm{const},\quad \mu=\mu(x)\,.$$

This shows that the superconducting condensate has

[30] Recently the validity of this generalization has been demonstrated experimentally (Amato and McLean, 1976).

[31] The TDGL type of equation may possibly hold true in S-N-S structures, as there is no gap in the excitation spectrum of a material with $\Delta=0$.

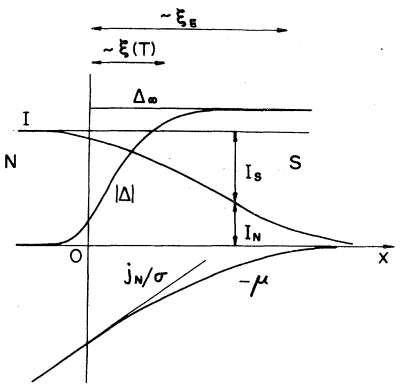

FIG. 17. Modulus $|\Delta|$ of order parameter, electric field potential μ, normal current and supercurrent vs distance from normal–superconductor interface (schematically).

the same potential μ_p, related to the order parameter phase by the Josephson equation (4), over the entire region with $\Delta \neq 0$ (even in those places where the electrical field $E = -\nabla\mu$ exists). As regards μ, it defines the potential of normal electrons, and its evolution in space is given by Eq. (161b)

$$\xi_\mu^2 \frac{d^2\mu}{dx^2} = (\mu - \mu_p)(\Delta^2/\Delta_0^2), \quad \xi_\mu = \xi(\tau_j/\tau_\Delta)^{1/2}. \tag{162}$$

This equation describes the change of μ from a constant value ($\mu = \mu_p$) inside the region S to a linear increase ($\partial\mu/\partial x = -j/\sigma_N$) inside the region N (Fig. 17). This change, and consequently the conversion of supercurrent into a normal current, takes place over a length ξ_μ.

Thus the TDGL equations contain two characteristic length constants (ξ and ξ_μ) which describe the scale of space variations in the modulus of the order parameter Δ and normal electrical current j_N, respectively. When Eqs. (156) or (159) are valid, ξ_μ is somewhat less than ξ.

3. Applications of TDGL equations

It is relatively easy to analyze the nonlinear ac processes occurring in superconductors with the help of TDGL equations. They have, therefore, been applied to many specific processes, such as the penetration of a strong microwave field into a bulk superconductor (Gor'kov and Eliashberg, 1968c), the action of a microwave field on thin films of infinite (Kulik, 1969a) and of finite (Likharev, 1971c) dimensions, the motion of Abricosov vortices under the action of dc current (Schmid, 1966; Gor'kov and Kopnin, 1971; Kupriyanov and Likharev, 1972; Danilov *et al.*, 1974) and microwave fields (Kupriyanov and Likharev, 1975), fluctuations at $T > T_C$ (Schmid, 1969) and $T < T_C$ (Kulik, 1970), and processes in superconducting thin filaments when $\bar{I} > I_C$ (Fink, 1973; Fink and Poulsen, 1974, 1975; Likharev, 1974; Kramer and Baratoff, 1977). These equations have also been used in analyzing the processes in weak links (Reiger *et al.*, 1972; Volkov, 1974; Likharev and Yakobson, 1974, 1975b, c; Volkov and Kasatkin, 1974; Jensen and Lindelof, 1976; Kramer and Baratoff, 1977).

Setting aside the last group of papers for the time being, we find that a comparison of the results derived from the TDGL equations with the experimental data on gap superconductors shows (Kupriyanov and Likharev, 1976) that this approximation does not hold true for all the above processes. This is quite evident, especially, in the experiments on the measurement of the uniform relaxation time of the order parameter. Thus, for thin film strips of tin (Peters and Meissner, 1973; Andratskii *et al.*, 1976), it was found that τ_Δ is $\sim 10^{-10}$ s for $T \approx 0.9\, T_C$, and the temperature dependence of τ_Δ is close to $(T_C - T)^{1/2}$. This is not consistent with Eqs. (156) and (159), which give $\tau_\Delta \sim 10^{-11} - 10^{-12}$s and $\tau_\Delta \propto (T_C - T)^{-1}$.

A noticeable discrepancy is also observed for the processes in long filaments when $\bar{I} > I_C$, for which the experiments (Scopol *et al.*, 1974b; Meyer and Tidecks, 1976; Klapwijk *et al.*, 1977) give somewhat greater length for the penetration of normal current into superconductors than the length derived from Eq. (162). Essentially, a value of τ_Δ cannot be chosen so as to obtain agreement with the two groups of experiments, because in the first group τ_Δ has to be greater than τ_j, whereas in the second group it is vice versa. (The discrepancy can be explained only by taking into account the nonequilibrium distributions of quasiparticles—see Sec. V.D.)

In a large group of experiments (mainly on the motion of Abricosov vortices) however, the TDGL equations give results in satisfactory agreement with experiment, provided $\tau_\Delta/\tau_j \sim 10$. In these experiments Δ changes at distances $\sim \xi(T)$, i.e., approximately as in weak links of length $L \sim \xi$. This gives grounds for believing that the TDGL equations may, at least qualitatively, give a correct description of some of the effects in weak links if we take $\tau_\Delta \sim 10\tau_j$.

4. Processes in weak links

Several essential errors were committed in the paper (Reiger *et al.*, 1972) in which the TDGL approximation was first applied to an analysis of ac processes in weak links.[32] They were subsequently detected and eliminated by Likharev and Yakobson (1975b, c).

For weak links of sufficiently small length [$L \lesssim \xi(T)$], according to the results derived in Sec. III, we may neglect the term $\Delta (\doteq 1 - |\Delta|^2/\Delta_0^2)$ in Eq. (160a) as compared to the gradient term $\sim (\xi/L)^2\Delta$ and to the relaxation term $\sim (\tau_\Delta \partial\Delta/\partial t)$. The characteristic value of $\partial/\partial t$ is $\sim \tau_j^{-1}$, where τ_j is a parameter of the electrode material, or $\sim \tau_j^{-1}A^2$, if we mean τ_j of the weak link material. From

[32] The fundamental error is that τ_Δ has been taken as zero in all numerical calculations. It can easily be shown that in this case the system (160) is reduced to a phase equation similar to that given by the RSJ model.

$$I = I_S(\varphi) + V/R_N,$$

where $I_S(\varphi)$ is the dc current-phase relation. It follows, in particular, from this equation that an excess current only exists in weak links for which $I_S(\varphi)$ is multivalent, which is in obvious contradiction to experiment. The validity of this model for not very large currents inferred by Jackel *et al.* (1976a) is, in all probability, a consequence of the rather limited amount of experimental data used in the analysis.

Eq. (160a) it then follows that the TDGL equations for short links have a dimensionless parameter

$$\gamma = \frac{\tau_\Delta}{\tau_j}\left(\frac{L}{\xi}\right)^2 A^2, \tag{163}$$

which characterizes the influence of the finite relaxation time of the order parameter. According to the estimate of τ_Δ/τ_j made above, γ can be taken as small for short structures, i.e., $\gamma \to 0$ if $L/\xi \to 0$. In this case the system of equations (160) under the boundary conditions of the ODSEE model [Eq. (64)] makes possible a complete analytical solution.

First, let us consider a region near the critical current: $\bar{I} \gtrsim I_C$. Since $\gamma \to 0$, the relaxation terms make only a small correction to the AL theory. According to these equations, Δ is given by Eq. (71), and μ is the same as in the normal state

$$\mu = \mu_1 - \frac{x}{L}\mu_2, \quad V = \mu_1 - \mu_2. \tag{164}$$

After substituting the solution into the left-hand side of (160a), we obtain the correction $\tilde{\Delta}$ to this solution. Now by substituting the total solution $(\Delta_{AL} + \tilde{\Delta})$ in (160b), and then integrating it with respect to length $(0 \lesssim x \lesssim L)$, we obtain an expression for the current

$$I = I_C \sin\varphi + \frac{V}{R_N}\left[1 + \frac{\gamma}{15}(1 - \cos\varphi)\right], \quad \text{if } \gamma/15 \ll 1, \tag{165}$$

where I_C has the same value as in the dc effect.

Now consider the region $\bar{I} \gg I_C$, in which the normal current is much greater than the supercurrent, allowing us to use Eq. (164) as a first approximation for μ. In this case the solution of the TDGL equation for Δ may be written as

$$\Delta(x,t) = \Delta\left[\Psi\left(\frac{x}{x_0}\right)\exp(i\chi_1) + \Psi\left(\frac{L-x}{x_0}\right)\exp(i\chi_2)\right], \tag{166}$$

where the function Ψ describes the decay of the electrode wave function inside the weak link and satisfies the equation

$$\frac{d^2\Psi(u)}{du^2} + iu\Psi(u) = 0, \quad \Psi(0) = 1, \quad \Psi(L/x_0) = 0. \tag{167}$$

Here x_0 is the characteristic length which depends on $\bar{V}$, i.e., on the position of the bias point on the $I-V$ curve

$$x_0/L = \eta^{-1/3}, \quad \eta = \gamma\frac{\bar{I}}{I_C} = \left(\frac{L\Delta}{\xi\Delta_0}\right)^2 \omega_V \tau_\Delta. \tag{168}$$

After finding the solution of Eq. (167) in terms of Airy functions (see, for example, Abramowitz and Stegun, 1965), then substituting (166) in Eq. (160b), and integrating with respect to x, we obtain an expression for the current, which may be written as follows (Jensen and Lindelof, 1976)

$$I = I_1(\eta)\sin\varphi + I_2(\eta)\cos\varphi + (V - \Delta V(\eta))/R_N. \tag{169}$$

The dependences of I_1, I_2, and ΔV on η, i.e., on the position of the bias point, are shown in Fig. 18.

We note here that Eqs. (165) and (169) agree in the intermediate range $1 \ll \bar{I}/I_C \ll \gamma^{-1}$; therefore together they give a complete solution which is valid for any current through the weak link.

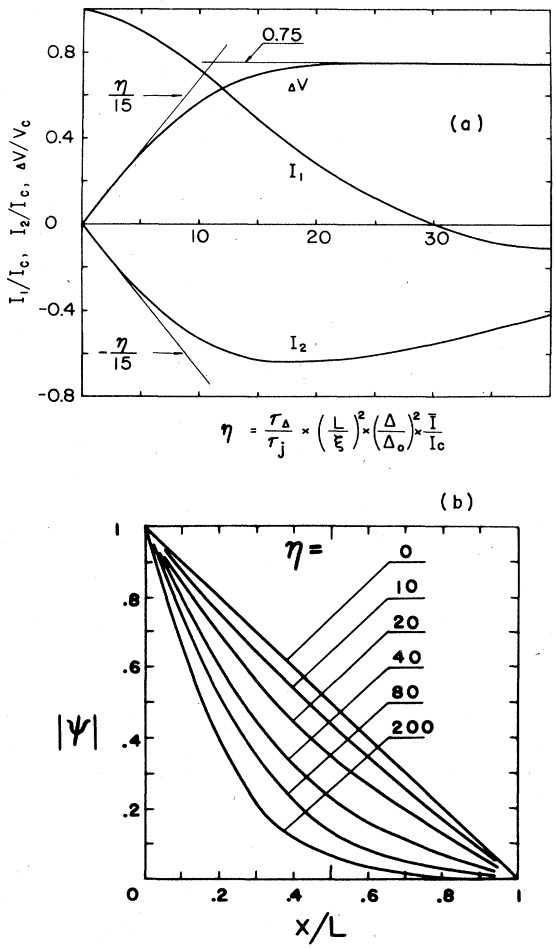

FIG. 18. (a) Frequency dependence of I_1, I_2, and ΔV from Eq. (169), and (b) $|\psi|$ distribution over the length of a weak link at different currents in TDGL approximation. Quantities $I_{1,2}$ give the amplitudes of Josephson supercurrent and fall as $\eta^{\frac{1}{4}}\exp(-\frac{\sqrt{2}}{3}\eta^{\frac{1}{2}})$ at $\eta \to \infty$. Deviation of V from the normal value (ΔV) is close to $\bar{V}(\gamma/15) = V_C(\eta/15)$ when $\eta \lesssim 5$, and is almost constant $(\Delta V \approx V_{def})$ at $\eta \gtrsim 20$, describing the "excess current" effect: $I_{ex} = \Delta V/R_N \approx 0.75\, I_C$. Function ψ enters in to Eq. (166) and shows the decrease of the electrode wave function in the weak link. At $\eta = 0$ $\psi = 1 - x/L$, and ψ tends to the universal function of x/x_0 (Fig. 19) when $\eta \to \infty$. After Likharev and Yacobson, 1975b,c; Jensen and Lindelof, 1976.

5. Discussion

Equation (165) shows that the $I-V$ curve of a short weak link is nearly hyperbolic (as predicted in the RSJ model). Its asymptote, however, differs from the normal $I-V$ curve by ΔV (Fig. 18). For small currents this gives only a slight decrease in the effective resistance of the weak link

$$\frac{R_N - R_{eff}}{R_N} = \frac{\gamma}{15} = \frac{1}{15}\frac{\tau_\Delta}{\tau_j}\left(\frac{L\Delta}{\xi\Delta_0}\right)^2. \tag{170}$$

For large current ΔV tends to the constant

$$\Delta V \to V_{def} = 2\epsilon V_C/R_N, \quad \epsilon \approx 0.375, \quad V_{def}[\mu V] \approx 475(T_C - T)[K]. \tag{171}$$

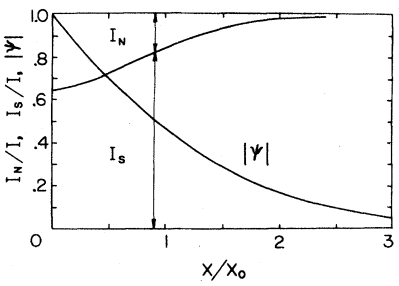

FIG. 19. Space dependences of $\psi \propto \Delta$, I_N, and I_S near the weak link–bank boundary at the large currents ($x_0 \ll L$; $\eta \gg 1$) according to the ODSEE–TDGL model. Normal current I_N is equal to zero in the bank, so I_N and I_S have jumps at the boundary. Variables Δ and μ are continuous. After Likharev and Yacobson, 1975b, c.

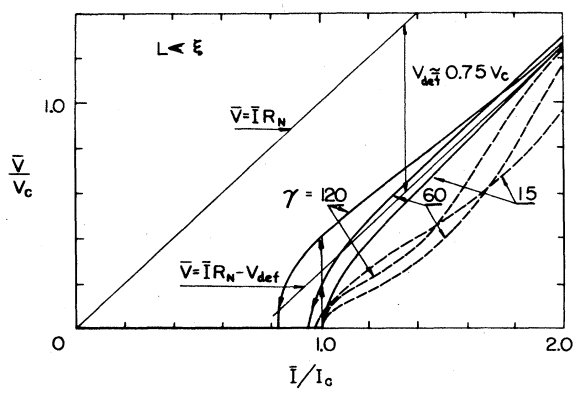

FIG. 20. $I-V$ curve of short ($L \lesssim \xi$) weak link, calculated numerically from Eqs. (160) for various γ [Eq. (163)]. Dashed lines show results of Jensen and Lindelof (1976) obtained from Eq. (169), which is really applicable only if $\gamma \ll 1$ and/or $\bar{I} \gg I_C$. Figure shows that TDGL equations in fact do not describe the "bumps" on $I-V$ curves. Small hysteresis appears on $I-V$ curves at very large γ.

Consequently the $I-V$ curve tends to the straight line (152) with an excess current $I_{ex} = V_{def}/R_N \approx 0.75 I_C$ which does not depend on τ_Δ and other parameters of the weak link material (T_C', ξ), and on L as well.

The reason for the nonzero values of I_{ex} within the framework of the TDGL equations is that with increasing current, the distribution of $|\Delta|$ over the link length begins to deviate from that derived in the AL theory [Eq. (71)], where $\Psi = 1 - x/L$ (see Fig. 18b). When the length x_0, which characterizes the level of current-caused suppression of the order parameter, becomes less than L, the function Ψ begins to decay from 1 at the banks to zero just over this range. Thus the electrode wave functions overlap range decreases and the Josephson effect, characterized by the supercurrent amplitude $I_A = (I_1^2 + I_2^2)^{1/2}$, is suppressed.

For large currents ($\eta \gg 1$), the wave functions decay so rapidly that they are hardly overlapped at all. Therefore the weak link is wholly in a normal state, except that $|\Delta|$ is different from zero in regions of length x_0 near the banks, where the superconductivity is supported by the proximity effect between the weak link and the banks (Fig. 19). In these regions, part of the current is transported by the superfluid component, hence the total voltage drop V across the weak link is less than the normal one by V_{def}. Thus the "excess current" effect[33] is a natural phenomenon in the TDGL model, and it is described by Eq. (171), which does not depend on τ_Δ. The latter fact suggests that the result is not very critical to changes in the model.

Other effects, such as bumps and hysteresis on the $I-V$ curves, do not appear for short weak links in this model. The following procedure was adopted by Jensen and Lindelof (1975) and Clark and Lindelof (1976): the equation for the phase $\varphi(t)$ derived from Eq. (169) was solved for all currents. A bump resembling the experimentally observed one appears on the $I-V$ curves if $\gamma \gg 1$.

It should, however, be borne in mind that Eq. (169) is only valid when either $\gamma \ll 1$, or $\gamma \sim 1$ and $\bar{I} \gg I_C$. If $\gamma \gtrsim 1$, and $\bar{I} \sim I_C$, the system of equations (160) has to be solved numerically (Likharev and Yakobson, 1975b, c; Kramer and Baratoff, 1977). Such numerical results are shown in Fig. 20 by solid lines. It is obvious that there is no bump on the $I-V$ curves, and the only new situation is the appearance of slight hysteresis on the $I-V$ curve near the critical current. Such a "relaxation" mechanism (Likharev, 1974b; Likharev and Yakobson, 1975b; Song, 1976) can hardly explain the experimentally observed hysteresis, since a very large τ_Δ/τ_j has to be introduced.

It is also easy to demonstrate that potential variations inside the weak links (Yu and Mercereau, 1976) can be explained within the framework of the TDGL equations.

D. Nonequilibrium quasiparticles

1. Nonequilibrium excitations

In the TDGL approximation no account is taken of possible deviations from the equilibrium concentration and the energy distribution of the two most important types of quasiparticle excitations in superconductors, namely, normal electrons and phonons.[34] These deviations, however, can be quite high in weak links, as nonequilibrium electrons are intensively generated when the order parameter suffers periodic variations. On relaxing in energy, these electrons transfer this energy in the form of phonons to the crystal lattice. Therefore the concentration and distribution of quasiparticles may differ markedly from their equilibrium values.

On the other hand, the quasiparticle distribution has considerable influence on the order parameter. For example, the suppression of Δ as $T \to T_C$ is due to the in-

[33] Our analysis has shown that this should be called a "voltage deficiency" effect.

[34] The influence of photons is only significant at the external irradiation, because the probability of photon generation in the bulk of the superconductor itself is extremely low (Fife and Gygax, 1972).

creasing number of quasiparticles with increasing temperature. Therefore even a small deviation in this number from the equilibrium value will have a significant influence on $|\Delta|$, especially when $T \approx T_C$.

Today, we know how the excitation and relaxation of nonequilibrium excitations occur in spatially uniform specimens carrying no current: see, for example, comprehensive reviews by Langenberg (1975) and by Chang and Scalapino (1977). The generation and relaxation of quasiparticles under strong gradients of Δ have, however, as yet been little studied, because the condensate and quasiparticles form here a rather complicated coupled system. At present, therefore, we can only give a qualitative description of these processes.

We shall begin with the important case in which the deviations of the phonon subsystem from equilibrium may be disregarded, and consequently only the distribution of normal electrons is out of equilibrium.

2. Nonequilibrium electrons

A general picture of the relaxation of a superconductor to its stationary state from an initial nonequilibrium state has been examined in several papers (Galaiko, 1971; Eliashberg, 1971; Larkin and Ovchinnikov, 1973; Aronov and Gurevich, 1974; Kulik, 1976). Qualitatively, it can be explained as follows: an ordered condensate of the Cooper pairs and a particular density of states of normal electrons is formed in a time interval $\hbar/|\Delta| \sim 10^{-12}$ s. As is known (Bardeen *et al.*, 1957), this density is

$$N(\epsilon) = \begin{cases} N(0)\epsilon/(\epsilon^2 - |\Delta|^2)^{1/2}, & \text{at } \epsilon > |\Delta|, \\ 0, & \text{at } \epsilon < |\Delta|, \end{cases} \tag{172}$$

where ϵ is the energy measured from the Fermi level.

These states are populated by electrons with the equilibrium density

$$n(\epsilon) = [\exp(\epsilon/k_B T) + 1]^{-1} \tag{173}$$

in a much larger time interval, which is of the order of the energetic relaxation time in the normal state τ_ϵ. The frequent (in times of $\sim l/v_F \sim 10^{-13} - 10^{14}$ s) collisions of electrons with impurities do not contribute to this relaxation, as they are elastic and do not change the energy of electrons. Therefore τ_ϵ is of the order of the electron–phonon collisions time. The density of phonons at temperatures far below the Debye temperature $T_D \sim 10^2$ K is rather low ($\propto T^3$)

$$\frac{\tau_\epsilon}{\hbar} \approx \frac{1}{k_B T}\left(\frac{T_D}{T}\right)^2 \gg \frac{1}{k_B T_C}. \tag{174}$$

Calculations (Kaplan *et al.*, 1976) give τ_ϵ of the order of 10^{-9} to 10^{-10} s for a majority of superconductors, and $\tau_\epsilon \sim 10^{-6}$ s for aluminum ($T_C \approx 1.19$ K) and zinc ($T_C \approx 0.87$ K).

On the other hand, this equilibrium value of $|\Delta|$ itself depends on the distribution of the normal electrons $n(\epsilon)$ by virtue of the self-consistency equation

$$|\Delta| = \lambda N(0) \int_{|\Delta|}^{k_B T_D} \frac{|\Delta| f(\epsilon) d\epsilon}{(\epsilon^2 - |\Delta|^2)^{1/2}}, \quad f(\epsilon) = 1 - 2n(\epsilon), \tag{175}$$

where λ is an electron–phonon coupling parameter.

Therefore the equilibrium values of $f(\epsilon)$ and $|\Delta|$ are established simultaneously in the time $\sim \tau_\epsilon$ [near T_C in a time $\sim \tau_\epsilon(k_B T_C/\Delta)$], i.e., in $\sim 10^{-9}$ s for a typical case.

If for some reason $|\Delta|$ varies with a frequency greater than τ_ϵ^{-1}, then some stationary electron distribution is established in the specimen, which in general differs from the equilibrium distribution. Its influence on the order parameter may be accounted for as follows.

Let the temperature be close to the critical value, i.e., we are dealing with a region where the GL equations (21) are applicable. The term in square brackets appears in (21a) from Eq. (175) after substitution of the stationary distribution, $f(\epsilon) \approx \epsilon/2k_B T$, from Eq. (173), and taking into account the smallness of $|\Delta|$. Making the same calculations for an arbitrary $f(\epsilon)$ and taking as before $|\Delta| \ll k_B T$, we find that Eq. (21a) is satisfied if T_C in (12) is replaced by a new effective critical temperature

$$k_B T_C' = k_B T_C \left\{1 + \int_{|\Delta|}^{\infty} \left[f(\epsilon) - \frac{\epsilon}{2k_B T}\right] \frac{d\epsilon}{(\epsilon^2 - |\Delta|^2)^{1/2}}\right\}. \tag{176}$$

Equation (176) shows that if $f(\epsilon)$ is greater than its value in equilibrium (i.e., the electron density $n(\epsilon)$ is less than its equilibrium value), T_C' may increase, i.e., enhancement of superconductivity occurs. The value of T_C' is especially sensitive to changes of $f(\epsilon)$ in the region $\epsilon \approx |\Delta|$, and therefore even a simple redistribution of electrons towards higher energies, with the total concentration conserved, can raise T_C'.

3. Current enhancement of superconductivity

Aslamazov and Larkin (1976) advanced a theory which provides an explanation of the bumps on the $I-V$ curves of weak links. They considered a one-dimensional geometry identical with the ODSEE model for the case of small lengths ($L \ll \xi$). The critical current in this case is given by the AL theory [Eq. (41)]. If the current exceeds the critical value, the frequency of the Josephson oscillations rapidly exceeds τ_ϵ^{-1}, and a stationary nonequilibrium distribution $f(\epsilon)$ is established in the specimen. After calculating this distribution with the help of equations derived earlier (Larkin and Ovchinnikov, 1975), Aslamazov and Larkin obtained the following expression

$$f(\epsilon) = \begin{cases} (\Delta/2k_B T) \times [1 - (1 - \epsilon/\Delta)^{5/4}], & \text{at } \epsilon < \Delta, \\ \epsilon/2k_B T, & \text{at } \Delta < \epsilon \ll k_B T, \end{cases} \tag{177}$$

where Δ is the equilibrium value of $|\Delta|$ at the banks [Eq. (12)]. The deviation of $f(\epsilon)$ from its equilibrium value occurs only for $\epsilon < \Delta$, because high-energy electrons may easily diffuse from weak links into the banks in a time $\sim L^2/D \ll \tau_\epsilon$. For low-energy electrons there are no free states in the banks [Eq. (172)], and they are reflected back into the weak link from those points where $|\Delta|$ is equal to their energy ϵ (Andreev, 1964).

Since $f(\epsilon)$ appears to be greater than the equilibrium value, superconductivity is enhanced, i.e., the amplitude of the supercurrent in ac Josephson effects becomes greater than the critical current I_C. Therefore the Josephson oscillations take place just as in the RSJ model with increased critical current I_C' and the $I-V$

curves are close to hyperbolic everywhere, except in a small region when $\overline{V} \to 0$, where the average current $\overline{I}$ sharply falls from I'_C to I_C. This corresponds to the usual "bump" on the $I-V$ curve.

In order to find I'_C, we have to substitute Eq. (177) into Eq. (176), and thus find the new value of the critical current from Eq. (21) for the new effective value of T'_C. For T very close to T_C, there appears to be a region of lengths $\xi \times (T_C - T/T_C)^{1/4} \ll L \ll \xi$ where I'_C is independent of the length, and is given by the expression

$$I'_C \approx 0.12\, C_j S (8/\pi\hbar D)^{1/2} \Delta^{5/2} \approx 0.2\, I_C [L/\xi(T)] \times [T/(T_C - T)]^{1/4} \gg I_C . \quad (178)$$

In this region $|\Delta|$ is almost constant over the whole length of the weak link, and tends to Δ only at the boundaries with the banks.

Another explanation of the bump on the $I-V$ curve was given by Deaver *et al.*, (1976a, b). They assumed that an increase in the number of quasiparticles with a decrease in Δ at the phase shifts $\varphi \approx \pi$ is responsible for the bump (see the discussion in Sec. VI.A). One more approach to nonequilibrium in weak links was discussed by Golub (1976).

4. Balance of holes and electrons

Quasiparticle excitations, which we have so far called electrons, change their properties depending on whether their momentum p is more or less than the Fermi momentum p_F. When $p > p_F$, a quasiparticle resembles an ordinary conduction electron: it has a negative charge $(-e)$ and differs from an electron only in that its dispersion at $p \gtrsim p_F$ is different

$$\epsilon = [\,|\Delta|^2 + v_F^2 (p - p_F)^2]^{1/2}, \quad (179)$$

which is just the cause of the anomalous density of states [Eq. (172)]. If $p < p_F$, a quasiparticle behaves like a hole, i.e., like a particle with a positive charge $(+e)$ and with the same dispersion law [Eq. (179)].

As a result of the different signs of the charge, the elastic conversion of an electron into a hole (or vice versa) is impossible, because in this process an additional Cooper pair with an energy corresponding to the Fermi level should appear (or disappear). If, therefore, an imbalance exists between the electrons and holes in a superconductor, it relaxes to zero in a time of the order of $\tau_Q \sim \tau_\epsilon$ [more exactly, $\tau_Q \approx \tau_\epsilon (k_B T/|\Delta|)$ when $T \to T_C$ (Kaplan *et al.*, 1976)].

The nonzero space charge of a superconductor has been shown to be directly connected with imbalance in the number of the electrons and holes (Tinkham and Clarke, 1972; Clarke, 1972; Tinkham, 1972). But, by virtue of the Maxwell equation, a space charge must appear on any interface between superconducting and normal phases crossed by a current. Since $\mathbf{E} = 0$ in the superconducting phase and $\mathbf{E} = \mathbf{j}/\sigma_N$ in the normal phase, a space charge appears at the interface with a total density

$$\int \rho\, dx = j/4\pi\sigma_N . \quad (180)$$

Thus, an imbalance between the electron and the hole components always arises at the $S-N$ interface when the current flows through this boundary. Since, during the relaxation time τ_Q, electrons and holes diffuse from the boundary to a distance

$$\xi_\epsilon \approx (D\tau_Q)^{1/2} = (v_F l \tau_Q/3)^{1/2} \propto (T_C - T)^{-1/4}, \quad \text{at } T \to T_C , \quad (181)$$

the electrical field and the normal current should penetrate into the superconductor to a depth of the same order. The magnitude of ξ_ϵ derived from Eq. (181) is much greater (several units or tens of microns) than that predicted by the TDGL theory [Eq. (162)]. The results obtained in experiments with long specimens (Skocpol *et al.*, 1974b, c; Meyer and Tidecks, 1976; Yu and Mercereau, 1975; Klapwijk *et al.*, 1976b) are generally in satisfactory agreement with Eq. (181), although it is not easy to detect the weak temperature dependence of T at $T \to T_C$.

There can be no doubt that slow relaxation of the normal current in time and space should have some kind of influence on the ac processes in weak links, on the "excess current" effect in particular, thereby giving rise to deviations from the TDGL result [Eq. (171)]. But the excess currents recorded in the experiments are quite well described by Eq. (171) [see, for example, Gubankov *et al.* (1977)]. The Andreev reflection of electrons at the $S-N$ interface (Andreev, 1964) seems to have a rather strong influence on this effect, resulting in partial changes in the electrical field at distances $\sim \xi \ll \xi_\epsilon$. In other words, just as in the case of the TDGL model, part of the electrical charge [Eq. (180)] is localized in a layer of thickness $\sim \xi(T)$. (See also the works Artemenko and Volkov, 1976, 1977; Schmid and Schön, 1975; Artemenko *et al.*, 1978.)

5. Self-heating

Scattering of the nonequilibrium electrons by the phonons leads to an increase in phonon concentration. Although the nonequilibrium spectrum of these phonons can differ markedly from the equilibrium one, qualitatively these phonons have the same effect as would be produced by a simple increase in their concentration, i.e., as the heating of the crystal lattice. Without giving an exact description of the thermal effects, which differ depending upon the weak link form and substrate properties, etc., we shall demonstrate that even a simple account of these effects (Gubankov *et al.*, 1972) gives rise to a negative slope region on the $I-V$ curve of the weak link.

Let us suppose that dissipation of energy P in a weak link leads to a proportional increase in the temperature of the system[35]

$$\Delta T = T' - T = \kappa P = \kappa \overline{I}\,\overline{V} , \quad (182)$$

where T is the temperature of the cryostat (surrounding medium). The temperature increase leads to a drop in the critical current. Let T be close to T_C; then Eq. (14) holds valid; hence

$$V_C(T') = V_C(T) - \alpha(T' - T) = V_C(T) - \overline{I}\,\overline{V}/I_T , \quad (183)$$

[35] For $L \lesssim \xi$, only the temperature of those bank regions which border on the weak link is essential.

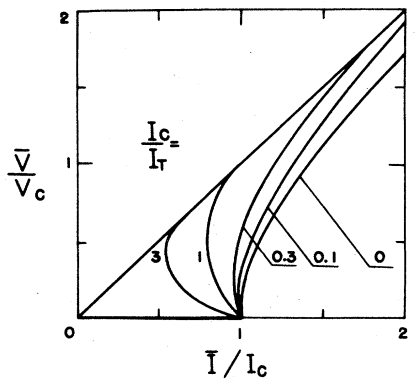

FIG. 21. $I-V$ curves according to the RSJ model with finite self-heating [Eq. (184)]. Parameter is the relation of the critical current I_C to the thermal current $I_T=|dV_C/dT|^{-1}(dT/dP)^{-1}$, which is larger, thermoconductivity is better. After Gubankov *et al.*, 1972.

where the larger the constant $I_T=(\alpha\kappa)^{-1}$, the better the heat transfer from the weak link. Substituting Eq. (183) into Eq. (147) derived in the RSJ model, we obtain a relationship for the resistive part on the $I-V$ curve for a nonisothermic case

$$\bar{I}^2R_N^2-\bar{V}^2=\begin{cases}(V_C-\bar{I}\bar{V}/I_T)^2, & \text{at } T'<T_C,\\ 0, & \text{at } T'>T_C,\end{cases} \tag{184}$$

which is shown in Fig. 21.

This figure shows that any nonzero value of κ gives rise to a region of negative slope on the $I-V$ curve due to the diminished critical current of the junction owing to heating in resistive state ($\bar{V}\neq 0$). We know that the initial portion of the resistive part can really be smoothed out as a result of the dc current enhancement of superconductivity. Consequently, a negative slope region appears only for finite κ (Fig. 16).

From Fig. 21 it is also evident that the thermal effects are enhanced with the increasing I_C, i.e., with decreasing temperature of the cryostat. This is in complete agreement with experiment. The dependence of the self-heating effect on geometry is not so pronounced. Although the dependence of $\alpha=|dV_C/dT|$ on the link dimensions, as a rule, is not very great, nonetheless it may be quite significant in some cases; therefore the specific calculation varies for different cases (Iwanishin and Smith, 1972; Nad' and Polyanskii, 1973; Fulton and Dunkleberger, 1974; Skocpol *et al.*, 1974a,b; Kaminaga, 1975; Desmons, Martin, and Thomas, 1975; Jahn and Kao, 1976; Tinkham *et al.*, 1977; Decker and Palmer, 1977).

Outwardly, the changes in the $I-V$ curves caused by the self-heating effect resemble those induced under the influence of finite capacitance of the structure (McCumber, 1968; Stewart, 1968): for β [Eq. (17)] greater than unity, a negative slope region appears on $I-V$ curves. Its depth increases with the growing β, i.e., with the growth of the critical current (for fixed R_N and C). Such a close similarity between the two phenomena has resulted in the fallacious opinion that the negative slope regions on $I-V$ curves, usually observed as hysteresis if the current source ($R_e\gg R_N$) is used, originate from the capacitance of the structure. Although even the simplest estimates give $\beta\ll 1$ for weak links, this opinion has persisted long after the publication of the first paper in which the thermal nature of hysteresis was proved (Gubankov *et al.*, 1972). In all probability, the unending stream of publications in which the influence of heat on $I-V$ curves of weak links is rediscovered, is an illustration of poor communication even in this narrow branch of physics.

In structures without current concentration or with weak current concentration a specific type of heating may take place in the electrodes, i.e., field-induced heating of electrons even without lattice heating (Aslamazov and Larkin, 1976). This effect is also observed in long superconducting films (Shklovskii, 1975; Volotskaya *et al.*, 1976). Qualitatively it leads to the same results as the "true" heating described above.

VI. OTHER NONSTATIONARY PROCESSES

From the preceding section it is evident that we are still in need of a complete theory of the nonstationary processes occurring in weak links, that would adequately explain the phenomena observed in real structures. The difficulty encountered in verifying the theoretical hypotheses experimentally is that the $I-V$ curves of weak links are not the best touchstone for them.

On the one hand, certain special features of $I-V$ curves (say, bumps) may be described by various theories. On the other hand, in the total voltage range from fractions of a microvolt (typical of the fluctuation bend on $I-V$ curves) to several tens of millivolts (where the Josephson effect is still frequently observed), the frequency of the processes (ω_V) changes by a factor of 10^4–10^5. Therefore it is hard to believe that a theory that describes the processes satisfactorily for a fixed $\bar{V}$, could give an exact description of the $I-V$ curve as a whole.

Use of other nonstationary phenomena, even if more complicated in experimentation, seems promising in comparing theories with experiments. In this section we shall discuss some of the possible experiments.

A. High-frequency impedance

1. Impedance in a superconducting state

Let a bias point be located on the superconducting part of the $I-V$ curve, i.e., let the constant current through the weak link be less than the critical current: $\bar{I}<I_C$, and the ac current of frequency ω and amplitude I_ω be superimposed on it. The current I_ω will cause the phase to deviate from its constant value $\bar{\varphi}$, corresponding to the current $\bar{I}$, the amplitude of these deviations being small for small I_ω. Finite-frequency oscillations in φ, by virtue of the Josephson relation (4), will give rise to voltage oscillations with an amplitude

$$V_\omega=i(\hbar\omega/2e)\varphi_\omega. \tag{185}$$

proportional to I_ω when $I_\omega\to 0$

$$V_\omega=Z(\omega)I_\omega,\quad Z(\omega)=i(\hbar\omega/2e)\varphi_\omega/I_\omega. \tag{186}$$

The complex quantity Z is the total ac resistance (im-

pedance) of a weak link. Frequently it is more convenient to use the inverse of impedance, i.e., the total conductance (admittance)

$$Y(\omega)=Z^{-1}(\omega)=-i(2e/\hbar\omega)I_\omega/\varphi_\omega . \tag{187}$$

In order to estimate impedance, we shall first determine it at low and high frequencies. If $\omega \ll \omega_C$, then I_S and φ are related by the dc $I_S(\varphi)$ relationship, hence

$$I_\omega/\varphi_\omega = dI_S/d\varphi|_{\varphi=\bar\varphi}, \quad Z(\omega)=i(\omega/c^2)\mathfrak{L}(\bar\varphi), \quad \mathfrak{L}^{-1}=\frac{2e}{\hbar c^2}\frac{dI_S}{d\varphi} . \tag{188}$$

We find that the impedance is inductive. For example, for short weak links with a sinusoidal $I_S(\varphi)$, we have

$$\mathfrak{L}^{-1}=\mathfrak{L}_C^{-1}\cos\bar\varphi, \quad \mathfrak{L}_C=c^2R_N/\omega_C , \tag{189}$$

therefore the impedance is much less than R_N

$$Z=iR_N(\omega/\omega_C)\cos^{-1}\bar\varphi . \tag{190}$$

On the other hand, the main current component at very high frequencies is the normal current, and

$$Z=R_N, \text{ at } \omega \gg \omega_C, \Delta/\hbar . \tag{191}$$

Thus the impedance grows with increasing frequency, and it is therefore easiest to measure it at microwave frequencies, where ω is of the order of ω_C. A typical experiment here is measurement of the reflection coefficient from the resonator or stub containing a weak link in a microwave guide (see, for example, Vystavkin *et al.*, 1973).

The impedance can also be measured at relatively low frequencies (units or tens of megahertz) by inserting a weak link into a superconducting ring of low inductance ($l_R<1$), i.e., with the help of a quantum interferometer (SQUID) operating in a nonhysteretic mode (see, for example, Hansma, 1975; Danilov and Likharev, 1975). One merit here is that in this method any value of $\bar\varphi$ can steadily be set up if $l+l_R<1$, not only values in the range $|\varphi|\leq\pi/2$ as in the absence of the ring.

2. $G_1 \cos\varphi$ term

In the RSJ model we have

$$I_\omega = I_C\cos\bar\varphi\ \varphi_\omega + V_\omega/R_N , \tag{192}$$

hence, with the help of (185), we get

$$\mathrm{Re}\,Y(\omega)=R_N^{-1}, \quad \mathrm{Im}\,Y(\omega)=-(2eI_C/\hbar\omega)\cos\bar\varphi . \tag{193}$$

This expression shows that with increasing ω, the transition from the asymptote of Eq. (190) to the asymptote of Eq. (191) occurs gradually. We may note that in the RSJ model the losses in the weak link (Re Y) do not depend on $\bar\varphi$. In the experiments, however, Re Y always increases as $\bar\varphi$ approaches π.

The dependence of Re Y on φ appears in the tunnel theory [Eqs. (7) and (8)]. Indeed, taking φ as

$$\varphi=\bar\varphi+\varphi_\omega\exp(i\omega t)+\text{c.c.},$$

we express $\exp(i\varphi/2)$ contained in Eq. (7) in the first approximation of φ_ω as

$$\exp(i\varphi/2)=\exp(i\bar\varphi/2)[1+i(\varphi_\omega/2)\exp(i\omega t)+\text{c.c.}] . \tag{194}$$

Hence we obtain an expression for the coefficients A_n

$$A_0=1, \quad A_{\pm1}=\pm\varphi_\omega/2; \quad A_n=0, \quad \text{at } |n|>1 . \tag{195}$$

Substituting these coefficients into Eq. (8), and retaining as before only the first terms with respect to $|A_{\pm1}|\ll A_0$, we get

$$I=I_C\sin\bar\varphi+Y(\omega)V_\omega\exp(i\omega t)+\text{c.c.}, \tag{196}$$

where the admittance $Y(\omega)$ has the following components (R. Harris, 1975)

$$\begin{aligned}\mathrm{Re}\,Y&=\frac{e}{\hbar\omega}\{\mathrm{Im}\,I_q(\omega)+\cos\bar\varphi\,\mathrm{Im}\,I_p(\omega)\},\\ \mathrm{Im}\,Y&=\frac{e}{\hbar\omega}\{\mathrm{Re}\,I_q(\omega)-\cos\bar\varphi[\mathrm{Re}\,I_p(\omega)+\mathrm{Re}\,I_p(0)]\}.\end{aligned} \tag{197}$$

Since $\mathrm{Re}\,I_p(0)$ is simply the critical current, from Eq. (187) we get for low frequencies ($\omega\ll\Delta(T)/e$)

$$\begin{aligned}\mathrm{Re}\,Y&=G_0+G_1\cos\bar\varphi, \qquad G_0=d[\mathrm{Im}\,I_q(2e\bar V/\hbar)]/d\bar V ,\\ \mathrm{Im}\,Y&=-(2eI_C/\hbar\omega)\cos\bar\varphi, \quad G_1=d[\mathrm{Im}\,I_p(2e\bar V/\hbar)]/d\bar V .\end{aligned} \tag{198}$$

We can see that the basic distinction from the RSJ model is that Re Y becomes a function of $\cos\bar\varphi$. Equation (198) and Fig. 2, however, show that $G_1>0$ and the losses (Re Y) diminish as $\varphi\to\pi$ in the tunnel theory, a fact which is in contradiction to the experiments both with tunnel junctions (Pedersen *et al.*, 1972) and with weak links (Vincent and Deaver, 1974; Nisenoff and Wolf, 1975; Callegari *et al.*, 1976; Rifkin and Deaver, 1976; Rifkin et al., 1976). The discrepancy between theory and experiment was discussed by Poulsen (1973), Langenberg (1974), and Harris (1974). Recently it was found (Zorin and Likharev, 1978b) that the observed negative sign of G_1 can be explained if the finite width of the Riedel peak is taken into account in tunnel theory.

The sign of the fourth term in Eq. (197) also seems unsatisfactory. Indeed, we see from Fig. 2, that at high frequencies

$$\mathrm{Re}\,I_q(\omega)\approx\mathrm{Re}\,I_p(\omega)+\mathrm{Re}\,I_p(0)\approx I_C, \text{ at } \omega\gg\Delta/\hbar , \tag{199}$$

hence Im Y is positive for any $\bar\varphi$. This means that the equivalent circuit of the Josephson junction at high frequencies consists of a normal resistance R_N in parallel with a *negative* inductance

$$L=-L_C(1-\cos\bar\varphi)/2 . \tag{200}$$

Consequently, the stationary state of the junction for any (i.e., for any $\bar I$) is unstable to high-frequency perturbations, a result which at present seems unphysical. However, because of the complex type of $\mathrm{Re}\,I_q$ frequency dependence, the problem needs some further analysis.

In conclusion, we may note that Eqs. (15) and (198) tempt one to modify the RSJ model as follows:

$$I=I_C\sin\varphi+(G_0+G_1\cos\varphi)V/R_N . \tag{201}$$

Expressions with a structure similar to Eqs. (15) and (198) really follow from Eq. (201). But even within the framework of these particular effects, Eq. (201) is contradictory in the sense that $G_{0,1}$ has different values in two effects. It is, moreover, meaningless to assert that the approximation (201) is valid in more complicated cases, say for instance during strong oscillations of

$V(t)$, which take place on the resistive part of the $I-V$ curve.

3. Other theories

The expression for current [Eq. (165)] which directly follows from the TDGL equations may also be used for finding the impedance. For low frequencies it gives Eq. (198), where we now have to take

$$G_0 = R_N^{-1}, \quad G_1 = -(\gamma/15)R_N^{-1} \ll R_N^{-1}. \tag{202}$$

Thus, in this theory, in agreement with the experiments, we have $G_1 < 0$ and the ratio G_1/G_0 just equal to the correction to normal resistance [Eq. (170)]. In particular, as $T \to T_C$ and $\Delta = \Delta_0$ (i.e., $A = 1$), G_1 should vary as $(T_C - T)^{-1}$.

Volkov and Kasatkin (1974) obtained the same sign as for the $V\cos\varphi$ term in analyzing, with the help of the same equations, the proximity effect bridges where the banks are to a considerable extent involved in the nonlinear processes.

Proceeding from the microscopic theory, Mitsai (1976) calculated the admittance of a short weak link which had the same geometry as the ODSEE model. For the most interesting case $\hbar\omega \ll \Delta \ll k_B T$ he derived the following expressions

$$\begin{aligned} \mathrm{Re}\, Y &= R_N^{-1}\left[\left(1 - \frac{7\Delta}{8k_BT}\right) + \frac{5\Delta}{8k_BT}\cos\bar{\varphi}\right], \\ \mathrm{Im}\, Y &= -(2eI_C/\hbar\omega)\left[\frac{1}{2}(\bar{\varphi} - 2\sin\bar{\varphi})\cot\frac{\bar{\varphi}}{2} + \cos\bar{\varphi}\right], \\ &\qquad \text{at } |\bar{\varphi}| \leq \pi. \end{aligned} \tag{203}$$

Note that the function in square brackets in the expression for $\mathrm{Im}\, Y$ is less than or equal to zero for any $\bar{\varphi}$. As a result the stationary state $\varphi = \bar{\varphi}$ is unstable to high-frequency perturbations for the same reason which we have discussed above. The Mitsai theory, in contradiction to experiment, also gives a positive sign to the $\cos\bar{\varphi}$ term in $\mathrm{Re}\, Y$.

Remarkably, the Mitsai theory of nonlinear nonstationary processes has been derived on the basis of the Green's function formulation of the superconductivity theory. None of the other results deduced in this way has as yet been confirmed by experiment.[36] Probably the wrong signs of two current amplitudes are due to the difficulties involved in analytical continuation procedure in a nonstationary case (Chang and Scalapino, 1977). Therefore this fact deserves the utmost attention.

Deaver *et al.* (1974, 1976a, b) have advanced a phenomenological model in which increased losses when $\bar{\varphi} \approx \pi$ are attributed to decrease of $|\Delta|$ under these phase values in a noticeable part of the bulk of the weak link. They believe that this situation should lead to the increased density n of the normal electrons, and consequently, to increased active conductivity $\mathrm{Re}\, Y$. Nonetheless, we may note that when $T \approx T_C$, this effect should hardly be noticeable, as the variation of $|\Delta|$ does not change the value of n

$$n = \int_{|\Delta|}^{\infty} n(\epsilon)N(\epsilon)\,d\epsilon = N(0)\int_{|\Delta|}^{\infty} \times \frac{1}{2}\,\frac{\epsilon\,d\epsilon}{(\epsilon^2 - |\Delta|^2)^{1/2}} = \mathrm{const}(|\Delta|). \tag{204}$$

Recently (Soerensen *et al.*, 1977) the first attempt has been made to measure Y as a function of the temperature near T_C. Such experiments with weak links of a geometry corresponding to the ODSEE model (for instance, with variable-thickness bridges) could give a better idea of the adequacy of the various existing theories.

4. Impedance in resistive state

It has been demonstrated (Vystavkin *et al.*, 1972; see also Vystavkin *et al.*, 1974; Likharev and Ulrich, 1978) that if the bias point is located on the resistive part of the $I-V$ curve ($\bar{V} \neq 0$), for a low-capacitance Josephson junction, we obtain quite an unusual dependence of the impedance on the bias voltage $\bar{V}$, i.e., on the frequency of the Josephson oscillations ω_V. In the RSJ model without fluctuations, in particular, it was found that impedance

$$\begin{aligned} \mathrm{Re}\, Z(\omega) &= R_N[F(\omega_V/\omega_C) + 1] \\ &\quad \times [\omega_C/(\omega + \omega_V) + \omega_C/(\omega - \omega_V)], \ \omega_V \neq \omega, \\ \mathrm{Im}\, Z(\omega) &= -R_N \pi F(\omega_V/\omega_C)\omega_C \delta(\omega - \omega_V), \\ F(x) &= [(1 + x^2)^{1/2} - x]/2, \end{aligned} \tag{205}$$

has a resonance-type singularity at $\omega \approx \omega_V$. The real part of Z is negative in the range of frequencies ω slightly greater than ω_V (Fig. 22)

$$\mathrm{Re}\, Z < 0, \text{ at } \omega_V^2 < \omega^2 < \omega_V(\omega_C^2 + \omega_V^2)^{1/2}. \tag{206}$$

If account is taken of even small fluctuations, then the singularity in Z at $\omega = \omega_V$ vanishes (Likharev and Semenov, 1973; Likharev and Kuzmin, 1977)

$$(\omega - \omega_V) \to (\omega - \omega_V) + i\gamma, \tag{207}$$

where γ is the half-width of the Josephson oscillation line. This gives only a small reduction in the frequency range where $\mathrm{Re}\, Z < 0$ (Fig. 22).

This "anomalous" impedance results from the complicated nature of the interaction between the signal and the Josephson oscillations (see Likharev and Ulrich, 1978, for details). This effect was first observed in 1972 in point contacts (Vystavkin *et al.*, 1973) and since then has been a topic for repeated investigations in point contacts as well as in weak links of well-defined geometry, such as variable-thickness bridges (Gubankov *et al.*, 1977), Dayem bridges (Pedersen *et al.*, 1977), and proximity effect bridges (Franson and Mercereau, 1976). The results of the experiments are in qualitative agreement with Eq. (205) of the RSJ model. With decreasing temperature, however, the resonance at $\omega = \omega_V$ is noticeably less than the theoretical value. Unfortunately, so far the impedance at $\bar{V} \neq 0$ has not been calculated by means of any other theory.

[36] For instance, the results obtained for the viscous motion of Abricosov vortices (Gor'kov and Kopnin, 1973) are in apparent contradiction to experiment (see Danilov *et al.*, 1975).

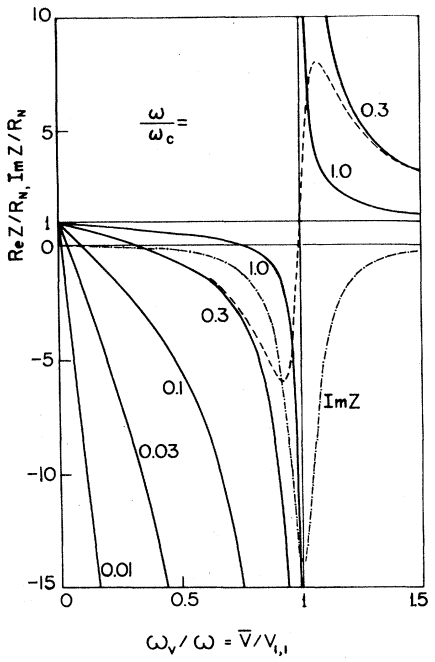

FIG. 22. Weak link impedance at the resistive branch of the $I-V$ curve as a function of the Josephson frequency ω_V for different frequencies ω of signal, as calculated from the RSJ model. Singularity in impedance occurs at $\omega=\omega_V$; dashed lines show smoothing of the singularity by small fluctuations. After Vystavkin *et al.*, 1972; Likharev and Semenov, 1973.

B. $I_A(\omega)$ function and current steps on I-V curves

The shape of nonstationary equations should, of course, vary for the different types of weak links. But for large voltages they should all give an expression of a form similar to Eq. (15)

$$I=\bar{I}(\bar{V})+I_A\sin(\omega_V t+\vartheta),\quad \omega_V=(2e/\hbar)\bar{V}, \tag{208}$$

describing the Josephson oscillations with an amplitude $I_A(\omega_V)$. Clearly, great interest lies in the measurement of the $I_A(\omega)$ dependence. This, in principle, may be carried out by measuring the impedance at frequencies $\sim\omega_V$ or by direct measurement of the Josephson oscillations at the frequency ω_V. But technically all these measurements involve difficulties, especially at frequencies ω_C, which may be as high as 10^{11}–$10^{12}\,\mathrm{s}^{-1}$ or even greater.

Therefore, of considerable interest for $I_A(\omega)$ determination are the straight parts ("current steps") on I–V curves, first predicted by Josephson in his pioneering paper (1962). These current steps appear at the voltages $V_{m,n}$ [Eq. (117)] on the junction when it is irradiated by external microwaves of frequency ω. The magnitude of these steps varies with signal power, i.e., with the amplitude A of the microwave current through the weak link. At the same time, the superconducting region changes as well, and it is convenient to regard it as the "zero current step" ($m=0$). The step heights can easily be measured in experiments, and may serve as a way of measuring the $I_A(\omega)$ dependence.

1. High-frequency approximation

If the voltage $V_{m,n}$ is sufficiently high ($\gg V_C$), the main contribution to the current is made by the normal component

$$V=IR_N=(I+A\cos\omega t)R_N; \tag{209}$$

hence we obtain a simple formula for the phase

$$\varphi=(2e/\hbar)\int V dt=\omega_V t+a\sin\omega t+\vartheta,\quad \vartheta=\text{const}, \tag{210}$$

$$a=2eAR_N/\hbar\omega,$$

which now has to be substituted in the expression for the supercurrent. For example, if the supercurrent amplitude I_A does not depend on the frequency in the range, which is the case, say, in the RSJ model, then we directly obtain:

$$\bar{I}_S=I_A\,\overline{\sin\varphi}=I_A\sum_m J_m(a)\,\overline{\sin}(\omega_V t+\vartheta+m\omega t), \tag{211}$$

where J_m is the Bessel function of the first kind. Equation (211) shows that I_S is only nonzero when $\omega_V=m\omega$, i.e., there are no subharmonic steps ($n\neq 1$) in this approximation, while the harmonic steps oscillate with A according to the "Bessel law"[37]:

$$\Delta I_m=2I_A\,|J_m(a)|,\quad V_m=m(\hbar\omega/2e). \tag{212}$$

It is known that the maximum value of J_m decays very slowly with increasing m, for $m\gg 1$ only as $\sim 0.67m^{-1/3}$ (see, for example, Abramowitz and Stegun, 1965). Therefore even steps with very high numbers up to $\sim 10^3$ can readily be observed in experiments (McDonald *et al.*, 1971; Ainitdinov *et al.*, 1976; Octavio *et al.*, 1977a).

It is now important to notice the following. The fact that noticeable steps are observed at voltages V_m does not necessarily mean that the Josephson effect has to take place in the junction at this voltage, i.e., that $I_A(m\omega)$ should be finite. To prove this, consider the time dependence of the phase [Eq. (210)], taking $\omega_V=m\omega$ and the value $a\approx m$, at which the size of the mth step is maximum (Fig. 23). During a part of the period $T=2\pi/\omega$ the phase grows rapidly, hence the voltage across the weak link is rather high

$$d\varphi/dt\approx 2m\omega,\quad V\approx 2V_m, \tag{213}$$

and during the other part φ is almost constant, hence the voltage is almost zero. The contribution to the average supercurrent is made in just these slow phase variation periods, and this contribution depends on the phase shift ϑ, which shows the position of the bias point on the current step. During the fast phase change, the supercurrent oscillates almost sinusoidally, and there is, therefore, no contribution to $\bar{I}_S$.

Even if $I_A(m\omega)$ is zero, i.e., there is no supercurrent flow during rapid phase variations, nevertheless, from Fig. 23, it is evident that the contribution to the mean current is nonzero providing $I_A\neq 0$ at frequencies of the order of ω (i.e., the rate at which the phase changes on

[37] Strictly speaking, $\bar{I}_S\neq 0$ also in a voltage range of width $\sim\Delta I_m R_N$ near each step, where the I–V curve becomes hyperbolic in shape (Volkov and Nad', 1970; Likharev and Kuzmin, (1977).

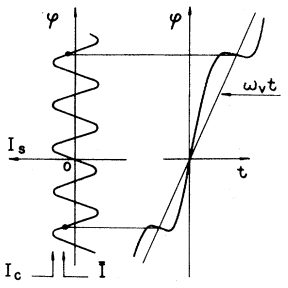

FIG. 23. Time dependence of phase difference φ when the bias point is located at the mth current step [Eq. (210)]. The figure shows that the main contribution to average supercurrent I_S occurs during the slow change of φ, when only frequencies $\sim\omega$ (but not $m\omega>>\omega$) are present in its spectrum.

the flat portion of its time evolution). Thus, for $m\gg1$, we have $\Delta I_m\propto I_A(\omega')$, $\omega'\sim\omega\ll m\omega$.

This fact, first noticed by Borovitskii and Malinovskii (1975) for the case of tunnel theory, shows that the high steps (for instance, of the order of units or tens of millivolts) observed with a relatively low-frequency source (say, X-band oscillator) show nonzero amplitude of the supercurrent only at frequencies ~10^{10} Hz, but not at ~10^{12} Hz. On the other hand, the first step ($m=1$) at the same voltage induced by a very-high-frequency source is proportional to the amplitude of the Josephson current at this frequency: $I_1\propto I_A(\omega)$. Therefore, measurement of the first step may serve as a good way of measuring the $I_A(\omega)$ dependence, say, to observe the smoothed Riedel singularity in relatively clean weak links at $\omega_V\approx4\Delta/\hbar$ (Thome and Couder, 1975; Kofoed and Saermark, 1975; see also Vernet and Adde, 1976). In contrast, the observation of high-order steps from relatively low-frequency sources is merely an indication of the absence of heating in weak links (Octavio *et al.*, 1977a). Such heating, being an inertial effect with a time constant $\tau\gg\omega^{-1}$, totally suppresses superconducting phenomena, including current steps.

2. Theoretical $I_A(\omega)$ dependences

As yet the frequency dependence of the supercurrent amplitude has only been calculated within the framework of two theories. In the tunnel theory it is expressed by Eq. (15) and formulas for the coefficients I_a, I_b (see, for example, Poulsen, 1973)

$$I_A=|I_b(\omega_V)|=\begin{cases} I_C, & \text{at } \omega_V\ll2\Delta/\hbar,\\ \dfrac{2\Delta}{eR_N}\dfrac{\Delta}{\hbar\omega_V}\ln\dfrac{\hbar\omega_V}{\Delta}, & \text{at } \omega_V\gg2\Delta/\hbar.\end{cases}\tag{214}$$

For $\omega_V=4\Delta/e$, the amplitude I_A has a weak "gap" singularity (Fig. 2). At frequencies behind the gap the amplitude slowly decreases with increasing ω_V (slightly slower than ω_V^{-1}). Any other theory probably will cause a faster drop in I_A.

In the TDGL model, as follows from Eq. (169), the amplitude $I_A=(I_1^2+I_2^2)^{1/2}$, as Fig. 18 shows, decreases exponentially for η greater than 10–20

$$I_A\approx3I_C\eta^{1/4}\exp[-(\sqrt{2}/3)\eta^{1/2}].\tag{215}$$

Within the framework of this theory, the decrease in I_A starts approximately where the I–V curve becomes a straight line of the excess current. This result still has to be verified experimentally.

3. Low frequencies

Measurements of current step heights as functions of microwave power not only provide a means of determining the dispersion of supercurrent amplitude, but also give an indirect method of verifying the sinusoidal shape of the dc $I_S(\varphi)$ relationship. Experimentally, this may be a much easier way than direct measurement of this relationship.

Indeed, for not-too-high frequencies ($\omega\lesssim(\omega_V)_{max}$) the dispersion of I_S may be disregarded. Therefore, if $I_S=I_C\sin\varphi$ we may use the RSJ model [Eq. (145)] to determine the height of the steps. Such calculations have been made by several workers and their results are well known (see, for example, Fack and Kose, 1971; Likharev and Semenov, 1971; Russer, 1972; Vystavkin *et al.*, 1974). In this model only the harmonic steps ($n=1$) are nonzero; their sizes and positions on the current axis depend on two dimensionless variables: current amplitude A and reduced frequency ω/ω_C. These dependences are not very suitable for comparison with experiment, and therefore the curves shown in Fig. 24 (Likharev and Semenov, 1971) are used frequently.

The solid lines show the functions $\kappa_m(\omega/\omega_C)$ defined by the equation

$$\kappa_m=(P_m^{(2)}/P_m^{(1)})^{1/2}-1,\tag{216}$$

where $P_m^{(k)}$ is the value of power P of the microwave signal ($\propto A^2$), at which the height of the mth current step has its kth zero. The experimental values of κ_m are to be plotted along the Y axis (Fig. 24) and then the corresponding values of ω/ω_C are to be found. If, within the limits of experimental error, all the values of κ_m give one value of reduced frequency, then the experimental weak link is consistent with the RSJ model. Such a "κ criterion" is convenient in that, firstly, there is no need for the use of absolute values of the power [Eq. (216)], and secondly the procedure is stable to slight smoothing of

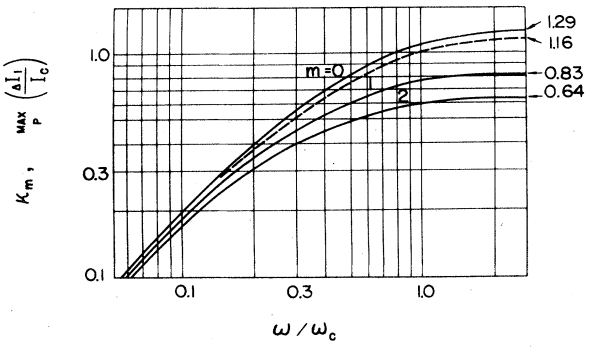

FIG. 24. Magnitudes κ_m [Eq. (216)] (solid lines) and maximum size of the first current step (dashed line) vs frequency ω of external microwave signal, reduced to the characteristic frequency ω_C of the weak link [Eq. (18)]. Results are based on the RSJ model (Likharev and Semenov, 1971; Fack and Kose, 1971).

current step edges by the fluctuations. Sometimes it is also convenient to use the maximum size of the first current step height which is shown by a dashed line in Fig. 24 (Fack and Kose, 1971).

It should be noted that even a slight deviation of $I_S(\varphi)$ from its sinusoidal shape gives rise to noticeable changes in the magnitude of the steps; in particular, the step heights do not disappear periodically when P changes (Vystavkin *et al.*, 1974), and subharmonic steps appear (Lübbig and Luther, 1974).

4. Other methods for I_A measurements

Several other methods are also available for measuring the frequency dependence of the supercurrent amplitude, among which the self-detection methods deserve special mention. For example, in the RSJ model [Eq. (147)] even for relatively high $\overline{V} \gg V_C$ the mean current is not equal to the normal current, and the difference is

$$\Delta\overline{I} = \overline{I} - \overline{V}/R_N \approx I_C^2/2\overline{V}R_N . \tag{217}$$

This results from the fact that even when $\overline{V} \gg V_C$, the law of change of phase $\varphi(t)$ is slightly different from the linear law [Eq. (135)] for the reasons mentioned in Sec. V.A. We can say that $\overline{I}$ is a consequence of self-detection of the Josephson oscillations by the weak link itself (see, for example, Likharev and Ulrich, 1978, for details).

On connecting a weak link to an external circuit with an impedance Z_e (reduced to the junction), comparable to R_N, the self-detection effect is weakened and thus $\overline{I}$ is decreased. Extending the results obtained in the RSJ model (Likharev and Semenov, 1972; Volkov, 1972) for an arbitrary $I_A(\omega)$ dependence, we find

$$\Delta I = -\frac{I_A^2(\omega_V)}{2\overline{V}} \mathrm{Re} Y_{\parallel}, \quad Y_{\parallel} = R_N^{-1} + Z_e^{-1}, \quad \text{at } \overline{V} \gg V_C. \tag{218}$$

Thus I_A can be measured by varying Z_e in a controlled manner. Such experiments have been described by Ganz and Mercereau (1975).

As $Z_e/R_N \to 0$, we have $\overline{I}_S \to 0$; this result is valid for any arbitrary $\overline{V}$. Consequently, by shunting the weak link heavily at all frequencies, the I–V curve can be made to coincide with the "quasiparticle current" curve $I_N(\overline{V})$ for $\overline{V} \neq 0$. Such an experiment was recently performed by Chiao and Levinsen (1977). However, they did not succeed in obtaining the relation $|Z_e| \ll R_N$, due, probably, to the noticeable contribution of kinetic inductance of bridge banks to Z_e. More recently, Yeh and Buhrman (1977) obtained somewhat lower values of $|Z_e|_N$.

The function $I_A(\omega)$ may also be determined from the mixing between the frequencies of two external signals at the Josephson junction (Grimes and Shapiro, 1968; McDonald *et al.*, 1974), or between an external frequency and the Josephson oscillations' frequency (Zimmerman, 1970; Vernet and Adde, 1976). The more convenient of these two experiments—mixing between two close external frequencies ω_1 and ω_2 with measuring of a low frequency difference component $\omega_- = \omega_1 - \omega_2$—can unfortunately again give information only about $I_A(\omega_-)$, for the same reasons as mentioned above for the high current steps. The same can also be said of mixing with frequency multiplication (see, for example, McDonald *et al.*, 1972): $\omega_- = m\omega_1 - \omega_2$, where the output signal is also proportional to $I_A(\omega_-)$, but not to $I_A(\omega_2)$.

C. Microwave enhancement of superconductivity

According to the RSJ model, the critical current is always less in the presence of an external microwave irradiation than without it. It was found (Wyatt *et al.*, 1966; Dayem and Wiegand, 1967), however, that in some weak links at temperatures close to τ_C the critical current increases somewhat at first, with the increasing power, and begins to decrease thereafter. Later this "enhancement of the superconductivity by microwaves" was repeatedly verified experimentally. Owing to the recent publication of a review (Klapwijk *et al.*, 1977a), we shall outline this topic only briefly.

1. Main experimental results

Critical current shows an increase only in a specific frequency range, i.e., the effect has lower (Dayem and Wiegand, 1967) and upper (Latyshev and Nad', 1974) frequency limits. These limits shift upward as the temperature decreases, although the behavior far from T_C has not been investigated in detail.

Essentially, critical temperature does not rise as the critical current increases.[38] The insignificant increase in T_C, observed in some experiments, does not usually exceed the width of the S-N phase transition, and consequently may easily be attributed to the proximity effect between regions with different T_C.

Microwave-induced enhancement shows a strong dependence on the size of the specimen. This effect is rarely observed in point contacts (Dmitriev *et al.*, 1973; Fjordbøge *et al.*, 1976), i.e., in structures containing microshorts, or in small bridges (submicron dimensions) where the "ideal" Josephson effect exists. On the contrary, in bridges of the dimensions of one or several microns, where the Josephson effect is weakly exhibited, enhancement of superconductivity is distinctly pronounced. A further increase in the specimen dimensions, say, the length of the film strip, almost inhibits the effect. In those rare instances where it has been observed on long specimens (Shepard, 1971; Latyshev and Nad', 1976) this effect probably takes place at minute inhomogeneities of either a geometrical or a physical nature.

This effect seems not to be dependent upon whether the current is concentrated in one direction or in two. In any case, it was observed both in Dayem bridges [current concentration only along the width, Fig. 1(e)], and in variable-thickness bridges [current concentration along the width and thickness, Fig. 1(f)].

2. Theoretical interpretations

Microwave enhancement of superconductivity has been treated differently in phenomenological terms (see, for example, Hunt and Mercereau, 1967; Shepard, 1971;

[38] The only exception is the recent experiment (Klapwijk and Mooij, 1976) with Al bridges. So far these results have not been confirmed by others.

Notarys *et al.*, 1973; Lindelof, 1976). None of these interpretations, however, is based on modern concepts of the physics of superconductors and is able to give a proper explanation to the whole body of experimental data.

At present, most of the workers in this field are inclined towards the hypothesis proposed by Eliashberg (1970), who attributed this effect to the fact that microwave oscillations cause a redistribution of normal electrons in the energy scale, the maximum of this distribution shifting from $|\Delta|$ to higher ϵ. By virtue of Eq. (175), such a redistribution should lead to a weakening of $|\Delta|$ suppression by normal electrons, i.e., to an increase in $|\Delta|$ at $T \approx T_c$. Accordingly, all critical parameters of the superconducting state, including the critical current, should increase.

Although several works have been published with regard to Eliashberg's idea (Ivlev, 1970; Ivlev and Eliashberg, 1971; Ivlev *et al.*, 1973; Schmid, 1977), this theory still cannot explain all the experimentally observed facts, especially the dependence of microwave enhancement on the dimensions of the weak link. This can, probably, be done with the help of the ideas developed by Aslamazov and Larkin (1976) for the dc current enhancement of superconductivity. Indeed, an ac current of frequency $\omega \gtrsim \tau_\epsilon^{-1}$ flowing through a weak link should affect the distribution of normal excitations approximately as the Josephson oscillations do. Consequently, the critical current should raise approximately to I_c', the height of the bump on the $I-V$ curve. Such an equality of superconductivity enhancement by dc and ac (microwave) currents has actually been observed in experiment (Gubankov *et al.*, 1977).

Recently Aslamazov and Larkin (1978) advanced a theory where the discussion runs along these lines.

D. Fluctuations

The nonstationary properties of weak links also have an influence upon the fluctuations taking place in them. In analyzing fluctuations, a clear distinction should be made between real (measurable) fluctuations of a particular quantity (say, voltage) and the intensity of the fluctuation sources, which may conveniently be represented as a "fluctuating current" I_f source connected in parallel to the weak link. In fact, the current fluctuations I_f interact with the supercurrent in a rather complex way, especially in the presence of the ac Josephson effect. Therefore the observed dependences of the real fluctuations on the parameters may be quite complicated. Conversely, I_f is directly associated with the physics of conductivity of the structure.

1. The nature of sources

The most important result of all the theories of fluctuations in the Josephson effect is that the only intrinsic source of fluctuations is the normal current rather than the supercurrent of the junction.[39] The reason is that the superconducting condensate is an ordered set of electron pairs, which cannot fluctuate independently. The collective fluctuations of the condensate as a whole under the usual conditions are negligibly small. Indeed, the order parameter can noticeably vary only at distances of the order of the coherence length. Therefore, in a bulk specimen, for example, the probability of a large fluctuation is of the order

$$p \sim \exp(-|\Delta| n\xi^3/k_B T),$$

and since $|\Delta| \sim k_B T$ and $n\xi^3 \gg 1$, is negligibly small.

The intensity of fluctuation sources in a superconducting weak link differs from the intensity in the normal state only to the extent that the normal (but not the total) conductivity of the structure differs. When this difference is not essential (say, within the framework of the RSJ model), the intensity of the sources is simply the same as in the normal state.

In the literature we sometimes come across wrong statements that the Stephen theory (1969) shows that the supercurrent also contributes to the source of fluctuations. Actually, the Stephen equations, valid only for a particular case, are obtained when only the normal conductivity of the junction and the equilibrium fluctuations of a resonator connected to the junction are taken as the fluctuation sources (see Likharev and Kuzmin, 1977, for details).

2. Equilibrium fluctuations

The fluctuation-dissipation theorem (see, for example, Stratonovich, 1962) holds true as long as the process occurring in the weak link is an equilibrium one. This theorem gives a simple relationship between the active conductivity $\mathrm{Re}Y$ of the two-terminal circuit with the spectral density $S_I(\omega)$ of the fluctuating current I_f source

$$S_I(\omega) = (2/\pi)\,\mathrm{Re}Y(\omega)(\hbar\omega/2)\coth(\hbar\omega/2k_B T).$$

In particular, at low frequencies ($\hbar\omega \lesssim k_B T$) we obtain the Nyquist formula

$$S_I(\omega) = \mathrm{Re}Y(\omega) 2k_B T/\pi. \tag{219}$$

For example, in the RSJ model, the value of Y is the same as in a normal structure and

$$S_I(\omega) = 2k_B T/\pi R_N. \tag{220}$$

3. Shot noise

As was shown by Larkin and Ovchinnikov (1967), when the voltage across a tunnel junction is greater than $\sim k_B T/e$ (about 360 μV at $T = 4.2$ K), the noise level is greater than that predicted by the fluctuation-dissipation theorem. For example, if the voltage across the junction is constant, Eq. (220) takes the form (for details see also Dahm *et al.*, 1969).

$$S_I(0) = (e\overline{V}/\pi R_N)\coth(e\overline{V}/2k_B T). \tag{221}$$

On increasing the factor $e\overline{V}/k_B T$ to a value slightly greater than unity, coth may be taken to be unity, and thus the noise is not dependent on temperature. Therefore we obtain the well known formula

[39] The only exception is the recent publication by Landa and Tarankova (1977). The author of this review is not convinced of the correctness of the results reported therein.

$$S_I(0) = e\bar{I}/\pi, \tag{222}$$

for the shot noise of a diode.

The physical meaning of the noise change at $e\bar{V} \sim k_B T$ lies in the following: normal electrons, responsible for the noise and usually having random energy of thermal motion $k_B T$, begin to be "overheated" in passage from one electrode to another due to the absorption of electrostatic energy $e\bar{V}$. Such a change should take place not only in tunnel contacts, but also in any case where the length ξ_ϵ, over which an electron transfers the energy $e\bar{V}$ gained in a field to lattice phonons, is much greater than the length of the weak link L. According to the facts mentioned in the previous section, we obtain the condition

$$L \lesssim (v_F \ell \tau_\epsilon/3)^{1/2},$$

which is generally satisfied in weak links of small or moderate lengths. So the transition from thermal noise to shot noise should take place in such weak links under voltage increase.

4. 1/f noise

Besides the noise sources described above, which have a wide frequency spectrum, low-frequency noise of the $1/f$ type (flicker noise) also arises in weak links. This noise can be of a diverse nature, and has a spectral density proportional to approximately $\omega^{-\alpha}$, $\alpha \sim 1$. The noise may be characterized by the cutoff frequency ω_{cf} at which the spectral density becomes equal to that of thermal noise.

Flicker noise is especially strong in point contacts (Kurdyumov, 1976), in which the cutoff frequency may be as high as hundreds of kilohertz. In all other types of weak links this noise is much less; for example, the cutoff frequency in the proximity effect bridges was found to be less than 20 Hz (Decker and Mercereau, 1975).

Recently it was found that some fluctuations of the $1/f$ type might appear even in an equilibrium case, where they are originated by the fundamental temperature fluctuation $\tilde{T}$ (Clarke and Voss, 1974). Thus, for "zero-dimensional" objects (particles) with a total heat capacity C_V and connected with the thermal bath via the total heat conductivity G, the general equations of statistical physics show that

$$\langle \tilde{T}^2 \rangle = k_B T^2 / C_V. \tag{223}$$

The spectral density of these fluctuations is constant up to a frequency of the order of the inverse thermal time constant $\tau = C_V/G$, and then falls as $\omega^{-3/2}$. For larger specimens the frequency dependence is more complicated; in particular, it may be proportional to ω^{-1} over a wide frequency range (Clarke and Voss, 1974; Voss and Clarke, 1976).

5. Fluctuation measurement

It is reasonable to measure the intensity of fluctuation sources in a weak link only in those experiments which provide the best controlled conditions for the transformation of S_I to the measured variable. Some examples of these conditions are the following (for details see Chap. 6 in Likharev and Ulrich, 1978).

(i) If the bias point is located far along the resistive branch of the $I-V$ curve ($\bar{V} \gg V_C$), then $V = IR_N$ and the spectral density of low-frequency voltage fluctuations is simply connected with the density of I_f.

$$S_V(0) = S_I(0) R_N^2. \tag{224}$$

Essentially, no such relationship exists for an arbitrary $\bar{V}$, even if the differential resistance R_d at the bias point is taken instead of R_N (see, for example, Likharev and Semenov, 1972).

(ii) If the fluctuation intensity is not very high, instead of S_V, we can measure the half-width of the Josephson oscillations line, which is simply connected with S_V (Larkin and Ovchinnikov, 1967)

$$\Delta\omega = (\pi/2)(2e/\hbar)^2 S_V(0). \tag{225}$$

The half-width $\Delta\omega$ may be measured either directly (by microwave emission of the weak link at the frequency ω_V) or indirectly by means of the width of the current step "embryo" formed on the $I-V$ curve by the action of a weak, external, monochromatic signal of frequency ω. This embryo is of the following form (see, for example, Likharev and Ulrich, 1978)

$$\Delta\bar{I} \propto (\bar{V} - V_\omega)/[(\bar{V} - V_\omega)^2 + (\Delta V)^2], \quad \Delta V = (\hbar/2e)\Delta\omega, \tag{226}$$

$$V_\omega = (\hbar/2e)\omega.$$

Measurements of $\Delta\omega$ (or ΔV) suffer from one drawback: all the fluctuations (including the low-frequency external interferences and flicker noise) whose spectra are located on the frequency axis between zero and $\sim\Delta\omega$, make a contribution to these quantities. Therefore the influence of undesirable fluctuations has to be effectively controlled in the experiments.

VII. MORE COMPLICATED WEAKLY LINKED STRUCTURES

In terms of circuit theory all the types of weak links considered in Sec. IV are simple two-terminal devices, i.e., they have two electrodes, which serve as terminals. In the last few years more complicated weakly linked structures have been acquiring increasing importance. We shall deal with these structures in this section. They can be formed either as single weak links of a complicated geometry, or by several ordinary weak links (two-terminal structures) connected in a complicated manner.

A. Multiterminal weak links

The multiterminal structure considered by Likharev (1975) is an example of the first type of structure. It contains a few superconducting electrodes connected by a common weak link. The possible realization of a three-electrode structure ("Josephson triode") is shown in Fig. 25(a), where a spot of thin film connects three superconducting electrodes made of a bulk superconducting film.

In order to analyze the processes occurring in a multiterminal structure we shall assume that the conditions of the AL theory are satisfied. In particular, all the di-

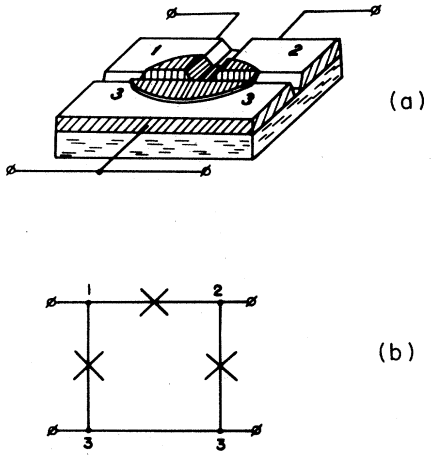

FIG. 25. Possible realization of Josephson triode, i.e., a weak link connecting three superconducting electrodes (a), and its equivalent circuit (b). Crosses denote usual Josephson junctions, which are really superimposed in the space. These imaginary junctions can have different values of I_C and R_N, but their characteristic voltages $V_C = I_C R_N$ are equal if the material of all electrodes is the same.

mensions of the structure are supposed to be less than ξ [if the weak link dimensions are great, then the currents from different terminals are simply added (Prans and Meissner, 1974)]. The solution to the Laplace equations for the order parameter $\Delta(\mathbf{r}, t)$ Eq. (29)] and the electrical field potential $\mu(\mathbf{r}, t)$ [Eq. (35)] may now be written in the form

$$\Delta = \sum_k \Delta_k f_k \exp(i\chi_k), \quad \mu = \sum_k f_k \mu_k, \quad f_k = f_k(\mathbf{r}), \tag{227}$$

where f_k is a particular solution to the Laplace equation for a given geometry of the structure, which is equal to unity inside the kth electrode and to zero in other electrodes. Variables $\Delta_k, \chi_k(t)$, and $\mu_k(t)$ are values of the modulus and phase of the order parameter and scalar potential inside the kth electrode.

Substituting Eq. (227) into the GL equation for current (21b), we easily find the current in the nth electrode in the general case

$$I_n = \sum_k [(I_C)_{k,n} \sin\varphi_{k,n} + V_{k,n}/(R_N)_{k,n}], \qquad \varphi_{k,n} = \chi_n - \chi_k, \quad V_{k,n} = \mu_k - \mu_n, \tag{228}$$

where the constants I_C and R_N are interrelated by the condition

$$(I_C)_{k,n}(R_N)_{k,n} = V_C. \tag{229}$$

Equation (228) is a generalization of the RSJ model [Eq. (145)] for the case of several electrodes. It shows that the equivalent circuit of a multiterminal structure consists of "ordinary" (two-terminal) Josephson junctions interconnecting each pair of electrodes. For example, three such imaginary "junctions" represent the triode [Fig. 25(b)]. The critical currents and normal resistances of these junctions depend on the geometry of the structure, but products V_C [Eq. (229)] are expressed by the usual formula (40), and therefore depend on the product $\Delta_k \Delta_n$ only. If all the electrodes are made from the same material, the quantities Δ_k and V_C are the same for all two-terminal junctions.

From Fig. 25(b) it is evident that the Josephson triode properties are close to the properties of three separate junctions inserted into a superconducting ring. The electrodynamical properties of the triode have been analyzed by Likharev (1975a), and it has been proven that, given a proper choice of parameters, a triode can be utilized particularly for microwave mixing, using the Josephson oscillations from one of the two-terminal junctions as the local oscillator signal.

B. Connections of weak links

Some interesting new processes may also take place in those structures where the usual (two-terminal) weak links are interconnected in a system by means of superconducting electrodes. The properties of the two simplest types of connections, series and parallel ones (Fig. 26), appear to be radically different.

1. Series connection

In series connections (Palmer and Mercereau, 1974, 1975, 1977; Jillie *et al.*, 1975; Feldman *et al.*, 1975; Dupart and Baixeras, 1977) the processes occurring in weak links are independent in the first approximation (Likharev, 1973). In fact, in Sec. V.A we have seen that the processes in the weak link only affect the phase shift and voltage drop on it, but have hardly any influence on the time dependence of the current through it. Since current is the only common variable for the elements connected in series, the contacts hardly interact at all. Of course, in real situations, there is always some weak interaction due to one mechanism or another, discussed below.

First, owing to the finite magnitude of impedance Z_e of the external system, Josephson oscillations give rise to an ac current, although a very weak one, at the Josephson frequency ω_V. This current will have a synchronizing action on the other weak links in the system.

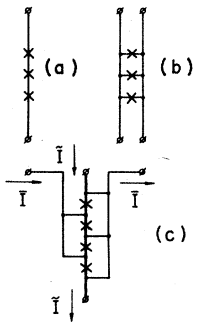

FIG. 26. Series (a), parallel (b), and one of the possible complex connections (c) of weak links. In the last case (Lukens, 1976) weak links are connected in series for the microwave signal (current $\tilde{I}$), but in parallel for dc bias (current $\bar{I}$), so that dc voltages $|\bar{V}|$ are equal at all junctions. Cross denotes a single element (weak link).

Therefore, mutual locking of the oscillations may take place if the link parameters are close in value, i.e., if the frequencies ω_V are almost the same for the same dc bias current.

Second, if the distance between the weak links is comparable to the coherence length of the electrodes ξ, there may be a finite interaction through the variation in the modulus of the order parameter at the banks. We have already seen that the greater the deviation of the weak links from the ODSEE model, the greater these variations will be. In other words, the variations are least in the variable-thickness bridges and greatest in one-dimensional structures with weak links and electrodes made from almost identical materials. This coupling mechanism has been theoretically analyzed in the literature (Blackburn *et al.*, 1972, 1975; Howard and Kao, 1975; Kovalenko, 1976; Way *et al.*, 1978).

Third, the generation of excess electron-like quasiparticles with an intensity varying with the Josephson frequency ω_V takes place in weak links during the ac Josephson effect. These normal electrons, on penetrating into the banks, may diffuse to distances $\sim\xi_\epsilon$ [Eq. (181)] which may be of the order of several microns (in aluminum tens or even hundreds of microns). If another weak link is located within this distance, the normal electrons will act upon it at a frequency ω_V. This mechanism has indeed been detected experimentally by Jillie *et al.* (1977a, b), but no detailed theoretical description is is yet developed.

Finally, for very low capacitances C between the connected electrodes: $e/C \gtrsim V_C$, one more specific coupling mechanism is also possible. In this case the passage of even one electron through one of the weak links changes the potential of the "middle" electrode (connected between two weak links) by a value e/C comparable to V_C. Therefore the conventional description of weak links (at least for those with a relatively large mean free path ℓ) is not valid, and the discrete nature of the current carriers has to be taken into consideration in the theory. Intuitively, it is evident that this will give a specific "electrostatic" mechanism of interaction between neighboring weak links. Although there are some communications describing such effects (Zeller and Giaver, 1969; Kulik and Shekhter, 1975, 1976), neither the exact boundaries, nor the main consequences of such interaction are as yet clear.

It should be pointed out that it may be rather difficult to separate the various synchronization mechanisms in the experiment.

2. Parallel connection

Unlike the case of series connection, weak links connected in parallel (two superconducting electrodes connected by several junctions) always interact between each other. Indeed, there can be no voltage drop across the sections of superconducting electrodes separating the junctions. Therefore the mean voltage $\overline{V}$, and consequently the Josephson oscillation frequency ω_V [Eq. (6)], is the same at all the weak links connected in parallel.

A similar strong interaction is observed in the stationary state too; it is responsible for a number of specific properties described in detail in the existing literature on the Josephson effect. Use of weak links in this case does not give rise to any new effects, and therefore we recommend that the reader consult some of the available publications (see Footnote 1).

3. Use of parallel and series connections

Parallel connections of Josephson junctions are used in dc SQUIDs (Clarke, 1977), and may also be used in cryotron-type (Zappe, 1975) and quantron-type (Fulton *et al.*, 1973; Likharev, 1977b) digital circuits. Moreover, distributed (wide) weak links (see below) can also be represented as a parallel connection of a large number of junctions.

Series connections of weak links into arrays seem to be highly promising for increasing the resistivity in microwave applications of the Josephson effect. The first experiments with such circuits (Feldman *et al.*, 1975; Chiao and Parrish, 1976), however, have shown that the inevitable variation of the parameters of the weak links in the array leads to noticeable differences in the values of dc voltage across them, and consequently to differences in the Josephson oscillation frequencies. It is, at the same time, highly desirable to fix a definite bias point $\overline{V}$ in most microwave devices. In this situation combined parallel-and-series connections can be used. An example of such a connection suggested by Lukens (1976) is shown in Fig. 26(c). In this circuit the ac current flows along a wide central line through all the elements in series. At the same time, thin lines of high inductance (to avoid shunting of the ac current) connect all the elements in parallel with respect to the dc bias; therefore $\overline{V}$ across them is the same even in the case of wide scattering of the parameters.

Some other weak link systems have also been studied (Mooij *et al.*, 1974; Tsang and Wang, 1974; Lindelof *et al.*, 1977), their utility for device applications being more doubtful. Moreover, a considerable number of papers have been published dealing with granular superconductors which may be looked upon as a complicated connection between chaotically located weak links with random parameters. Perhaps a separate paper is needed to review all these works. Today, regular weak link systems seem to be more promising both for physical research and for device applications.

C. Distributed structures

In the preceding pages we considered relatively narrow ($W \sim \xi \ll \lambda_{\text{eff}}$) weak links in which the current is uniformly distributed throughout the cross section. If the link width W becomes large, the phase difference φ and the current density J may depend on the transverse coordinate y. This dependence can be caused by an external magnetic field, and if the width W is greater than some characteristic size λ_{eff}, it can also be caused by the magnetic field of the current flowing through the weak link. In the case where the relation between J_s and φ is sinusoidal, a special term, the Josephson penetration depth λ_J, is used for λ_{eff}.

Such dependences [$J(y)$] are well understood for tunnel junctions (see, for example, Ferrell and Prange, 1963; Owen and Scalapino, 1967; Kulik and Yanson,

1970), and our aim here is only to show that they can have some specific features in weak links.

1. Local and nonlocal self-limitation

Self-limitation, that is variation of φ along the width of the structure under the influence of the current flowing through it, is conveniently described in the following way (Lapir *et al.*, 1975). An elementary current $J(\mathbf{r}')d\mathbf{r}'$ flowing through a particular region of a weak link penetrates into the banks, and thus creates a gradient $d(\nabla\chi)$ of the order parameter phase inside the bank. If the nonlinear processes are localized in the weak link itself, i.e., condition (64) of the ODSEE model is applicable, the electrodynamics of the banks is linear, and therefore $d(\nabla\chi(\mathbf{r})) \propto J(\mathbf{r}')d\mathbf{r}'$. Summing up the contributions of all regions of the weak link to the phase gradient, we obtain

$$\chi(\mathbf{r}) = \chi_0(\mathbf{r}) + \int K(\mathbf{r},\mathbf{r}')J(\mathbf{r}')d\mathbf{r}', \tag{230}$$

where the integral is taken along the weak link width, and is the phase distribution in the absence of the current through the link, for instance, under the effect of external magnetic fields or currents along the banks. $K(\mathbf{r},\mathbf{r}')$ is a kernel, which depends on the geometry and the material of the banks.

After subtracting Eq. (230) written for the points on opposite sides of the weak link, and taking into consideration that $\varphi(y) = \chi_2 - \chi_1$, we obtain the self-consistency equation:

$$\varphi(y) = \varphi_0(y) + \int_0^W K(y,y')J(y')dy', \tag{231}$$

where the kernel K is simply the sum of the kernels $K_{1,2}$ for the banks taken at $x = x' = 0$.

In sandwich-type structures [Fig. 1(a),(b)][40] the current penetrates into the banks only at distances of the order of penetration depth λ, which is usually much less than λ_J. Therefore at distances λ_J from the source the current flows parallel to the interlayer, and thus, by virtue of Eqs. (21b) and (24), creates a constant phase gradient:

$$\nabla\varphi = (2\pi/c\phi_0)\mathcal{L}_\square J, \quad \phi_0 = \pi ch/e, \tag{232}$$

along the y coordinate. Here $\mathcal{L}_\square$ stands for the inductance per square of the system consisting of two superconducting films, in which the currents flow in opposite directions along adjacent surfaces

$$\mathcal{L}_\square = 4\pi t_{\text{eff}}, \tag{233}$$

where, for the case under consideration, $t_{\text{eff}} = L + 2\lambda$, and L is the thickness of the interlayer.

From Eqs. (232) and (233) it follows that in sandwich-type structures we may take that

$$K(y,y') = (4\pi^2 t_{\text{eff}}/c\phi_0)\,|y - y'|. \tag{234}$$

Substituting this kernel in the self-consistency equation (231), and then differentiating twice with respect to y, we arrive at the usual result that the distribution of the phase over the width of the junction obeys the differential equation

$$\frac{\partial^2\varphi}{\partial y^2} = \frac{\partial^2\varphi_0}{\partial y^2} + \lambda_J^{-2} J(y)/J_C, \tag{235a}$$

$$\lambda_J = (c\phi_0/8\pi^2 t_{\text{eff}} j_C)^{1/2}. \tag{235b}$$

Here we can say that self-limitation is a local effect in which the current at a given point affects the phase changes only at the same point. However, Eq. (231) shows that this is not so in the general case, where self-limitation is described by an integral equation, i.e., is a nonlocal effect.

2. Variable-thickness bridge over ground plane

Consider the system shown in Fig. 27 (Lapir *et al.*, 1975) as an example of a structure with nonlocal self-limitation. In this system a variable-thickness bridge connecting two banks made of relatively thick ($d \gtrsim 2\lambda$) film is located above a superconducting ground plane, say, above a thick film ($d_{gp} \gtrsim 2\lambda_{gp}$). The spacing t between banks and ground plane, just like λ and d, is small compared to the planar dimensions of the systems, say the bridge width W. These systems are interesting not only for their unusual electrodynamics, but also for their application as Josephson cryotrons.

In this case, to find the kernel K in Eq. (231), note that Eq. (23) is also valid for the bank–ground plane gap, if $t_{\text{eff}} = t + \lambda + \lambda_{gp}$ is the effective spacing between the bank and the ground plane. In the dc state the current in the banks is conserved ($\text{div}_{x,y} J = 0$); therefore the phase χ satisfies the Laplace equation

$$\nabla^2_{x,y}\chi = 0, \tag{236a}$$

which has to be solved under the boundary condition following from (232)

$$\left.\frac{\partial\chi}{\partial n}\right|_C = \frac{8\pi^2 t_{\text{eff}}}{c\phi_0} J_n, \tag{236b}$$

where C is the contour of the bank boundaries, and n is

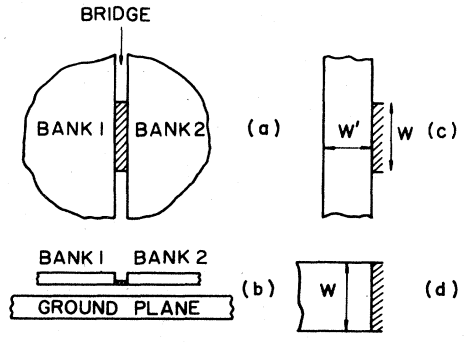

FIG. 27. Variable-thickness bridge over the superconducting ground plane: (a) view from above and (b) from the side, and also particular shapes of one of the banks (c), (d). Views from above (a,c,d) do not show the ground plane, sizes of which are much greater than the sizes of the banks.

[40] For the sake of simplicity, we consider a long sandwich with one of its dimensions (W') much less than the other (W), so that it can be regarded as a structure distributed in one dimension (along W) with a linear current density $J = jW'$.

a normal to this contour. Solving Eq. (236) by the usual potential method, we arrive at Eq. (231) in which the kernels $K_{1,2}$ satisfy the equations

$$\nabla^2_{x,y} K_{1,2} = 0, \quad K_{1,2} \to (2\pi\lambda_0 J_C)^{-1} \ln|\mathbf{r}-\mathbf{r}'|, \quad \text{at } \mathbf{r}\to\mathbf{r}'. \tag{237}$$

Here λ_0 is a constant

$$\lambda_0 = c\phi_0/16\pi^2 t_{\text{eff}} J_C, \quad \lambda_0[\mu\text{m}] \approx 1.31/J_C[A/\text{cm}]\, t_{\text{eff}}[\mu\text{m}], \tag{238}$$

which determines the characteristic scale of the self-limitation effect.[41] For the real values of the parameters ($t_{\text{eff}} \approx 0.3$ μm, $J_C \sim 1$–10 A/cm) λ_0 is in the range of units or tens of microns, i.e., much greater than the typical values of W and L (tenths of a micron).

The kernels $K_{1,2}$ essentially depend on the shape of the banks. If the bank planar dimensions are much greater than λ_0, the kernels are simple.

$$K_{1,2} = (2\pi\lambda_0 J_C)^{-1} \ln|\mathbf{r}-\mathbf{r}'|, \tag{239}$$

In this case the current from the bridge penetrates the bank–ground plane gap at large distances of the order of λ_0 and the self-limitation effect is essentially nonlocal, i.e., Eq. (231) cannot be reduced to a differential equation of the type (235a). In this case various electrodynamical characteristics of wide ($W \gg \lambda_0$) bridges (for example, field distribution across the width of structures, dependence of critical current on external magnetic field, shape and characteristics of Josephson vortices) are somewhat different from the characteristics of Josephson sandwich-type structures. A detailed analysis of these characteristics is given in papers by Lapir *et al.* (1975) and Kupriyanov *et al.* (1976a).[42]

But if the penetration of the current into the depths of the bank–ground plane gap is limited by the shape of the bank, the effective size becomes less than λ_0. For example, for the bank shape shown in Fig. 27(c), applying conformal transformation of a semi-infinite strip to half-plane, from Eq. (237) we find that

$$K_1 = (2\pi\lambda_0 J_C)^{-1} \ln\left|\sinh\frac{\pi(y-y')}{2W'}\right|. \tag{240}$$

If the bank "depth" W' decreases and becomes less than λ_0, the kernel K_1 [Eq. (240)] assumes the shape of Eq. (234) at the distances λ_J, which we are interested in. Therefore, here Eq. (231) is again reduced to the differential equation (235a) where we now have

$$\lambda_J = (2\lambda_0 W')^{1/2} = (c\phi_0 W'/8\pi^2 t_{\text{eff}} J_C)^{1/2} \ll \lambda_0. \tag{241}$$

Thus, if at least one of the banks is sufficiently narrow, the self-limitation effect once again becomes local and the expression for the characteristic size λ_J merely coincides with the expression for sandwich-type junctions (235b). The "depth" W' of the narrow bank now serves as the second planar dimension of the tunnel junction, and the effective gap between the bank and the ground plane functions as the effective thickness of the sandwich t_{eff}.

3. Applications of distributed weak links

It has been seen that the electrodynamical properties of variable-thickness bridges over the ground plane with at least one narrow bank are almost analogous to the properties of wide Josephson sandwich-type structures (for example, tunnel junctions), but have a negligibly small intrinsic capacitance and, therefore, single-valued I–V characteristics Hence variable-thickness bridges can easily be used as Josephson cryotrons (or "Josephson gates"), particularly diffraction-type cryotrons.

A cryotron (see, for instance, Bremer, 1962) is a four-terminal superconducting device, through which two currents can pass, usually without direct (galvanic) contact with each other: gate current I_g and control current I_c. Switching on the control current sharply decreases the critical value $(I_g)_{\max}$ of the gate current, resulting in decrease of gate current I_g. Figure 28 shows the simplest ("in-line") Josephson cryotron (Matisoo, 1967) and the distributions of the gate current (I_g) and the control current (I_c) density in it. These figures show that the equivalent circuit of such a cryotron is a distributed Josephson junction fed by the currents I_g and I_c as shown in Fig. 28(d). To find the main characteristics of the cryotron (control characteristics), i.e., the dependence of the critical value of the current I_g on the control current

$$(I_g)_{\max} = f(I_c), \tag{242}$$

we have to solve Eq. (235a) with $\partial^2\varphi_0/\partial y^2 = 0$ under the following boundary conditions (see, for example, Kulik and Yanson, 1970)

$$\lambda_J \frac{d\varphi}{dy}\bigg|_{y=0} = 2\frac{I(0)}{I_J}, \quad \lambda_J \frac{d\varphi}{dy}\bigg|_{y=W} = 2\frac{I(W)}{I_J}, \quad I_J = 2\lambda_J J_C. \tag{243}$$

Here $I(0)$ and $I(L)$ are the currents fed to the junction edges. From Fig. 28(d), it is evident that for an in-line cryotron

$$I(0) = I_c, \quad I(L) = I_c + I_g, \tag{244}$$

This problem has been analyzed both numerically (see, for example, Basavaiah and Broom, 1975), and analytically within the limits $W \ll \lambda_J$ (Jaklevic *et al.*, 1964) and $W \gg \lambda_J$ (Kupriyanov *et al.*, 1976b). Figure 28(e) shows the shape of the control characteristics for the case $W \gg \lambda_J$, where it is described by the equalities

$$g = -h + \begin{cases} (h^2+1)^{1/2}, & \text{at } h > 0 \\ 1, & \text{at } -1 < h < 0 \\ -(h^2-1)^{1/2}, & \text{at } h < -1 \end{cases} \qquad \begin{aligned} g &= (I_g)_{\max}/I_J, \\ h &= I_c/I_J. \end{aligned} \tag{245}$$

In actual wide junctions ($W \approx 4$–$10\lambda_J$), the curve lies slightly lower, and small oscillations exist at its edges, the curve (245) being the envelope of the oscillations.

From the above it follows that a structure based on

[41] For variable-thickness bridges without a ground plane, simple estimates give $\lambda_J = (c\phi_0/16\pi^2 J_C)^{\frac{1}{2}}$, i.e., about one micron at $J_C = 1$ A/cm.

[42] Nonstationary effects under nonlocal self-limitation, in particular, the shape of the I–V curves of wide weak links (Kupriyanov *et al.*, 1976a) likewise differ from those given by the local equation (235) (Clarke, 1971).

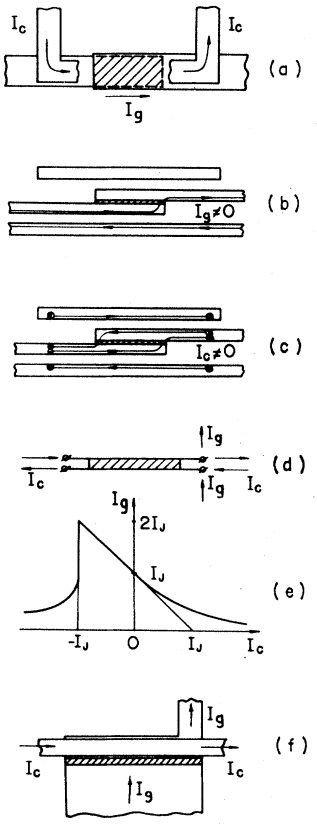

FIG. 28. In-line Josephson cryotron with sandwich-type junction: (a) view from above; (b) distributions of gate current; (c) distribution of control current; (d) equivalent circuit; (e) control characteristics for the case $W \gg \lambda_J$; and (f) possible realization of the cryotron with variable-thickness bridge.

a variable-thickness bridge will have the same control characteristics if the currents are fed into the bridge as shown in Fig. 28(f) (superconducting ground plane not shown). It is clear that the gate current I_g is fed precisely as shown in Fig. 28(d). In order to verify the validity of the circuit shown in Fig. 28(d) for the control current, we have to take account of the fact that I_c excites an equal countercurrent along the upper surface of the bank, which should return to the lower surface of the wide bank through the bridge.

As is clear from Fig. 28(e), the effective gain of an inline cryotron

$$G=|\Delta(I_g)_{\max}/\Delta I_c| \tag{246}$$

for relatively large logical signals $|\Delta I| \sim I_J$ is small: $G \lesssim 1$. Kupriyanov *et al.* (1976) have found that the gain G can be significantly increased by feeding the current in the middle of the Josephson junction. For example, for structures with an equivalent circuit shown in Fig. 29(a), the control characteristics are of the form [Fig. 29(b)]

$$g=\begin{cases}4, & \text{at } |h|<1,\\ 2[|h|+(h^2-1)^{1/2}]^{-1}, & \text{at } |h|>1.\end{cases} \tag{247}$$

The gain G of such a cryotron may be as high as 3 or 4,

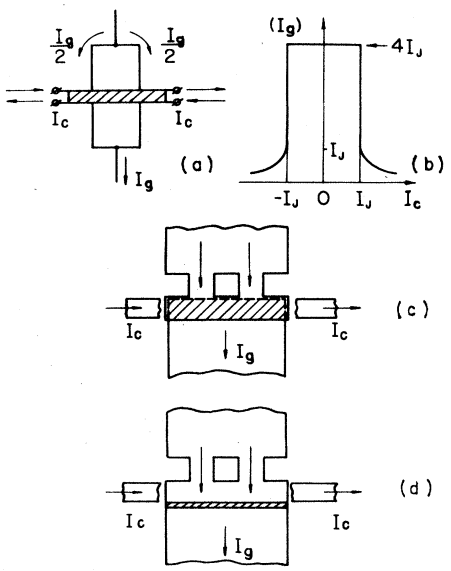

FIG. 29. Cryotron with gate current fed into two internal points: (a) equivalent circuit; (b) control characteristics; (c) realization of the cryotron with sandwich-type junction and (d) variable-thickness bridge (Kupriyanov *et al.*, 1976b; Likharev and Ulrich, 1978).

and this level is quite sufficient for most of the simple cryotron-based circuits (Bremer, 1962). Current fed into the internal points can easily be realized both with sandwich-type structures [Fig. 29(c)] and with variable-thickness bridges [Fig. 29(d)].

Interference cryotrons (Zappe, 1975, 1977) can easily be built up with microbridges too. These circuits do not have such good control characteristic as the cryotrons shown in Fig. 29, but may be somewhat simpler in fabrication. In particular, structures with $W \sim L$, for instance, Dayem bridges, can be used in these cryotrons.

VIII. CONCLUSIONS

Superconducting weak links—weak conducting connections between superconducting electrodes—are unique in their variety of electrodynamic phenomena. Intensive research in the past few years has explained many of these phenomena, but also brought to the fore many new questions. Below we attempt to list those phenomena that are clearly understood now, and those unresolved problems which are, in the author's opinion, key questions today.

A. Basic results

1. Stationary processes

(1) The Josephson effect occurs in all weak links of sufficiently small length, namely, in those having an ef-

[43] Of course, we can also use other types of wide ($W \gg L_{\text{eff}}$) bridges as well, say, one-dimensional structures where the nonlinear effects do not extend to the banks [Fig. 1(C), (D)], provided the critical current of such structures is small. But in this case the parameter V_C that determines the amplitude of the cryotron output signal is small.

fective length L_{eff} less than the coherence length of the weak link material (but not of the electrode material!). By the Josephson effect we mean that the dependence of supercurrent I_S flowing through a weak link on the phase difference φ of the electrodes is single-valued and 2π-periodic (Fig. 4). Thus the Josephson effect is not directly associated with superconducting tunneling: tunnel junctions are just one of the systems that exhibit the Josephson effect (Fig. 1).

(2) Only in some rare and very special cases does the Josephson effect take place in weak links in the same manner as in tunnel junctions. In most real weak links, even in a dc state, the function $I_S(\varphi)$ differs both in shape and in amplitude (the critical current) from the function in tunnel junctions. The function $I_S(\varphi)$ is substanstantially dependent, also, on the ratio of the effective length L_{eff} to the mean free path ℓ of electrons in a weak link (Fig. 6).

(3) For small weak links ($L_{\text{eff}} \lesssim \xi$) it is unimportant whether the link material at a given temperature is superconducting or normal, and the main characterizing parameter of the weak link $V_C = I_C R_N$ does not depend on the link material (but only on the electrode material). However, if the effective length of the weak link L_{eff} is increased to several coherence lengths of the link material, the function $I_S(\varphi)$ begins to be dependent of the parameters of the link material. If the weak link is made of a normal material, the Josephson effect is limited by an exponential drop in the supercurrent as the length increases (Fig. 7). If the link material is superconducting, then at approximately the same lengths, the dependence $I_S(\varphi)$ becomes multivalued (Figs. 7 and 8).

(4) The uniform flow of the superconducting condensate in weak links with a multivalent function $I_S(\varphi)$ [Fig. 4(b), 8(a)] may be violated even if their dimensions are relatively small ($L, W \sim \xi$), due to the onset of Abricosov vortices (if $W > W_C$) or the formation of phase-slip centers (if $W < W_C$) (see Fig. 12). Both these effects are highly sensitive to the small space inhomogeneities which are responsible for the strong irreproducibility of the phenomena. They are impossible if the $I_S(\varphi)$ relationship is single-valued, and thus the structure is stable with respect to small space inhomogeneities. Therefore the situation where the function $I_S(\varphi)$ ceases to be single-valued may reasonably be taken to be the limit of the "ideal" Josephson effect. For dirty weak links ($\ell \ll L_{\text{eff}}$) made from superconducting material, this limit lies within several coherence lengths of the link material.

(5) Different types of weak links (Fig. 1) mainly vary in the degree of involvement of the electrodes in the nonlinear processes occurring in the weak link. In the limit when this involvement is negligible, the simple model [One-Dimensional Structure with Electrodes in Equilibrium (ODSEE)] is applicable in which the values of the order parameter modulus at the weak link–electrode interfaces are taken to be equal to the equilibrium values inside the electrodes. In those types of weak links where geometric current concentration does not occur [constant cross-section, Fig. 1(d)], the ODSEE model can be made applicable if the parameter σ_N/ξ of the link material is much less than that of the bank material. For structures with strong current concentration the ODSEE model can be made valid practically for any material of the weak link and electrodes. Such behavior is only exhibited by variable-thickness bridges [Fig. 1(f)] among the structures with controllable geometry.

(6) The higher the V_C and R_N, the better the application properties of the weak links for utilization in most Josephson effect devices. The values of V_C are maximal if $L_{\text{eff}} \lesssim \xi$, a condition which is easier to obtain in structures approximately obeying the ODSEE model. At present, the most promising seem to be the sandwich-type structures with an interlayer made of low-conduction material, and variable-thickness bridges, which both are superior to tunnel junctions because of low intrinsic capacitance.

(7) When the cross section (i.e., width) is increased, the bridge-type weak links may exhibit self-limitation effects which differ from those in sandwich-type structures, for example, in tunnel junctions. In particular, the effect of the current on the phase changes along the structure width may be essentially nonlocal. Nonetheless, variable-thickness bridges can be utilized in the design of magnetic-field-controlled structures (Josephson cryotrons), just as can tunnel junctions.

2. Nonstationary processes

(1) In analyzing the nonstationary (ac) processes, one should bear in mind that the intrinsic capacitance of weak links is relatively small, since the capacitance of Josephson structures may have somewhat greater influence on their observed properties than the physics of their conductivity.

(2) The basic ac properties of short weak links [with single-valued $I_S(\varphi)$] may be interpreted even on the basis of very simple models, for example, the RSJ model in which the supercurrent and normal current are supposed to be superimposed in a simple linear manner. Among the main effects which this model fails to explain are enhancement of superconductivity by ac and dc currents, and the existence of "excess" current and of the upper frequency limit for the Josephson effect. The last two of these effects can easily be interpreted within the framework of simple TDGL equations, which are strictly suitable only for gapless superconductors. Enhancement of superconductivity is most likely to be associated with the decrease in the suppression of the order parameter by electron-like excitations of energies $\epsilon \sim |\Delta|$.

(3) In general, the nonstationary effects are highly complicated as a result of nonequilibrium distributions of quasiparticles (normal electrons and phonons) and of their consequent back response to the ac processes.

(4) For comparing theories of nonstationary processes with reality, it is frequently not simple experiments (say, observation of I–V curve of an autonomous weak link) but more complicated ones (usually with microwave irradiation from an external source) that are most convenient. For instance, a study of the real and imaginary parts of the high-frequency conductivity of a weak link as functions of the dc bias point in the superconducting region of the I–V curve and of temperature seems to be quite useful because the corresponding theoretical problems admit linearization with respect to variables. In contrast, such well known methods as observation of

current steps on $I-V$ curves with high serial numbers under microwave radiation can give only a limited amount of information.

(5) The weak links which satisfy the ODSEE model are remarkably useful for the comparison mentioned above. Since it is desirable to use structures with an arbitrary relation between the parameters of the weak link and the electrodes, variable-thickness bridges seem to be particularly promising.

B. Unsolved problems

1. dc processes

(1) Is it possible to derive the familiar theoretical results for clean ($\ell \gg \xi_0$), thick ($L \gg \xi_0$), S-N-S-type sandwiches from the Eilenberger equations? How does the transition to the "dirty" limit occur in these structures with decreasing mean free path?

(2) How does the finite critical temperature of the link material affect the critical current I_C and the $I_S(\varphi)$ relationship at arbitrary temperatures (dirty limit, ODSEE model)?

(3) Is it experimentally possible to prepare weak links which completely obey the tunnel theory? Are the microshort dimensions $L \lesssim \hbar/p_F$ unrealizable? What are the superconducting properties of one such microshort?

(4) What are the optimum parameters of the material of the interlayer and its thickness in a sandwich-type weak link, so that V_C would be maximum while $I_S(\varphi)$ is single-valued? How does the presence of the Schottky barriers in semiconductors affect these results?

2. ac processes

(1) Is the discrepancy in the signs of the same two terms between experiment and the Mitsai theory indicative of certain fundamental inconsistencies in the Green's function formulation of the theory of nonstationary superconductivity?

(2) What is the physical pattern of the distribution of normal electrons in a weak link during Josephson oscillations? What are the corresponding changes in the density of excitations? Can electrons with energy $\epsilon < |\Delta|$ exist in a weak link when the usual relation $\omega_V \tau_\epsilon \gg 1$ is satisfied?

(3) What is the distribution (at arbitrary temperatures) of an electric field when a weak current flows through the interface between the normal and superconducting phase? What is the effect of the current density on this distribution? How does this pattern affect the simple expression for the excess current of weak links obtained in the TDGL approximation?

(4) Why does the weak link length have such a considerable influence on superconductivity enhancement by microwaves? What is the relationship between this effect and the dc-induced enhancement?

(5) What is the high-frequency limit for the Josephson effect, i.e., the characteristic frequency from which the function $I_A(\omega_V)$ falls off, if one takes into account nonequilibrium excitations? How does the weak link length affect this limit?

(6) All the listed questions relate to the usual model of weak links (ODSEE model, for $l \ll L$). But how do the nonstationary processes occur in clean weak links, if only of small dimensions ($L_{\text{eff}} \ll l, \xi_0$)?

C. Concluding remarks

One can easily notice that while the unsolved problems in the dc field are rather particular in nature [although question (4) is quite essential for device applications], in the field of ac effects there are more questions than answers. This is due to the lack of an adequate theory to explain the nonstationary processes in superconductors and due to the complexity of the processes themselves, which depend to a greater extent on the various specific properties of weak links than do the stationary ones. In the first place, this results from the fact that excitation of the nonequilibrium electrons and phonons plays a decisive role in nonstationary processes; their subsequent diffusion, energy relaxation, and interaction are greatly affected by the properties of materials and the shape of both the weak link itself and the banks, and frequently by the properties of surrounding objects, e.g., of the substrate and cryogenic gas or liquid (helium) in contact with it.

It should be pointed out that the questions about the nonstationary behavior of weak links which still remain obscure have no direct immediate practical importance. Without even answering them, we are able to say to what extent a specific type of weak link is suitable for a particular device based on the Josephson effect. However, elucidating these problems may be very important for the development of the theory of nonlinear nonstationary processes in superconductors and, consequently, for their possible applications in future. The geometry of weak links (especially those obeying the ODSEE model) is remarkably useful for developing this theory. The recent advent of an appreciable number of theoretical studies and the development of such convenient structures for physical investigations as variable-thickness bridges gives us every hope that progress in this field is forthcoming.

ACKNOWLEDGMENTS

The author would like to express his gratitude to Dr. R. W. Keyes for preliminary discussion of this paper, to Dr. A. G. Aslamazov, Mr. A. B. Zorin, Dr. I. O. Kulik, Dr. M. Yu. Kupriyanov, Mr. V. F. Lukichev, and Dr. A. N. Omelyanchuk for discussion of particular problems. Dr. M. Yu. Kupriyanov, Dr. V. V. Shmidt. and Dr. A. F. Volkov were very kind in editing the manuscript and suggested a number of improvements. This review could not have been written without the support extended by the Chair of Oscillations, the Division of Radiophysics, and the Department of Physics of Moscow State University.

The author takes this opportunity to express his gratitude to the members of the "Josephson Effect Community" of the United States for their hospitality during his visit to the country in 1976, when the idea of writing this review did, in fact, take shape.

REFERENCES

Abrahams, E., and T. Tsuneto, 1966, Phys. Rev. **152**, 416.

Abramowitz, M., and I. A. Stegun, 1965, *Handbook of Mathematical Functions* (Dover, New York).

Abricosov, A. A., 1957, Zh. Eskp. Teor. Fiz. **32**, 1442 [Sov. Phys.-JETP **5**, 1174 (1957)].

Abricosov, A. A., L. P. Gor'kov, and I. E. Dzyaloshinski, 1963, *Quantum Field Theoretical Methods in Statistical Physics* (Pergamon, Oxford), 2nd edition.

Adde, R., P. Crozat, S. Gourrier, G. Vernet, M. Bernheim, and D. Zennatti, 1973, Rev. Phys. Appl. **8**, 455.

Adde, R., P. Grozat, S. Gourrier, G. Vernet, M. Bernheim, and D. Zennatti, 1974, Rev. Phys. Appl. **9**, 179.

Ainitdinov, H. A., S. I. Borovitskii, and L. L. Malinovskii, 1976, in *Proceedings of the 19th Soviet Conference on Low Temperature Physics* (Inst. Fiz. Tverd. Tela Akad. Nauk BSSR, Minsk), p. 376 (in Russian).

Albrecht, G., and W. Richter, 1976, in *Proceedings of the 5th International Conference on Cryogenic Engineering* (Tokyo), p. 119.

Amato, J. C., and W. L. Mc Lean, 1976, Phys. Rev. Lett. **37**, 930.

Ambegaokar, V., and A. Baratoff, 1963, Phys. Rev. Lett. **10**, 486; **11**, 104(E).

Ambegaokar, V., and B. I. Halperin, 1969, Phys. Rev. Lett. **22**, 1364.

Anacker, W., 1969, IEEE Trans. Magn. **5**, 968.

Anacker, W., and H. H. Zappe, 1973, U. S. Patent No. 37005393.

Anderson, P. W., and A. H. Dayem, 1964, Phys. Rev. Lett. **13**, 195.

Anderson, P. W., and J. M. Rowell, 1963, Phys. Rev. Lett. **10**, 230.

Andratskii, V. P., V. N. Gubankov, K. K. Likharev, and N. B. Pavlov, 1976, Zh. Eksp. Teor. Fiz. **70**, 292 [Sov. Phys.-JETP **43**, 151 (1976)].

Andreev, A. F., 1964, Zh. Eksp. Teor. Fiz. **46**, 1823 [Sov. Phys.-JETP **19**, 1228 (1964)].

Antsygina, T. N., E. N. Bratus, and A. V. Svidsinskii, 1975, Fiz. Nizk. Temp. **1**, 49 [Sov. J. Low Temp. Phys. **1**, 23 (1975)].

Antyukh E. V., and F. Ya. Nad', 1975, Cryogenics **15**, 224.

Aronov, A. G., and Yu. M. Gal'perin, 1974, Zh. Eksp. Teor. Fiz. Pis'ma Red. **19**, 281 [JETP Lett. **19**, 165 (1974)].

Aronov, A. G., and V. L. Gurevitz, 1974, Fiz. Tverd. Tela. **16**, 2656 [Sov. Phys.—Solid State **16**, 1722 (1974)].

Aronov, A. G., and B. Z. Spivak, 1975, Zh. Eksp. Teor. Fiz. Pis'ma Red. **22**, 218 [JETP Lett. **22**, 101 (1975)].

Arrington III, C. H., and B. S. Deaver, Jr., 1975, Appl. Phys. Lett. **26**, 204.

Artemenko, S. N., and A. F. Volkov, 1975, Phys. Lett A55, 113.

Artemenko, S. N., and A. F. Volkov, 1976, Zh. Eksp. Teor. Fiz. **70**, 1051 [Sov. Phys.—JETP **43**, 548 (1976)].

Artemenko, S. N., and A. F. Volkov, 1977, Zh. Eksp. Theor. Fiz. **72**, 1018 [Sov. Phys.-JETP].

Artemenko, S. N., A. F. Volkov, and A. V. Zaitsev, 1978, J. Low Temp. Phys. **30**, 487.

Aslamazov, L. G., A. I. Larkin, and Yu. N. Ovchinnikov, 1968, Zh. Eksp. Teor. Fiz. **55**, 323 [Sov. Phys.—JETP **28**, 171 (1969)].

Aslamazov, L. G., and A. I. Larkin, 1969, Zh. Eksp. Teor. Fiz. Pis'ma Red. **9**, 150 [JETP Lett. **9**, 87 (1969)].

Aslamazov, L. G., and A. I. Larkin, 1975, Zh. Eksp. Teor. Fiz. **68**, 766 [Sov. Phys.—JETP **41**, 381 (1975)].

Aslamazov, L. G., and A. I. Larkin, 1976, Zh. Eksp. Teor. Fiz. **70**, 1340 [Sov. Phys.—JETP **43**, 698 (1976)].

Aslamazov, L. G., and A. I. Larkin, 1978, Phys. Lett. 67A, 226.

Auracher, F., and T. Van Duzer, 1974, Rev. Phys. Appl. **9**, 233.

Balla, D. D., G. A. Zaitsev, M. A. Obolenskii, and H. B. Chashka, 1977, Fiz. Nizk. Temp. **3**, 438 [Sov. J. Low Temp. Phys.].

Baratoff, A., J. A. Blackburn, and B. B. Schwartz, 1970, Phys. Rev. Lett. **25**, 1096; **25**, 1738(E).

Bardeen, J., L. N. Cooper, and J. Schrieffer, 1957, Phys. Rev. **108**, 1175.

Bardeen, J., and J. L. Johnson, 1972, Phys. Rev. B **5**, 72.

Barone, A., P. Rissman, and M. Russo, 1974, Rev. Phys. Appl. **9**, 73.

Barone, A., and M. Russo, 1974, Phys. Lett. A**49**, 45.

Basavaiah, S., and R. F. Broom, 1975, IEEE Trans. Magn. **11**, 759.

Bevza, Yu. G., G. G. Tsakh, V. I. Karamushko, and I. M. Dmitrenko, 1976, Pis'ma V. Zh. Tekh. Fiz. **2**, 367 [Sov. Phys.—Tech. Phys. Lett.].

Bezuglyi, A. I., I. O. Kulik, and Yu. N. Mitsai, 1975, Fiz. Nizk. Temp. **1**, 57 [Sov. J. Low Temp. Phys. **1**, 27 (1975)].

Blackburn, J. A., B. B. Schwartz, and A. Baratoff, 1972, Phys. Lett. A**42**, 31.

Blackburn, J. A., B. B. Schwartz, and A. Baratoff, 1975, J. Low Temp. Phys. **20**, 523.

Bolton, J. E., and D. H. Douglass, Jr., 1971, Phys. Rev. B **4**, 3003.

Bondarenko, S. I., E. I. Balanov, L. E. Kolin'ko, and T. P. Narbut, 1970a, Cryogenics **10**, 508.

Bondarenko, S. I., I. M. Dmitrenko, and E. I. Balanov, 1970 b, Fiz. Tverd. Tela **12**, 1417 [Sov. Phys.-Solid State **12**, 1113 (1970)].

Bondarenko, S. I., V. A. Matveeva, N. M. Loboda, K. B. Lobanov, and A. S. Shul'man, 1976, Zh. Tekh. Fiz. **46**, 2440 [Sov. Phys.-Tech. Phys.].

Boone, B. G., C. H. Arrington, III, L.-K. Wang, and B. S. Deaver, Jr., 1977, IEEE Trans. Magn. **13**, 735.

Borovitskii, S. I., and L. L. Malinovskii, 1975, Radiotekh. Elektron. **20**, 1447 [Radio Eng. Electron. Phys.].

Bracken, T. dan, see Dan Bracken, T.

Bremer, J., 1962, *Superconducting Devices* (McGraw-Hill, New York).

Broom, R. F., E. Jutzi, and Th. O. Mohr, 1975, IEEE Trans. Magn. **11**, 755.

Buhrman, R. A., S. F. Strait, and W. W. Webb, 1971, J. Appl. Phys. **42**, 4527.

Callegari, A., H. A. Atwater, and B. S. Deaver, Jr., 1976, Phys. Lett. A**59**, 55.

Campbell, A. M., and J. E. Evetts, 1972, *Critical Currents in Superconductors* (Taylor and Francis, London).

Cardinne, Ph., J. Nordman, and M. Renard, 1974, Rev. Phys. Appl. **9**, 167.

Carelli, P., and I. Modena, 1976, J. Appl. Phys. **47**, 4649.

Chang, J.-J., and D. J. Scalapino, 1977, in *Superconductor Applications: SQUIDs and Machines*, edited by B. B. Schwartz and S. Foner (Plenum, New York), p. 447.

Chiao, R. Y., M. J. Feldman, M. Ohta, and P. T. Parrish, 1974, Rev. Phys. Appl. **9**, 183.

Chiao, R. Y., and M. T. Levinsen, 1977, Appl. Phys. Lett. **30**, 144.

Chiao, R. Y., and P. T. Parrish, 1976, J. Appl. Phys. **47**, 2639.

Christiansen, P. V., E. B. Hansen, and C. J. Sjöström, 1971, J. Low Temp. Phys. **4**, 349.

Clark, T. D., and P. E. Lindelof, 1976, Phys. Rev. Lett. **37**, 368.

Clarke, J., 1966, Phys. Mag. **13**, 115.

Clarke, J., 1968, Phys. Rev. Lett. **21**, 1566.

Clarke, J., 1969, Proc. R. Soc. Lond. A **308**, 447.

Clarke, J. 1970, Am. J. Phys. **38**, 1071.

Clarke, J., 1971, Phys. Rev. B **4**, 2963.

Clarke, J., 1972, Phys. Rev. Lett. **28**, 1363.

Clarke, J., 1977, in *Superconduction Applications: SQUIDs and Machines*, edited by B. B. Schwartz and S. Foner (Plen-

um, New York), p. 67.
Clarke, J., and R. F. Voss, 1974, Phys. Rev. Lett. **33**, 24.
Cohen, M. H., L. M. Falicov, and J. C. Phillips, 1962, Phys. Rev. Lett. **8**, 316.
Consadori, F., A. A. Fife, R. F. Frindt, and S. Gygax, 1971, Appl. Phys. Lett. **18**, 233.
Contaldo, A., 1967, Rev. Sci. Instrum. **38**, 1543.
Cross, N. R., and T. G. Blaney, 1977, J. Phys. E **10**, 146.
Dahm, A. J., A. Denenstein, D. N. Langenberg, W. H. Parker, D. Rogovin, and D. J. Scalapino, 1969, Phys. Rev. Lett. **22**, 1416.
Dan Bracken, T., and W. O. Hamilton, 1972, Phys. Rev. B **6**, 2603.
Danilov, V. V., and K. K. Likharev, 1975, Zh. Tekh. Fiz. **45**, 1110 [Sov. Phys.–Tech. Phys. **20**, 697 (1976)].
Danilov, V. V., M. Yu. Kupriyanov, and K. K. Likharev, 1974, Fiz. Tverd. Tela **16**, 935 [Sov. Phys.-Solid State **16**, 602 (1974)].
Dayem, A. H., and C. C. Grimes, 1966, Appl. Phys. Lett. **9**, 47.
Dayem, A. H., and J. J. Wiegand, 1967, Phys. Rev. **155**, 419.
Deaver, Jr., B. S., B. G. Boone, and R. Rifkin, 1976a, Phys. Lett. A **57**, 186.
Deaver, Jr., B. S., R. Rifkin, and R. D. Sandell, 1976b, J. Low Temp. Phys. **25**, 407.
Deaver, Jr., B. S., R. D. Sandell, and D. A. Vincent, 1974, Phys. Lett. A **46**, 411.
Deaver, Jr., B. S., and D. A. Vincent, 1974, in *Methods of Experimental Physics*, edited by R. V. Coleman (Academic, New York/London), Vol. 11, p. 199.
Decker, S. K., and J. E. Mercereau, 1973, Appl. Phys. Lett. **23**, 347.
Decker, S. K., and J. E. Mercereau, 1975a, Appl. Phys. Lett. **27**, 466.
Decker, S. K., and J. E. Mercereau, 1975b, IEEE Trans. Magn. **11**, 848.
Decker, S. K., and D. W. Palmer, 1977, J. Appl. Phys. **48**, 2043.
De Gennes, P. G., 1966, *Superconductivity of Metals and Alloys* (Benjamin, New York).
Deminova, G. F., and A. S. Kovalenko, 1976, in *Proceedings of the 19th Soviet Conference on Low Temperature Physics* (Inst. Fiz. Tverd. Tela Akad. Nauk BSSR, Minsk), p. 362 (in Russian).
Desmons, J. Y., M. Martin, and D. G. Thomas, 1975, Phys. Lett. A **51**, 123.
Dmitriev, V. M., E. V. Khristenko, and S. Shapiro, 1973, Fiz. Kond. Sost. **28**, 3 (in Russian).
Dmitriev, V. M., E. V. Khristenko, and L. V. Ysichko, 1976, Fiz. Nizk. Temp. **2**, 318 [Sov. J. Low Temp. Phys. **2**, 159 (1976)].
Dolan, G. J., and J. E. Lukens, 1977, IEEE Trans. Magn. **13**, 581.
Dupart, J. M., and J. Baixeras, 1977, Appl. Phys. Lett. **30**, 123.
Edrich, J., J. D. Cupp, and D. G. McDonald, 1974, Rev. Phys. Appl. **9**, 195.
Eilenberger, G., 1968, Z. Phys. **214**, 195.
Eliashberg, G. M., 1970, Zh. Eksp. Teor. Fiz. Pis'ma Red. **11**, 186 [JETP Lett. **11**, 114 (1970)].
Eliashberg, G. M., 1971, Zh. Eksp. Teor. Fiz. **61**, 1254 [Sov. Phys.–JETP **34**, 668 (1972)].
Fack, H., and V. Kose, 1971, J. Appl. Phys. **42**, 320.
Falco, C. M., and W. H. Parker, 1975, J. Appl. Phys. **46**, 3238.
Feldman, M. J., P. T. Parrish, and R. Y. Chiao, 1975, J. Appl. Phys. **46**, 4031.
Ferrell, R., and R. Prange, 1963, Phys. Rev. Lett. **10**, 479.
Fife, A. A., and S. Gygax, 1972, Appl. Phys. Lett. **20**, 152.
Fink, H. J., 1973, Phys. Status Solidi B **60**, 843.
Fink, H. J., and R. S. Poulsen, 1974, Phys. Rev. Lett. **32**, 762.
Fink, H. J., and R. S. Poulsen, 1975, Phys. Rev. B **11**, 1870.
Fiory, A. T., 1971, Phys. Rev. Lett. **27**, 501.
Fjordbøge, B. R., T. D. Clark, and P. E. Lindelof, 1976, Phys. Rev. Lett. **37**, 1302.
Franson, J. D., and J. E. Mercereau, 1976, J. Appl. Phys. **47**, 3261.
Froome, P. K. D., and A. H. Beck, 1976, Electron. Lett. **12**, 99.
Fujita, T., S. Kosaka, T. Ohtsuka, and Y. Onodera, 1975, IEEE Trans. Magn. **11**, 739.
Fulton, T. A., and L. N. Dunkleberger, 1974, J. Appl. Phys. **45**, 2283.
Fulton, T. A., and R. C. Dynes, 1970, Phys. Rev. Lett. **25**, 794.
Fulton, T. A., R. C. Dynes, and P. W. Anderson, 1973, Proc. IEEE **61**, 28.
Galaiko, V. P., 1971, Zh. Eksp. Teor. Fiz. **61**, 382 [Sov. Phys.–JETP **34**, 203 (1972)].
Galaiko, V. P., A. V. Svidzinskii, and V. A. Slyusarev, 1969, Zh. Eksp. Teor. Fiz. **56**, 835 [Sov. Phys.–JETP **29**, 454 (1969)].
Ganz, T., and J. E. Mercereau, 1975, J. Appl. Phys. **46**, 4986.
Giaever, I., 1960a, Phys. Rev. Lett. **5**, 147.
Giaever, I., 1960b, Phys. Rev. Lett. **5**, 464.
Giaever, I., 1965, Phys. Rev. Lett. **14**, 904.
Giffard, R. P., J. C. Gallop, and B. W. Petley, 1976, Prog. Quantum Electron. **5**, 1.
Gilabert, A., J. P. Laheurte, J. P. Romagnan, and J. C. Noiray, 1975, in *Proceedings of the 14th International Conference on Low Temperature Physics*, edited by M. Krusius and M. Vuorio (North-Holland, Amsterdam), Vol. 4, p. 92.
Gilabert, A., D. B. Ostrowsky, C. Vanneste, M. Papuchon, and B. Pench, 1977, Appl. Phys. Lett. **31**, 590.
Ginzburg, V. L., 1944, Zh. Eksp. Teor. Fiz. **14**, 177 (in Russian).
Ginzburg, V. L., 1958, Dokl. Akad. Nauk SSSR **118**, 464 [Sov. Phys.–Dokl. **3**, 102 (1958)].
Ginzburg, V. L., and L. D. Landau, 1950, Zh. Eksp. Teor. Fiz. **20**, 1064 (in Russian).
Golovashkin, A. I., I. S. Levchenko, A. N. Lykov, and L. I. Makhashvili, 1976, Zh. Eksp. Teor. Fiz. Pis'ma Red. **24**, 565 [JETP–Lett.].
Golovashkin, A. I., B. G. Zhurkin, A. N. Lykov, and V. I. Novikov, 1977, Pis'ma V. Zh. Tekh. Fiz. **3**, 865 [Sov. Phys.–Tech. Phys. Lett.].
Golub, A. A., 1976, Zh. Eksp. Teor. Fiz. **71**, 341 [Sov. Phys.–JETP **44**, 178 (1976)].
Goodkind, J. M., and D. L. Stolfa, 1970, Rev. Sci. Instrum. **41**, 799.
Gor'kov, L. P., 1958, Zh. Eksp. Teor. Fiz. **34**, 735 [Sov. Phys.–JETP **7**, 505 (1958)].
Gor'kov, L. P., 1959, Zh. Eksp. Teor. Fiz. **37**, 1407 [Sov. Phys.–JETP **10**, 998 (1960)].
Gor'kov, L. P., and G. M. Eliashberg, 1968a, Zh. Eksp. Teor. Fiz. Pis'ma Red. **8**, 329 [JETP Lett. **8**, 202 (1968)].
Gor'kov, L. P., and G. M. Eliashberg, 1968b, Zh. Eksp. Teor. Fiz. **54**, 612 [Sov. Phys.–JETP **27**, 328 (1968)].
Gor'kov, L. P., and G. M. Eliashberg, 1968c, Zh. Eksp. Teor. Fiz. **55**, 2430 [Sov. Phys.–JETP **28**, 1291 (1969)].
Gor'kov, L. P., and G. M. Eliashberg, 1970, J. Low Temp. Phys. **2**, 161.
Gor'kov, L. P., and N. B. Kopnin, 1973, Zh. Eksp. Teor. Fiz. **64**, 356 [Sov. Phys.–JETP **37**, 183 (1973)].
Gregers-Hansen, P. E., E. Hendricks, M. T. Levinsen, and G. R. Picket, 1973, Phys. Rev. Lett. **31**, 524.
Gregers-Hansen, P. E., M. T. Levinsen, L. Pederson, and C. L. Siöström, 1971, Solid State Commun. **9**, 661.
Gregers-Hansen, P. E., and M. T. Levinsen, 1971, Phys. Rev. Lett. **27**, 847.
Gregers-Hansen, P. E., M. T. Levinsen, L. Pedersen, and

C. L. Siöström, 1972a, in *Proceedings of the Applied Superconductor Conference* (IEEE, New York), IEEE Pub. No. 72–CH0682–5–TABSC, p. 597.
Gregers-Hansen, P. E., M. T. Levinsen, and G. Fog Pedersen, 1972b, J. Low Temp. Phys. **7**, 99.
Greiner, J. H., 1971, J. Appl. Phys. **42**, 5151.
Greiner, J. H., 1974, J. Appl. Phys. **45**, 32.
Grimes, C. C., P. L. Richards, and S. Shapiro, 1966, Phys. Rev. Lett. **17**, 432.
Grimes, C. C., and S. Shapiro, 1968, Phys. Rev. **169**, 397.
Gubankov, V. N., V. P. Koshelets, K. K. Likharev, and G. A. Ovsyannikov, 1973, Zh. Eksp. Teor. Fiz. Pis'ma Red. **18**, 292 [JETP Lett. **18**, 171 (1973)].
Gubankov, V. N., V. P. Koshelets, and G. A. Ovsyannikov, 1975, Zh. Eksp. Teor. Fiz. Pis'ma Red. **21**, 489 [JETP Lett. **21**, 226 (1975)].
Gubankov, V. N., V. P. Koshelets, and G. A. Ovsyannikov, 1976, Zh. Eksp. Teor. Fiz. **71**, 348 [Sov. Phys.–JETP **71**, 182 (1976)].
Gubankov, V. N., V. P. Koshelets, and G. A. Ovsyannikov, 1977a, IEEE Trans. Magn. **13**, 228.
Gubankov, V. N., V. P. Koshelets, and G. A. Ovsyannikov, 1977b, Zh. Eksp. Teor. Fiz. **73**, 1435 [Sov. Phys.–JETP].
Gubankov, V. N., K. K. Likharev, and N. M. Margolin, 1972, Fiz. Tverd. Tela **14**, 935 [Sov. Phys.–Solid State **14**, 819 (1972)].
Guthman, C., J. Maurer, M. Belin, J. Bok, and A. Libchaber, 1975, Phys. Rev. B **11**, 1909.
Hansma, P. K., 1975, Phys. Rev. B **12**, 1707.
Harding, G. L., A. B. Pippard, and J. R. Tomlinson, 1974, Proc. R. Soc. Lond. A **340**, 1.
Harris, E. P., 1975, IEEE Trans. Magn. **11**, 785.
Harris, E. P., and R. B. Laibowitz, 1977, IEEE Trans. Magn. **13**, 724.
Harris, R. E., 1974, Phys. Rev. B **10**, 84.
Harris, R. E., 1975, Phys. Rev. B **11**, 3329.
Hasselberg, L. E., M. T. Levinsen, and M. R. Samuelsen, 1974, Rev. Phys. Appl. **9**, 157.
Holdeman, L. B., and P. N. Peters, 1975, IEEE Trans. Magn. **11**, 782.
Holdeman, L. B., and P. N. Peters, 1976, Appl. Phys. Lett. **28**, 632.
Howard, W., and Y. H. Kao, 1975, in *Proceedings of the 14th International Conference on Low Temperature Physics*, edited by M. Krusius and M. Vuorio (North-Holland, Amsterdam), Vol. 4, p. 144.
Hu, E. L., L. D. Jackel, A. R. Strnad, R. E. Epworth, R. F. Lucey, C. A. Zogg, and E. Gornik, 1978, Appl. Phys. Lett. **32**, 584.
Huang, C. L., and T. Van Duzer, 1974, Appl. Phys. Lett. **25**, 753.
Huang, C. L., and T. Van Duzer, 1975, IEEE Trans. Magn. **11**, 766.
Huebener, R. P., and D. E. Chimenti, 1976, Phys. Lett. A **55**, 432.
Hunt, T. K., and J. E. Mercereau, 1967, Phys. Rev. Lett. **18**, 551.
Hurrell, J. P., 1977, Bull. Am. Phys. Soc. **22**, 374.
Ishii, C., 1970, Prog. Theor. Phys. **44**, 1525.
Ishii, C., 1972, Prog. Theor. Phys. **47**, 1464.
Ivlev, B. I., 1970, Zh. Eskp. Teor. Fiz. **59**, 1036 [Sov. Phys.–JETP **32**, 563 (1971)].
Ivlev, B. I., and G. M. Eliashberg, 1971, Zh. Eksp. Teor. Fiz. Pis'ma, Red. **13**, 464 [JETP Lett. **13**, 333 (1971)].
Ivlev, B. I., S. G. Lysitzyn, and G. M. Eliashberg, 1973, J. Low Temp. Phys. **10**, 449.
Iwanishin, O., and H. J. T. Smith, 1972, Phys. Rev. B **6**, 120.
Jackel, L. D., R. A. Buhrman, and W. W. Webb, 1974, Phys. Rev. B **10**, 2782.
Jackel, L. D., T. D. Clark, and R. A. Buhrman, 1975, IEEE Trans. Magn. **11**, 732.
Jackel, L. D., W. H. Henkels, J. M. Warlaumont, and R. A. Buhrman, 1976a, Appl. Phys. Lett. **29**, 214.
Jackel, L. D., J. M. Warlaumont, T. D. Clark, J. C. Brown, R. A. Buhrman, and M. T. Levinsen, 1976b, Appl. Phys. Lett. **28**, 353.
Jahn, M. T., and Y. H. Kao, 1973, J. Low Temp. Phys. **13**, 175.
Jahn, M. T., and Y. H. Kao, 1976, J. Phys. Soc. Jpn. **40**, 377.
Janocko, M. A., M. Ashkin, and C. K. Jones, 1973, Phys. Lett. A **43**, 345.
Janocko, M. A., J. R. Gavaler, C. K. Jones, and R. D. Blaugher, 1971, J. Appl. Phys. **42**, 182.
Janocko, M. A., J. R. Gavaler, and C. K. Jones, 1975, IEEE Trans. Magn. **11**, 880.
Jensen, H. H., and P. E. Lindelof, 1976, J. Low Temp. Phys. **23**, 469.
Jillie, D. W., J. E. Lukens, Y. H. Kao, and G. J. Dolan, 1976, Phys. Lett. A **55**, 381.
Jillie, D. W., J. E. Lukens, and Y. H. Kao, 1975, IEEE Trans. Magn. **11**, 671.
Jillie, D. W., J. E. Lukens, and Y. H. Kao, 1977a, IEEE Trans. Magn. **13**, 578.
Jillie, D. W., J. E. Lukens, and Y. H. Kao, 1977b, Phys. Rev. Lett. **38**, 915.
Josephson, B. D., 1962, Phys. Lett. **1**, 251.
Josephson, B. D., 1964, Rev. Mod. Phys. **36**, 216.
Josephson, B. D., 1965, Adv. Phys. **14**, 419.
Kaminaga, M., 1975, J. Phys. Soc. Jpn. **39**, 1621.
Kamper, R. A., 1977, in *Superconductor Applications: SQUIDs and Machines*, edited by B. B. Schwartz and S. Foner (Plenum, New York), p. 189.
Kandyba, P. E., D. P. Kolesnikov, V. A. Kolyasnikov, S. T. Koretskaya, V. P. Lavristchev, V. A. Ryzhkov, A. N. Samus', and V. K. Semenov, 1978, Mikroelektronika **7**, 184 (in Russian).
Kanter, H., and F. L. Vernon, Jr., 1970, Phys. Rev. B **2**, 4694.
Kaplan, S. B., C. C. Chi, D. N. Langenberg, J.-J. Chang, S. Jafarey, and D. J. Scalapino, 1976, Phys. Rev. B **14**, 4854.
Keyes, R. W., 1969, IEEE Spectrum **6**, 36.
Keyes, R. W., 1975, Proc. IEEE **63**, 740.
King, C. A., 1971, Rev. Sci. Instrum. **42**, 1717.
Kirshman, R. K., J. A. Hutchby, and J. W. Burgess, 1977, IEEE Trans. Magn. **13**, 731.
Kirshman, R. K., H. A. Notarys, and J. E. Mercereau, 1971, Phys. Lett. A **34**, 209.
Kirshman, R. K., H. A. Notarys, and J. E. Mercereau, 1975, IEEE Trans. Magn. **11**, 778.
Klapwijk, T. M., and J. E. Mooij, 1975, IEEE Trans. Magn. **11**, 858.
Klapwijk, T. M., and J. E. Mooij, 1976, Phys. Lett. A **57**, 97.
Klapwijk, T. M., M. Sepers, and J. E. Mooij, 1977a, J. Low Temp. Phys. **27**, 801.
Klapwijk, T. M., J. N. Van der Bergh, and J. E. Mooij, 1977b, J. Low Temp. Phys. **26**, 385.
Klapwijk, T. M., and T. B. Veenstra, 1974, Phys. Lett. A **47**, 351.
Kofoed, B., and K. Saermark, 1974, Phys. Rev. Lett. **31**, 1124.
Kofoed, B., and K. Saermark, 1975, Phys. Lett. A **55**, 72.
Komarovskikh, N. I., G. M. Lapir, A. N. Samus', and V. K. Semenov, 1975, Pis'ma V. Zh. Tekh. Fiz. **1**, 1002 [Sov. Phys.–Tech. Phys. Lett.].
Kovalenko, A. S., 1976, Pis'ma V. Zh. Tekh. Fiz. **2**, 715 [Sov. Phys.–Tech. Phys. Lett.].
Kramer, L., and A. Baratoff, 1977, Phys. Rev. Lett. **38**, 518.
Kravchenko, V. V., S. I. Bondarenko, K. B. Lobanov, and O. E. Shchastlivets, 1976, Fiz. Nizk. Temp. **2**, 200 [Sov. J. Low Temp. Phys. **2**, 100 (1976)].
Kulik, I. O., 1966, Zh. Eksp. Teor. Fiz. **50**, 1617 [Sov. Phys.–JETP **23**, 1077 (1966)].

Kulik, I. O., 1969a, Zh. Eksp. Teor. Fiz. **57**, 600 [Sov. Phys.–JETP **30**, 329 (1970)].
Kulik, I. O., 1969b, Zh. Eksp. Teor. Fiz. **57**, 1745 [Sov. Phys.–JETP **30**, 944 (1970)].
Kulik, I. O., 1970, Zh. Eksp. Teor. Fiz. **59**, 584 [Sov. Phys.–JETP **32**, 318 (1971)].
Kulik, I. O., 1976, Fiz. Nizk. Temp. **2**, 962 [Sov. J. Low. Temp. Phys. **2**, 471 (1976)].
Kulik, I. O., and Yu. N. Mitzai, 1975, Fiz. Nizk. Temp. **1**, 906 [Sov. J. Low Temp. Phys. **1**, 434 (1975)].
Kulik, I. O., and A. N. Omelyanchuk, 1975, Zh. Eksp. Teor. Fiz. Pis'ma Red. **21**, 216 [JETP Lett. **21**, 96 (1975)].
Kulik, I. O., and A. N. Omelyanchuk, 1977, Fiz. Nizk. Temp. **3**, 945 [Sov. J. Low Temp. Phys.].
Kulik, I. O., and R. I. Shekhter, 1975, Zh. Eksp. Teor. Fiz. **68**, 623 [Sov. Phys.–JETP **41**, 308 (1975)].
Kulik, I. O., and R. I. Shekhter, 1976, Fiz. Nizk. Temp. **2**, 21 [Sov. J. Low Temp. Phys. **2**, 9 (1976)].
Kulik, I. O., and I. K. Yanson, 1970, *Josephson Effect in Superconducting Tunnel Structures* (Nauka, Moscow) [Keter Press, Jerusalem (1972)].
Kulikov, V. A., N. N. Kurdyumov, G. P. Leshchenko, L. V. Matveetz, V. V. Migulin, and E. S. Soldatov, 1974, Rev. Phys. Appl. **9**, 293.
Kupriyanov, M. Yu., and K. K. Likharev, 1972, Zh. Eksp. Teor. Fiz. Pis'ma Red. **15**, 349 [JETP Lett. **15**, 247 (1972)].
Kupriyanov, M. Yu., and K. K. Likharev, 1975, Zh. Eksp. Teor. Fiz. **68**, 1506 [Sov. Phys.–JETP **41**, 755 (1976)].
Kupriyanov, M. Yu., K. K. Likharev, and L. A. Maslova, 1975, in *Proceedings of the 14th International Conference on Low Temperature Physics*, edited by M. Krusius and M. Vuorio (North-Holland, Amsterdam), Vol. 4, p. 104.
Kupriyanov, M. Yu., and K. K. Likharev, 1976, Fiz. Tverd. Tela **18**, 1947 [Sov. Phys.–Solid State **18**, 1133 (1976)].
Kupriyanov, M. Yu., K. K. Likharev, and V. K. Semenov, 1976a, Fiz. Nizk, Temp. **2**, 706 [Sov. J. Low Temp. Phys. **2**, 346 (1976)].
Kupriyanov, M. Yu., K. K. Likharev, and V. K. Semenov, 1976b, Fiz. Nizk. Temp. **2**, 1252 [Sov. J. Low Temp. Phys. **2**, 610 (1976)].
Kurdyumov, N. N., 1976, Pis'ma V. Zh. Tekh. Fiz. **2**, 973 [Sov. Phys.–Tech. Phys. Lett.].
Lahiri, S. K., 1976, J. Vac. Sci. Technol. **13**, 148.
Laibowitz, R. B., 1973, Appl. Phys. Lett. **23**, 407.
Laibowitz, R. B., C. C. Tsuei, J. C. Cuomo, J. F. Ziegler, and M. Hatzakis, 1975, IEEE Trans. Magn. **11**, 883.
Laibowitz, R. B., J. M. Viggiano, and M. Hatzakis, 1974, Rev. Phys. Appl. **9**, 165.
Lambe, J., A. H. Silver, J. E. Mercereau, and R. C. Jaklevič, 1964, Phys. Lett. **11**, 16.
Landa, P. S., and N. D. Tarankova, 1977, Fiz. Nizk. Temp. **3**, 32 [Sov. J. Temp. Phys. **3**, 15 (1977)].
Langenberg, D. N., 1974, Rev. Phys. Appl. **9**, 35.
Langenberg, D. N., 1975, in *Proceedings of the 14th International Conference on Low Temperature Physics*, edited by M. Krusius and M. Vuorio (North-Holland, Amsterdam), Vol. 5, p. 223.
Lapir, G. M., K. K. Likharev, L. A. Maslova, and V. K. Semenov, 1975, Fiz. Nizk. Temp. **1**, 1235 [Sov. J. Low Temp. Phys. **1**, 590 (1975)].
Lapir, G. M., K. K. Likharev, and V. K. Semenov, 1977, Zh. Tekh. Fiz. **47**, 1069 [Sov. Phys.-Tech. Phys. **22**, 638 (1977)].
Larkin, A. I., and Yu. N. Ovchinnikov, 1966, Zh. Eksp. Teor. Fiz. **51**, 1535 [Sov. Phys.–JETP **24**, 1035 (1967)].
Larkin, A. I., and Yu. N. Ovchinnikov, 1967, Zh. Eksp. Teor. Fiz. **53**, 2159 [Sov. Phys.–JETP **26**, 1219 (1968)].
Larkin, A. I., and Yu. N. Ovchinnikov, 1973a, J. Low Temp. Phys. **10**, 407.
Larkin, A. I., and Yu. N. Ovchinnikov, 1973b, Zh. Eksp. Teor. Fiz. **65**, 1704 [Sov. Phys.–JETP **38**, 854 (1974)].
Larkin, A. I., and Yu. N. Ovchinnikov, 1975, Zh. Eksp. Teor. Fiz. **68**, 1915 [Sov. Phys.–JETP **41**, 960 (1975)].
Latyshev, Yu. I., and F. Ya. Nad', 1974, Zh. Eksp. Teor. Fiz. Pis'ma Red. **19**, 737 [JETP Lett. **19**, 380 (1974)].
Levinsen, M. T., 1974, Rev. Phys. Appl. **9**, 153; Appl. Phys. Lett. **24**, 247.
Likharev, K. K., 1971a, Izv. Vyssh. Uchebn. Zaved. Radiofiz. **14**, 909 [Radiophys. Quant. Electron.].
Likharev, K. K., 1971b, Izv. Vyssh. Uchebn. Zaved. Radiofiz. **14**, 919 [Radiophys. Quant. Electron.].
Likharev, K. K., 1971c, Izv. Vyssh. Uchebn. Zaved. Radiofiz. **14**, 1232 [Radiophys. Quant. Electron.].
Likharev, K. K., 1971d, Zh. Eksp. Teor. Fiz. **61**, 1700 [Sov. Phys.–JETP **34**, 906 (1972)].
Likharev, K. K., 1973, Fiz. Tverd. Tela **15**, 2524 [Sov. Phys.–Solid State **15**, 1679 (1974)].
Likharev, K. K., 1974a, Radiotekh. Elektron. **19**, 1494 [Radio Eng. Electron. Phys. **19**, 109 (1974)].
Likharev, K. K., 1974b, Zh. Eksp. Teor. Fiz. Pis'ma Red. **20**, 730 [JETP Lett. **20**, 338 (1974)].
Likharev, K. K., 1975a, Radiotekh. Elektron. **20**, 660 [Radio Eng. Electron. Phys. **20**, 135 (1975)].
Likharev, K. K., 1975b, Fiz. Tverd. Tela **17**, 2787 [Sov. Phys.–Solid State **17**, 1856 (1976)].
Likharev, K. K., 1976, Pis'ma V. Zh. Tekh. Fiz. **2**, 29 [Sov. Phys.–Tech. Phys. Lett.].
Likharev, K. K., 1977a, IEEE Trans. Magn. **13**, 242.
Likharev, K. K., 1977b, IEEE Trans. Magn. **13**, 244.
Likharev, K. K., and Kuzmin, L. S., 1977, Radiotekh. Elektron. **22**, 1689 [Radio Eng. Electron. Phys.].
Likharev, K. K., G. M. Lapir, V. K. Semenov, and L. A. Yakobson, 1974, *Some Properties of Variable Thickness Bridges*, Report on Applied Superconductivity Conference, Oakbrook (unpublished).
Likharev, K. K., G. M. Lapir, and V. K. Semenov, 1976, Pis'ma V. Zh. Tekh. Fiz. **2**, 809 [Sov. Phys.–Tech. Phys. Lett.].
Likharev, K. K., and V. K. Semenov, 1971, Radiotekh. Elektron. **16**, 2167 [Radio Eng. Electron. Phys. **16**, 1917 (1971)].
Likharev, K. K., and V. K. Semenov, 1972a, Zh. Eskp. Teor. Fiz. Pis'ma Red. **15**, 625 [JETP Lett. **15**, 442 (1972)].
Likharev, K. K., and V. Semenov, 1972b, Radiotekh. Elektron. 17, 1983 [Radio Eng. Electron Phys. 18, 1290 (1973)].
Likharev, K. K., and V. K. Semenov, 1973, Radiotekh. Elektron, 18, 1757 [Radio Eng. Electron Phys. 18, 1290 (1973)].
Likharev, K. K., and B. T. Ulrich, 1978, *Josephson Junction Circuits and Applications* (Izd. Mosk. Universiteta, Moscow), English edition to be published.
Likharev, K. K., and L. A. Yakobson, 1975a, Zh. Tekh. Fiz. **45**, 1503 [Sov. Phys.–Tech. Phys. **20**, 950 (1975)].
Likharev, K. K., and L. A. Yakobson, 1975b, IEEE Trans. Magn. **11**, 860.
Likharev, K. K., and L. A. Yakobson, 1975c, Zh. Eksp. Teor. Fiz. **68**, 1150 [Sov. Phys.–JETP **41**, 570 (1976)].
Lindelof, P. E., 1976, Solid State Commun. **18**, 283.
Lindelof, P. E., J. B. Hansen, J. Mygind, N. F. Pedersen, and O. H. Sørensen, 1977, Phys. Lett. A **60**, 451.
Lobanov, K. B., S. I. Bondarenko, A. G. Davydova, and V. B. Bondarev, 1976, Zh. Tekh. Fiz. **46**, 2443 [Sov. Phys.–Tekh. Phys.].
Lubbig, H., and H. Luther, 1974, Rev. Phys. Appl. **9**, 29.
Lukens, J. E., 1976, private communication.
Lum, W. Y., and T. Van Duzer, 1975, J. Appl. Phys. **46**, 3216.
Macfarlane, J. C., 1973, Appl. Phys. Lett. **22**, 549.
Macfarlane, J. C., 1976, J. Phys. E **9**, 167.
Maki, K., 1963, Prog. Theor. Phys. **30**, 573.
Mamaladze, Yu. G., and O. D. Cheishvili, 1966, Zh. Eksp. Teor. Fiz. **50**, 169 [Sov. Phys.–JETP **23**, 112 (1966)].
Martinoli, P., O. Daldini, C. Leemann, and B. Van den Brandt, 1976, Phys. Rev. Lett. **36**, 382.

Matisoo, J., 1967, Proc. IEEE **55**, 172.
Mattis, D. C., and J. Bardeen, 1958, Phys. Rev. **111**, 412.
McCarthy, S. L., and J. Stanko, 1974, Rev. Sci. Instrum. 45, 335.
McCumber, D. E., 1968, J. Appl. Phys. **39**, 3113.
McDonald, D. G., K. M. Evenson, J. S. Wells, and J. D. Cupp, 1971, J. Appl. Phys. **42**, 179.
McDonald, D. G., E. G. Johnson, and R. E. Harris, 1976, Phys. Rev. B **13**, 1028.
McDonald, D. G., F. R. Petersen, J. D. Cupp, B. L. Danielson, and E. G. Johnson, 1974, Appl. Phys. Lett. **24**, 335.
McDonald, D. G., A. S. Risley, J. D. Cupp, K. M. Evenson, and J. R. Ashley, 1972, Appl. Phys. Lett. **20**, 296.
Mercereau, J. E., 1974, Rev. Phys. Appl. **9**, 47.
Meservey, J. E., and P. M. Tedrow, 1969, J. Appl. Phys. 40, 2028.
Meservey, J. E., and P. W. Tedrow, 1975, IEEE Trans. Magn. **11**, 720.
Meyer, J. D., and R. Tidecks, 1976, Solid State Commun. **18**, 305.
Mitsai, Yu. N., 1976, Fiz. Nizk. Temp. **2**, 189 [Sov. J. Low Temp. Phys. **2**, 94 (1976)].
Mooij, J. E., C. A. Gorter, and J. E. Nordman, 1974, Rev. Phys. Appl. **9**, 173.
Murata, K., T. Kawai, Y. Sato, Y. Nohmi, and S. Kobayashi, 1976, Jpn. J. Appl. Phys. **15**, 733.
Nad', F. Ya., 1971, Prib. Tekh. Eksp. No. 6, 179 [Instrum. Exp. Tech. **14**, 1794 (1971)].
Nad', F. Ya., 1975, Prib. Tekn. Eksp. No. 1, 7 [Instrum. Exp. Tech. **18**, 1 (1975)].
Nad'F. Ya., and O. Yu. Polyanskii, 1973, Radiotekh. Elektron. **18**, 2445 [Radio Eng. Electron. Phys.].
Neumaier, K., 1976, Cryogenics **16**, 117.
Niemeyer, J., and V. Kose, 1976, Appl. Phys. Lett. **29**, 380.
Nisenoff, M., and S. Wolf, 1975, Phys. Rev. B **12**, 1712.
Notarys, H. A., and J. E. Mercereau, 1971, Physica (Utr.) **55**, 424.
Notarys, H. A., M. L. Yu, and J. E. Mercereau, 1973, Phys. Rev. Lett. **30**, 743.
Octavio, M., W. J. Skocpol, and M. Tinkham, 1977a, IEEE Trans. Magn. **13**, 739.
Octavio, M., W. J. Skocpol, and M. Tinkham, 1977b, Phys. Rev. B **17**, 159.
Ohta, H., M. J. Feldman, P. T. Parrish, and R. Y. Chiao, 1974, Rev. Phys. Appl. **9**, 187.
Omelyanchuk, A. N., I. O. Kulik, and R. I. Shekhter, 1977, Zh. Eksp. Teor. Fiz. Pis'ma Red. **25**, 465 [JETP Lett. **25**, 437 (1977)].
Owen, C. S., and D. J. Scalapino, 1967, Phys. Rev. **164**, 538.
Palmer, D. W., and S. K. Decker, 1973, Rev. Sci. Instrum. **44**, 1621.
Palmer, D. W., and J. E. Mercereau, 1974, Appl. Phys. Lett. **25**, 467.
Palmer, D. W., and J. E. Mercereau, 1975, IEEE Trans. Magn. **11**, 667.
Palmer, D. W., and J. E. Mercereau, 1977, Phys. Lett. A **61**, 135.
Pankove, J. I., 1966, Phys. Lett. **21**, 406.
Parks, R. D., and J. M. Mochel, 1964, Rev. Mod. Phys. **36**, 284.
Pedersen, N. F., T. F. Finnegan, and D. N. Langenberg, 1972, Phys. Rev. B **6**, 4151.
Pedersen, N. F., O. H. Soerensen, J. Mygind, P. E. Lindelof, M. T. Levinsen, and T. D. Clark, 1976, Appl. Phys. Lett. **28**, 562.
Pedersen, N. F., O. H. Soerensen, J. Mygind, M. T. Levinsen, P. E. Lindelof, T. D. Clark, and M. Danielsen, 1977, IEEE Trans. Magn. **13**, 248.
Peters, P., and H. Meissner, 1973, Phys. Rev. Lett. **30**, 965.
Pines, D., 1963, *Elementary Excitations in Solids* (Benjamin, New York).
Pippard, A. B., J. G. Shepherd, and D. A. Tindall, 1971, Proc. R. Soc. Lond. A **324**, 17.
Poulsen, U. K., 1973, *A Theoretical Treatment of Tunnel Currents in Superconducting Junctions* Rept. Fys. Lab. I DTH, (Lyngby, Denmark) No. 121.
Prans, G. P., and H. Meissner, 1974, IEEE Trans. Electron Devices **21**, 605.
Puma, M., and B. S. Deaver, Jr., 1971, Appl. Phys. Lett. **19**, 539.
Rachford, F. J., J. K. Hirvonen, S. A. Wolf, J. Kennedy, and M. Nisenoff, 1977, IEEE Trans. Magn. **13**, 875.
Reiger, T. J., D. J. Scalapino, and J. E. Mercereau, 1971, Phys. Rev. Lett. **27**, 1787.
Reiger, T. J., D. J. Scalapino, and J. E. Mercereau, 1972, Phys. Rev. B **6**, 1734.
Richter, W., and G. Albrecht, 1973, Phys. Status Solidi A **17**, 531.
Riedel, E., 1964, Z. Naturforsch. **19a**, 1634.
Rifkin, R., and B. S. Deaver, Jr., 1976, Phys. Rev. B **13**, 3894.
Rifkin, R., D. A. Vincent, B. S. Deaver, Jr., and P. K. Hansma, 1976, J. Appl. Phys. **47**, 2645.
Rogovin, D., and D. J. Scalapino, 1971, Physics (Utr.) **55**, 399.
Romagnan, J. P., A. Gilabert, J.-P. Laheurte, J. C. Noiray, and E. Guyon, 1975, Solid State Commun. **16**, 359.
Rothwarf, A., and B. N. Tyalor, 1967, Phys. Rev. Lett. **19**, 27.
Rowell, J. M., 1963, Phys. Rev. Lett. **11**, 200.
Russer, P., 1972, J. Appl. Phys. **43**, 2008.
Sandell, R. D., G. J. Dolan, and J. E. Lukens, 1977, in *SQUIDs and their Applications*, edited by H. D. Hahlbohm and H. Lubbig (Walter de Gruyter, West Berlin), p. 26.
Säss, A. R., and W. C. Stewart, 1968, J. Appl. Phys. **39**, 1956.
Schmid, A., 1966, Phys. Kondens. Mater. **5**, 302.
Schmid, A., 1969, Phys. Rev. **180**, 527.
Schmid, A., 1977, Phys. Rev. Lett. **38**, 922.
Schmid, A., and W. Hauger, 1973, J. Low Temp. Phys. **11**, 667.
Schmid, A., and G. Schön, 1975, J. Low Temp. Phys. **20**, 207.
Schroen, W., 1968, J. Appl. Phys. **39**, 2671.
Schuller, I., and K. E. Gray, 1976, Phys. Rev. Lett. **36**, 429.
Schwartz, B. B., 1966, Bull. Am. Phys. Soc. **11**, 106.
Schyfter, M., J. Maah-Sango, N. Raley, B. T. Ulrich, and T. Van Duzer, 1977, IEEE Trans. Magn. **13**, 862.
Shapiro, S., 1963, Phys. Rev. Lett. **11**, 80.
Shepard, K. W., 1971, Physica (Utr.) **55**, 786.
Shepherd, J. G., 1972, Proc. R. Soc. Lond. A **326**, 421.
Shklovskii, V. A., 1975, Fiz. Tverd. Tela **17**, 3076 [Sov. Phys.–Solid State **17**, 2040 (1976)].
Shmidt, V. V., and G. S. Mkrtchyan, 1974, Usp. Fiz. Nauk **112**, 459 [Sov. Phys.–Usp. **17**, 170 (1974)].
Seto, J., and T. Van Duzer, 1971, Appl. Phys. Lett. **19**, 488.
Simmonds, M. B., 1974, J. Appl. Phys. **45**, 366.
Simmonds, M. B., 1977, in *Superconductor Applications: SQUIDs and Machines*, edited by B. B. Schwartz and S. Foner (Plenum, New York), p. 403.
Skocpol, W. J., M. R. Beasley, and M. Tinkham, 1974a, Rev. Phys. Appl. **9**, 19.
Skocpol, W. J., M. R. Beasley, and M. Tinkham, 1974b, J. Appl. Phys. **45**, 4054.
Skocpol, W. J., M. R. Beasley, and M. Tinkham, 1974c, J. Low Temp. Phys. **16**, 145.
Soerensen, O. H., 1974, Cryogenics **14**, 166.
Soerensen, O. H., J. Mygind, and N. F. Pedersen, 1977, Phys. Rev. Lett. **39**, 1018.
Solymar, L., 1972, *Superconducting Tunneling and Applications* (Chapman and Hall, London).
Song, Y., 1976, J. Appl. Phys. **47**, 2651.
Song, Y., and G. I. Rochlin, 1972, Phys. Rev. Lett. **29**, 416.
Stephen, M. J., 1969, Phys. Rev. **182**, 531.

Stewart, W. S., 1968, Appl. Phys. Lett. **12**, 277.
Stratonovich, R. L., 1967, *Topics in the Theory of Random Noise* (Gordon and Breach, New York).
Sugahara, M., **1977**, J. Appl. Phys. **48**, 234.
Svidzinskii, A. V., 1972, Fiz. Kondens. Sost. **19**, 42 (in Russian).
Svidzinskii, A. V., T. N. Antsygina, and E. N. Bratus, 1971, Zh. Eksp. Teor. Fiz. **61**, 1612 [Sov. Phys.–JETP **34**, 860 (1972)].
Svidzinskii, A. V., T. N. Antsygina, and E. N. Bratus, 1973, J. Low Temp. Phys. **10**, 131.
Taguchi, I., and H. Yoshioka, 1972, J. Phys. Soc. Jpn. **33**, 92.
Taguchi, I., and H. Yoshioka, 1973, J. Phys. Soc. Jpn. **34**, 1106.
Taylor, B. N., W. H. Parker, and D. N. Langenberg, 1969, *The Fundamental Constants and Quantum Electrodynamics* (Academic, New York).
Testardi, L. R., Phys. Rev. B **4**, 2189.
Thomé, H., and Y. Couder, 1975, in *Proceedings of the 14th International Conference on Low Temperature Physics*, edited by M. Krusius and M. Vuorio (North-Holland, Amsterdam), Vol. 4, p. 156.
Tinkham, M. , 1972, Phys. Rev. B **6**, 1747.
Tinkham, M., 1975, *Introduction to Superconductivity* (McGraw-Hill, New York).
Tinkham, M., and J. Clarke, 1972, Phys. Rev. Lett. **28**, 1366.
Tinkham, M., M. Octavio, and W. J. Skocpol, 1977, J. Appl. Phys. **48**, 1311.
Tsang, W. T., and S. Wang, 1974, Appl. Phys. Lett. **24**, 519.
Ulrich, B. T., and T. Van Duzer, 1977, in *Superconductor Applications: SQUIDs and Machines*, edited by B. B. Schwartz and S. Foner (Plenum, New York), p. 321.
Usadel, K. D., **1970**, Phys. Rev. Lett. **25**, 507.
Vernet, G., and R. Adde, 1976, Appl. Phys. Lett. **28**, 559.
Vincent, D. A., and B. S. Deaver, Jr., 1974, Phys. Rev. Lett. **32**, 212.
Volkov, A. F., 1971, Zh. Eskp. Teor. Fiz. **60**, 1500 [Sov. Phys.–JETP **33**, 811 (1971)].
Volkov, A. F., 1972, Radiotekh. Electron. **17**, 2581 [Radio Eng. Electron. Phys.].
Volkov, A. F., 1973, Fiz. Tverd. Tela **15**, 1364 [Sov. Phys.–Solid State **15**, 925 (1973)].
Volkov, A. F., 1974, Zh. Eksp. Teor. Fiz. **66**, 758 [Sov. Phys.–JETP **39**, 366 (1974)].
Volkov, A. F., and A. L. Kasatkin, 1974, Zh. Eksp. Teor. Fiz. **67**, 1527 [Sov. Phys.–JETP **40**, 760 (1975)].
Volkov, A. F., and F. Ya. Nad', 1970, Zh. Eksp. Teor. Fiz. Pis'ma Red. **11**, 92 [JETP Lett. **11**, 56 (1970)].
Volkov, A. F., and A. V. Zaitzev, 1976, Pis'ma V. Zh. Tekh. Fiz. **2**, 188 [Sov. Phys.–Tech. Phys. Lett.].
Volotskaya, V. G., L. E. Musienko, I. M. Dmitrenko, and Yu. V. Kalekin, 1976 Fiz. Nizk. Temp. **2**, 500 [Sov. J. Low Temp. Phys. **2**, 248 (1976)].
Voss, R. E., and J. Clarke, 1976, Phys. Rev. B **13**, 556.
Vystavkin, A. N., V. N. Gubankov, L. S. Kuzmin, K. K. Likharev, and V. V. Migulin, 1972, Radiotekh. Electron. **17**, 896 [Radio Eng. Electron. Phys. **17**, 705 (1972)].
Vystavkin, A. N., V. N. Gubankov, L. S. Kuzmin, K. K. Likharev, V. V. Migulin, and A. M. Spytsyn, 1973, Zh. Eksp. Teor. Fiz. Pis'ma Red. **17**, 284 [JETP Lett. **17**, 204 (1973)].
Vystavkin, A. N., V. N. Gubankov, L. S.Kuzmin, K. K. Likharev, V. V. Migulin, and V. K. Semenov, 1974, Rev. Phys. Appl. **9**, 79.
Waldram, J. R., 1975, Proc. R. Soc. Lond. A **345**, 231.
Waldram, J. R., 1976, Rep. Prog. Phys. **39**, 751.
Waldram, J. R., and J. M. Lumley, 1975, Rev. Phys. Appl. **10**, 7.
Wang, L.-K., A. Callegari, B. S. Deaver, Jr., D. W. Barr, R. J. Mattauch, 1977, Appl. Phys. Lett. **31**, 306.
Way, Y. C., K. C. Hsu, and Y. H. Kao, 1978, Interactions between Two Superconducting Weak Links in the Stationary ($V = 0$) States,[11] preprint.
Werthamer, N. R., 1966, Phys. Rev. **147**, 255.
Wong, T.-W., J. T. C. Yeh, and D. N. Langenberg, 1976, Phys. Rev. Lett. **37**, 150; **38**, 795E.
Wong, T.-W., J. T. C. Yeh, and D. N. Langenberg, 1977, IEEE Trans. Magn. **13**, 743.
Wu. C. T., and C. M. Falco, 1977, Appl. Phys. Lett. **30**, 609.
Wyatt, A. F. G., V. M. Dmitriev, W. S. Moore, and F. W. Sheard, 1966, Phys. Rev. Lett. **16**, 1166.
Yanson, I. K., 1975, Fiz. Nizk. Temp. **1**, 141 [Sov. J. Low Temp. Phys. **1**, 67 (1975)].
Yanson, I. K., V. M. Svistunov, and I. M. Dmitrenko, 1965, Zh. Eksp. Teor. Fiz. **48**, 976 [Sov. Phys.–JETP **21**, 650 (1965)].
Yeh, J. T. C., 1974, J. Appl. Phys. **45**, 4617.
Yu, M. L., and J. E. Mercereau, 1972, Phys. Rev. Lett. **28**, 1117.
Yu, M. L., and J. E. Mercereau, 1975, Phys. Rev. B **12**, 4909.
Yu, M. L., and J. E. Mercereau, 1976, Phys. Rev. Lett. **37**, 1148.
Zaitzev, A. V., 1976, Fiz. Tverd. Tela **18**, 2744 [Sov. Phys.–Solid State **18**, 1599 (1976)].
Zaitzev, R. O., 1966, Zh. Eksp. Teor. Fiz. **50**, 1055 [Sov. Phys.–JETP **23**, 702 (1966)].
Zappe, H. H., 1975, Appl. Phys. Lett. **27**, 432.
Zappe, H. H., 1977, Jpn. J. Appl. Phys. **16**, Suppl., 247.
Zavaritskii, N. V., 1974, Zh. Eksp. Teor. Fiz. Pis'ma Red. **19**, 205 [JETP Lett. **19**, 126 (1974)].
Zeller, H. R., and I. Giaever, 1969, Phys. Rev. **181**, 789.
Ziman, J. M., 1972, *Principles of the Theory of Solids* (Cambridge University, Cambridge, England), 2nd. ed.
Zimmerman, J. E., 1970, J. Appl. Phys. **41**, 1589.
Zimmerman, J. E., 1972, in *Proceedings of the Applied Superconductor Conference* (IEEE, New York) IEEE Pub. No. 72-CH0682-TABSC, p. 544.
Zimmerman, J. E., J. A. Cowen, and A. H. Silver, 1966, Appl. Phys. Lett. **9**, 353.
Zimmerman, J. E., and J. E. Mercereau, 1965, Phys. Lett. **13**, 125.
Zimmerman, J. E., and A. H. Silver, 1964, Phys. Lett. **10**, 47.
Zimmerman, J. E., and A. H. Silver, 1966a, Phys. Rev. **141**, 376.
Zimmerman, J. E., and A. H. Silver, 1966b, Solid State Commun. **4**, 133.
Zimmerman, J. E., P. Thiene, and J. T. Harding, 1971, J. Appl. Phys. **41**, 1572.
Zorin, A. B., and K. K. Likharev, 1977a, Fiz. Nizk. Temp. **3**, 148 [Sov. J. Low Temp. Phys. **3**, 70 (1977)].
Zorin, A. B., and K. K. Likharev, 1978a, Fiz. Nizk. Temp. **3**, 713 [Sov. J. Low Temp. Phys.].
Zorin, A. B., and K. K. Likharev, 1978b, Some Problems in the Tunnel Theory of the Josephson Effect, Report at 15-th Conf. on Low Temp. Phys. (Grenoble, Aug. 1978), to be published.